

Muscarinic Receptors Mediated Stimulation and Intracellular Signaling Pathways Involved in Human Lung Fibroblast Proliferation

Dissertation

zur

Erlangung des Doktorgrades (Dr. rer. nat)

der

Mathematisch-Naturwissenschaftlichen Fakultät

der

Rheinischen Friedrich-Wilhelms-Universität Bonn

vorgelegt von

Amit Bahulayan

aus

Mumbai

2009

Angefertigt mit der Genehmigung der

Mathematisch-Naturwissenschaftlichen Fakultät der Rheinischen
Friedrich-Wilhelms-Universität Bonn

1. Referent: Prof. Dr. med. Kurt Racké

2. Referent: Prof. Dr. med. Klaus Mohr

Tag der Promotion: 13.05.2009

Dedicated to my parents for their support all these years

Table of Contents

Abbreviations

1 Introduction	1
1.1 Neuronal and Non Neuronal Acetylcholine	2
1.2 Cholinoceptors	3
1.2.1 Nicotinic Receptors	3
1.2.2 Muscarinic Receptors	4
1.3 Molecular and Pharmacological Classification of Muscarinic Receptor Subtypes	5
1.3.1 Molecular Biology of Muscarinic Receptors	5
1.3.2 Pharmacological Classification of Muscarinic Receptor Subtypes	6
1.4 Muscarinic Coupling to G-proteins and Effector Molecules	8
1.4.1 Adenylyl Cyclase	10
1.4.2 Phospholipase C	11
1.5 Mitogen Activated Protein Kinases	12
1.5.1 MAPKs in Regulation of Cell Cycle	14
1.6 G-protein Coupled Receptor Signaling to MAPK	16
1.7 Intracellular Signaling Pathways Linking G-protein Coupled Receptors to MAPK	17
1.7.1 The Ras Mediated Activation of MAPK Cascade via G-protein Coupled Receptors	18
1.7.2 Rho Mediated Activation of MAPK Cascade via G-protein Coupled Receptors	21
1.7.3 Phosphatidylinositol 3-Kinase (PI3K) Mediated Activation of MAPK Cascade via G-protein Coupled Receptors	23
1.7.4 Phospholipase C (PLC) Mediated Activation of MAPK Cascade via G-protein Coupled Receptors	25
1.8 Transactivation of Classical Receptor Tyrosine Kinases by GPCRs	26
1.9 Apoptosis and G-protein Coupled Receptor Signaling Interaction	27
2 Materials and Methods	29
2.1 Materials	29
2.1.1 Reagents	29
2.1.2 Test Drugs	30

2.1.3 Buffers and Reagents for Cell Culture	34
2.1.4 Solution and Buffers for Proliferation Assay	35
2.1.5 Reagents for Protein Determination using the Lowry Method	36
2.1.6 Primers for Polymerase Chain Reaction	37
2.1.7 Buffers and Solutions for RT/PCR	38
2.1.8 Human Lung Fibroblast Cells	40
2.1.9 Buffers and Reagents for Protein Gel Electrophoresis and Immunoblot	40
2.1.10 Antibodies	42
2.1.11 Reagents and Solutions for Caspase-3 Fluorimetric Assay	42
2.1.12 Equipment	44
2.1.13 Tools for Statistical Analysis	44
2.2 Methods	46
2.2.1 Culture of Human Lung Fibroblast	46
2.2.2 RNA Preparation	47
2.2.3 Reverse Transcription	48
2.2.4 Polymerase Chain Reaction (PCR)	49
2.2.5 Agarose Gel Electrophoresis	50
2.2.6 DNA Preparation	50
2.2.7 Protein Preparation	51
2.2.8 Protein Determination	52
2.2.9 Protein Gel Electrophoresis and Immunoblot	52
2.2.9.1 Protein Gel Electrophoresis	52
2.2.9.2 Immunoblot	53
2.2.9.3 Membrane Stripping	55
2.2.10 (³ H)-Thymidine Incorporation Proliferation Assay	55
2.2.11 Caspase-3 Fluorimetric Assay	56
3 Results	59
3.1 Muscarinic Receptor Expression in Human Lung Fibroblasts	59
3.1.1 Muscarinic Receptor Expression in MRC-5 Human Lung Fibroblasts	59
3.1.2 Muscarinic Receptor Expression in Primary Human Lung Fibroblasts	62
3.2 Muscarinic Stimulation of Proliferation of Human Lung Fibroblasts	65
3.2.1 Muscarinic Stimulation of Proliferation of MRC-5 Human Lung Fibroblasts	65
3.3 Characterisation of Muscarinic Receptor Sub-Type	68
3.3.1 Inhibition of Muscarinic Proliferation using Receptor Sub-Type Specific Antagonists in MRC-5 Human Lung Fibroblasts	68
3.3.1.2 Effect of Pertussis Toxin on Muscarinic Stimulation of Proliferation of MRC-5 Human Lung Fibroblasts	71

3.3.1.3 Muscarinic Stimulation and Effect of Pertussis Toxin on Proliferation in Primary Human Lung Fibroblasts (pHLFb)	72
3.4 Muscarinic Stimulation Mediated Activation of MAPK Pathway in Human Lung Fibroblasts	73
3.4.1 Muscarinic Receptor Stimulation and Activation of p-42/44 MAPK Pathway in proliferation of Human Lung Fibroblast	73
3.4.1.2 Western Blot Analysis of p42/44 MAPK (ERK1, ERK2) Activation in MRC-5 Human Lung Fibroblast	74
3.5 Effect of Kinase Inhibitors on Muscarinic Stimulation of MRC-5 Human Lung Fibroblast Proliferation	76
3.5.1 Effects of the Rho-kinase Inhibitor Y27632 on Muscarinic Stimulation of MRC-5 Human Lung Fibroblast Proliferation	76
3.5.1.2 Effects of the Phospholipase C Inhibitor U73122 on Muscarinic Stimulation of MRC-5 Human Lung Fibroblast Proliferation	78
3.5.1.3 Effects of the PI3-kinase Inhibitor Wortmannin on Muscarinic Stimulation of MRC-5 Human Lung Fibroblast Proliferation	80
3.5.1.4 Effects of the Raf-1 Inhibitor GW5074 on Muscarinic Stimulation of MRC-5 Human Lung Fibroblast Proliferation	82
3.5.1.5 Effects of the Raf-1 Inhibitor GW5074 (GW) on Muscarinic Stimulation of the ERK-MAP Kinase in MRC-5 Human Lung Fibroblasts	84
3.5.1.6 Effects of the Tyrosine-Kinase Inhibitor Tyrphostin AG1295 on Muscarinic Stimulation of MRC-5 Human Lung Fibroblasts	85
3.6 Muscarinic Stimulation of proliferation of MRC-5 Human Lung Fibroblast and Anti-apoptotic effects	87
3.7 Nicotinic Receptor Expression and Function in MRC-5 Human Lung Fibroblasts	89
4 Discussion	92
4.1 Muscarinic Receptor Expression in Human Lung Fibroblasts	92
4.2 Muscarinic Stimulation of Proliferation of Human Lung Fibroblasts	92
4.3 Inhibition of Muscarnic Proliferation using Receptor Sub-Type Specific Antagonists in MRC-5 Human Lung Fibroblasts and Effect of Pertussis Toxin on Muscarinic Stimulation of Proliferation of Human Lung Fibroblasts	94
4.4 Muscarinic Receptor Stimulation and Activation of p-42/44 MAPK Pathway in Proliferation of Human Lung Fibroblast	95

4.5 Intracellular Signaling Mechanism Involved in Muscarinic Stimulation Mediated Activation of MAPK Cascade in MRC-5 Human Lung Fibroblast Proliferation	96
4.5.1 Effects of the Rho-kinase Inhibitor Y27632 on Muscarinic Stimulation of MRC-5 Human Lung Fibroblast Proliferation	96
4.5.1.2 Effects of the Phospholipase C Inhibitor U73122 on Muscarinic Stimulation of MRC-5 Human Lung Fibroblast Proliferation	97
4.5.1.3 Effects of the PI3-kinase Inhibitor Wortmannin on Muscarinic Stimulation of MRC-5 Human Lung Fibroblast Proliferation	98
4.5.1.4 Effects of the Raf-1 Inhibitor GW5074 on Muscarinic Stimulation of MRC-5 Human Lung Fibroblast Proliferation	99
4.5.1.5 Effects of the Tyrosine-Kinase Inhibitor Tyrphostin AG1295 on Muscarinic Stimulation of MRC-5 Human Lung Fibroblasts	100
4.6 Muscarinic Stimulation of Proliferation of MRC-5 Human Lung Fibroblast and Anti-apoptotic Effects	101
4.7 Nicotinic Receptor Expression and Function in MRC-5 Human Lung Fibroblasts	102
5 Conclusion	104
6 References	106
7 Seminars and Publications	127
8 Acknowledgements	128
9 Curriculum Vitae	129

Abbreviations

ACh	Acetylcholine
AC	Adenylyl cyclase
ADP	Adenosine diphosphate
Akt	Protein kinase B
Arg	Arginine
Asp	Aspartic acid
ATP	Adenosine triphosphate
cAMP	Cyclic adenosine monophosphate
COPD	Chronic obstructive pulmonary disease
cDNA	Complementary Deoxyribonucleic acid
CDK	Cyclin dependent kinase
CKI	Cyclin dependent kinase inhibitor
DAG	Diacyl glycerol
DNA	Deoxyribonucleic acid
DMSO	Dimethylsulfoxide
DEPC	Diethylpyrocarbonate
EGF	Epidermal growth factor
EGFR	Epidermal growth factor receptor
EDTA	Ethylenediaminetetraaceticacid
ERK	Extracellular signal regulated kinase
FCS	Fetal calf serum
GAPs	GTPase Activating Proteins
GEFs	Guanine nucleotide exchange factors
G-protein	Guanine nucleotide binding proteins
GPCR	G-protein-coupled receptor
GDP	Guanosine diphosphate
GTP	Guanosine Triphosphate
GTPase	Guanosine triphosphatase
gDNA	Genomic DNA

IP ₃	Inositol triphosphate
LPA	Lysophosphatidic acid
MAPK	Mitogen activated protein kinase
mAChR	Muscarinic acetylcholine receptor
mRNA	Messenger RNA
PCR	Polymerase chain reaction
PBS	Phosphate buffered saline
PDGF	Platelet derived growth factor
PtdIns	Phosphatidylinositol
PIP2	Phosphotidylinositol-4,5-biphosphate
PLC	Phospholipase C
PKC	Protein kinase C
PI3K	Phosphatidylinositol 3 Kinase
PKA	Protein kinase A
PTX	Pertussis toxin
RNA	Ribonucleic acid
RT	Reverse transcription
RTK	Receptor tyrosine kinase
SEM	Standard error of the mean
SAPK	Stress activated protein kinase
TNF α	Tumor necrosis factor

1 Introduction

Asthma and chronic obstructive pulmonary disease (COPD) are two diseases characterized by airflow limitation due to either reduced driving pressure (loss of elastic recoil of the lung parenchyma) or an increased resistance (airway obstruction) which is mostly reversible in asthma and mostly irreversible in COPD (1, 2). Airway remodeling is a pathological feature observed both in asthma and COPD. The most important difference between asthma and COPD is the nature of inflammation, which is primarily eosinophilic and CD-4 driven in asthma, and neutrophilic and CD-8 driven in COPD (3). In spite of these differences fibrotic alterations are observed in both these diseases (4). Cholinergic pathway represents key mechanisms in control of airway smooth muscle tone. Anticholinergic bronchodilators reduce vagal cholinergic tone, the main reversible component in COPD hence constitute an essential element in the therapy of obstructive airways diseases especially in COPD (5, 6). Furthermore tiotropium bromide (Spiriva[®]) a long acting muscarinic antagonist was found to delay the decline in airway function in COPD (7, 8, 9), suggesting that cholinergic mechanisms plays a pivotal role in the structural changes associated with airway remodeling. In studies carried out on human and bovine airway smooth muscle it was seen that muscarinic agonists enhanced the proliferative response to epidermal growth factor and platelet-derived growth factor respectively (10, 11). Moreover, tiotropium was found to attenuate the increase in airway smooth muscle mass and myosin expression induced by repeated allergen challenges (12). Almost every cell type in the airways expresses cholinergic receptor (13, 14) and hence could be a target for acetylcholine released from neuronal or nonneuronal sources (13, 15). Expression of mRNA encoding different nicotinic receptor subunits (16) and M₂ receptors in airway fibroblasts has been described, but a detailed study on expression of muscarinic receptor subtypes in lung and airway fibroblasts is still lacking. It has been shown that the activation of nicotinic receptors stimulates collagen gene expression and fibronectin synthesis (17, 18) whereas the functional role of muscarinic receptors in airway fibroblasts remains to be illuminated.

The purpose of this study was to determine the expression pattern of the muscarinic receptors in human lung fibroblasts and to investigate whether muscarinic receptors mediate effects on cell proliferation and if so, to elucidate the intracellular signaling pathways entailed.

1.1 Neuronal and Non-Neuronal Acetylcholine

ACh represents the 'classical' neurotransmitter of the parasympathetic nervous system. As neurotransmitter ACh is synthesized in the nerve endings by the enzyme choline acetyltransferase using acetyl-CoA and choline as substrates. It is then stored in the synaptic vesicles. Eventually, depolarization-induced calcium influx lead to an exocytotic release of the neurotransmitter into the extracellular space where it may interact with receptors located on the target cells as well as on the cholinergic nerve terminals themselves (13). In order to limit effector cell activation, after release, ACh is degraded by acetylcholinesterase to non-active choline (19).

Recent studies have revealed that choline acetyltransferase and its product ACh are present in a wide range of non-neuronal cells, including epithelial and endothelial cells, smooth muscle cells as well as various cells of the immune system such as lymphocytes, macrophages, eosinophils and neutrophils (20). In addition nicotinic and muscarinic receptors have been shown to be widely expressed on these non-neuronal cells (21, 22, 23, 24). The essential components of the cholinergic system are present, to a greater or lesser extent, in many of these non-neuronal inflammatory cells involved in airway physiology and pathophysiology. However unlike neuronal cells, where ACh is stored in discrete neurosecretory vesicles, cells of the non-neuronal cholinergic system appear to release acetylcholine directly upon synthesis via active transport mediated by members of the organic cation transporter (OCT) family. Although not much is know about the functional role of non-neuronal ACh it has been shown to act as a local cell molecule via paracrine and autocrine mechanisms to control basic cell functions such as proliferation, differentiation, maturation, migration, secretion, organization of the cytoskeleton and cell-cell contact (23,

24, 25, 26, 27). In a recent study it was shown that the dysfunction of the non-neuronal cholinergic system in the airways could contribute to the deleterious changes of epithelial ion and water movement involved in the pathogenesis of cystic fibrosis a hereditary disease that affects mainly the lungs and digestive system, causing progressive disability (28).

1.2 Cholinoceptors

1.2.1 Nicotinic Receptors

The nicotinic acetylcholine receptors are pentamers of homologous or identical subunits, symmetrically arranged to form a transmembrane cation channel (29). There are multiple nicotinic receptor isotypes existing. Muscle nicotinic receptors, localized at the end plate of the neuromuscular junctions, are assembled of two α -, one β -, one γ - or one ϵ - and one δ (30), whereas neuronal nicotinic receptors appear to be composed either of only two different types of subunits (α and β) or of five α - subunits. The activation of the nicotinic receptor causes a net influx of positively charged ions resulting in membrane depolarization, which can be detected for example as 'excitatory postsynaptic potential' at postganglionic neurons (13). At least 10 different α - and four β - subunits have been identified so far. In addition to the expression of neuronal nicotinic receptor subunits in autonomic ganglia, it was observed in almost every other cell type in the airways and lung tissues. The α -7 subunit was detected in many non-neuronal cells such as the bronchial epithelial cells, endothelial airway cells and airway fibroblasts (16). In vitro studies carried out on bronchial epithelial cells and pulmonary neuroendocrine cells indicated nicotinic receptor mediated activation of cell proliferation cascade (31, 32). It's worth mentioning that nicotinic receptors in non-neuronal cells have also been suggested to be involved in tobacco induced toxicity in the airways (33). Furthermore, chronic exposure of murine and human bronchial epithelial cells to nicotine both in vitro and in vivo caused an upregulation of α -7 and α -3 subunits (34, 35). In another study carried out on WI38 cells, a human embryonic pulmonary fibroblast cell line expressing α -3 and α -7 nicotinic receptor subunits, nicotine exposure disrupted the specific epithelial-

mesenchymal paracrine signaling pathways and resulted in pulmonary interstitial lipofibroblast (LIF)-to-myofibroblast (MYF) transdifferentiation, which could result in altered pulmonary development and function (36).

1.2.2 Muscarinic Receptors

The muscarinic ACh receptors (mAChRs) are members of the superfamily of hormones and neurotransmitter receptors. The muscarinic acetylcholine receptor is a seven transmembrane domain receptor that is coupled to a guanosine triphosphate (GTP) binding protein (G-protein). The muscarinic receptors regulate the activities of intracellular secondary messenger pathways through ion channel and enzyme activation/deactivation by interaction with their coupled G-proteins. Five different subtypes of muscarinic receptors have been identified by molecular biological techniques (m_1 - m_5) (37, 38, 39), but so far a sufficient pharmacological and functional characterization has been provided for only four of them (M_1 - M_4). Nonetheless, there is now significant evidence that the gene product of the m_5 gene forms a functional muscarinic receptor (M_5) (39). The 'odd numbered' (M_1 / M_3 / M_5) muscarinic receptor subtypes couple preferentially to the pertussis toxin (PTX) insensitive G-proteins of the G_q family, while the 'even numbered' (M_2 / M_4) muscarinic receptors bind with G-proteins belonging to the $G_{i/o}$ family. The former subtypes activates phospholipase C (PLC), phospholipase A2 (PLA2), phospholipase D (PLD), tyrosine kinase and calcium influx but do not inhibit adenylyl cyclase, while the latter group of receptors inhibit adenylyl cyclase but do not stimulate PLC. However this coupling specificity of the mAChRs subtypes is not absolute, for the M_2 and the M_4 subtypes can weakly activate PLC when expressed at high levels in certain cell types (40, 41, 42). The PTX-insensitive coupling to PLC is mediated by $G\alpha_q$, $G\alpha_{11}$, $G\alpha_{14}$, and $G\alpha_{16}$, while the PTX-sensitive coupling to adenylyl cyclase inhibition is mediated by $G\alpha_i$ or $G\alpha_o$ (43, 44).

1.3 Molecular and Pharmacological Classification of Muscarinic Receptor Subtypes:

1.3.1 Molecular Biology of Muscarinic Receptors

Subsequent to early pharmacological findings, molecular cloning studies revealed five different subtypes of muscarinic receptors (m_1 - m_5) (37). Numa and colleagues cloned the m_1 and the m_2 genes (45, 46). The m_3 , m_4 , and m_5 gene were thereafter discovered (47, 48, 49). The vertebrate cloned receptor genes are intronless, and similar across mammalian species (50, 51). These five genes encode mAChR glycoproteins that display the structural features of the seven transmembrane helix G-protein-coupled receptor family. Based on the pharmacological binding studies of each receptor resembling the cloned genes, it is now recommended that M_1 , M_2 , M_3 , M_4 and M_5 be used to describe both pharmacological subtypes and molecular subtypes encoded by the cloned genes.

Similar to most members of the G-protein-coupled receptor family whose ligand recognition site binds small molecules, there are several major features of muscarinic receptor structure. First, the ligand recognition site can be located within the outer half of the membrane-embedded part of the protein. To bind the neurotransmitter ACh, all muscarinic receptors have an Asp residue in the distal N-terminal part of the third transmembrane domain which is thought to interact with the polar head of the neurotransmitter and other amine ligands (52, 53). Second, the transmembrane segments are α -helical, whereby three helices are oriented approximately perpendicular to the membrane, and four helices are oriented at a more acute angle (54). Furthermore, there are two conserved cysteine residues that form a disulphide bond between the first and the third extracellular loops (55, 56). There exists a conserved triplet of amino acids (Asp, Arg, Tyr) at the cytoplasmic interface of TMIII with the second intracellular loop that is crucial for both the expression and function of the receptor (57, 58, 59). Moreover the carboxy terminus of the mAChR is located on the intracellular side of the membrane, while the amino terminus is located on the extracellular side of the membrane containing one or more glycosylation sites. On the other hand, the

fourth intracellular region plus regions near transmembrane area in the second and the third internal loops seem to be targeted for phosphorylation by ligand stimulated negative feedback loop mediated mAChR kinase (60). Yet, to distinguish between the different mAChR subtypes, a sequence divergence in the postulated third internal loop (i3) exists between the $M_1/M_3/M_5$ sequences compared with the M_2/M_4 sequences (38, 61, 62). The sequence divergence probably specifies the different coupling preferences of the two categorized groups of subtypes. In addition the sequence within the i3 loop differ sufficiently between each mAChR subtype that allows raising subtype specific antisera (63)

1.3.2 Pharmacological Classification of Muscarinic Receptor Subtypes

The task of pharmacologically characterizing mAChR subtypes has been a difficult process, especially with the initial lack of agonists with any selectivity in addition to the lack of any antagonist with high selectivity for any single receptor subtype. Studies were focused on discovering natural agonists or antagonist plus attempts to synthesize agonists or antagonists that can bind selectively to each subtype to distinguish between each of the five mAChRs. Yet the sites for Ach and other agonists were found to be similar among all five mAChR subtypes. This was further complicated by the presence of multiple muscarinic binding sites in most tissues which emphasized the need of the concept for high selective agonist and antagonist that are needed to be used in clinical application for disorders resulting from muscarinic aberrations.

The definition of antagonist affinities for the five muscarinic receptors has been aided greatly by the use of radioligand binding techniques, with ligands such as (^3H)pirenzepine and (^3H)N-methylscopolamine, in combination with membrane preparations from cells transfected with the gene for a particular receptor, and thereby expressing a single receptor subtype. Binding studies using two new antagonists, hexahydro-sila-difenidol (HHSiD) and its para-fluoro analogue (p-F-HHSiD), enabled researchers to distinguish between M_2 muscarinic binding sites in the heart and the glandular tissues (39). The heart M_2 receptor had a 70-fold lower affinity for p-F-HHSiD than for the ' M_2 ' glandular tissue receptor, which was

then found to be distinct from the M₂ subtype, and renamed M₃ mAChR. Recently two new highly selective M₂ antagonists that displays high selectivity between M₁ and M₄ subtypes has been developed (64).

Further studies have lead to more selective antagonist being synthesized including the M₂ preferential antagonist methoctramine, the M₃ antagonist 4-DAMP and its irreversible analogue 4-DAMP-mustard (65, 66, 67, 68). In addition two new snake toxins MT3 and MT7 which show high selectivity for muscarinic subtypes M₄ and M₁ respectively have been discovered (39). In another antagonist binding profile study done using a transformed Chinese hamster ovary cell line (CHO-K1) individually expressing the various muscarinic receptors it was observed that the 'M₃-selective' agent p-F-HHSiD (69, 70) showed similar affinities for M₁, M₃ and M₄ receptors, which were up to 9-fold higher than those found for M₂ and M₅ receptors. All five M₂-selective muscarinic antagonists employed in the study (methoctramine, himbacine, AF-DX 384, AQ-RA 741 and AF-DX 250) bound with high affinities to both M₂ and M₄ receptors and intermediate affinities for M₁ and M₃ receptors, with the exception of himbacine which showed about a 10-fold higher affinity for M₂/M₄ than for M₁ receptor (71).

Antagonist affinity constants (log affinity constants or pK_B values) for mammalian muscarinic receptors. Various selective muscarinic acetylcholine receptor antagonists are shown including their pK_B values. Data are from a variety of mammalian species, including human. Values are adapted from Caulfield and Birdsall (1998).

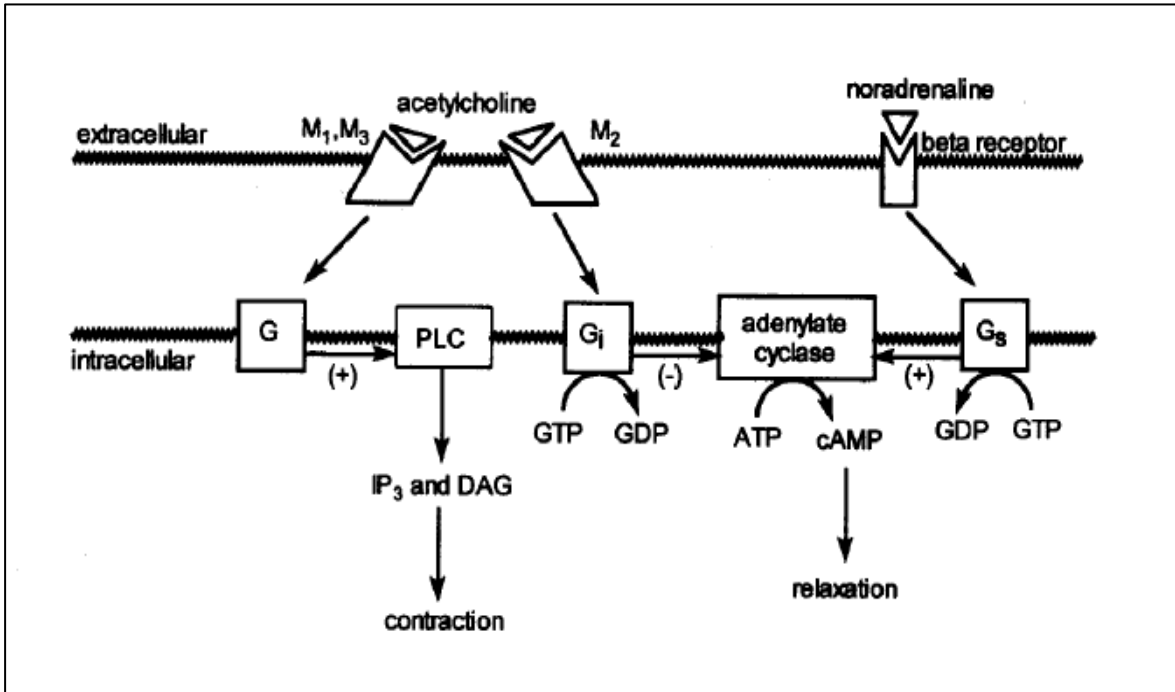
Antagonist	M ₁	M ₂	M ₃	M ₄	M ₅
Atropine	9.0-9.7	9.0-9.3	8.9-9.8	9.1-9.6	8.9-9.7
Pirenzepine	7.8-8.5	6.3-6.7	6.7-7.1	7.1-8.1	6.2-7.1
Methoctramine	7.1-7.8	7.8-8.3	6.3-6.9	7.4-8.1	6.9-7.2
4-DAMP	8.6-9.2	7.8-8.4	8.9-9.3	8.4-9.4	8.9-9.0
Himbacine	7.0-7.2	8.0-8.3	6.9-7.4	8.0-8.8	6.1-6.3
AF-DX 384	7.3-7.5	8.2-9.0	7.2-7.8	8.0-8.7	6.3
MT3	7.1	<6	<6	8.7	<6
MT7	9.8	<6	<6	<6	<6

1.4 Muscarinic Coupling to G-proteins and Effector Molecules

Similar to most seven transmembrane receptors, the mAChRs are coupled to G-proteins that can transduce the exterior signal in this case the binding of Ach to the mAChR and the receptor's subsequent activation, into an intracellular signal governed by specific second messenger cascade that cause many cellular responses. The link between the receptors and the effectors is in many cases mediated by the heterotrimeric G-proteins. G-protein transduced cellular responses include biochemical activities, metabolic changes, enzyme activation/deactivation, downstream gene transcription, protein synthesis, cell division and cell motility. The heterotrimeric G-proteins are composed of one α -, β - and γ - subunits each and are classified on the basis of their α -subunits. More than twenty different α -, five β - and ten γ -subunits have been identified at present, but based on primary sequence homology of the five α -subunits. G-proteins have been subdivided into four families: $G\alpha_s$, $G\alpha_{i/o}$, $G\alpha_q$, and $G\alpha_{12}$ (72, 73). G-proteins shift between their active and inactive state by binding to GTP or GDP nucleotide. When bound to the GTP nucleotide, G-protein is in its active stable state where it can activate directly diverse effector molecules. The G-proteins possess an intrinsic GTPase function in the α -subunit which hydrolyses

GTP to GDP, and thus induces the GDP binding inactive form. At this inactive stage the α -subunit associates with the $\beta\gamma$ -subunit. The stimulation of the muscarinic receptor induces the exchange of the GDP to GTP at the α -subunit. The binding of GTP results in the dissociation of the α -subunit and the $\beta\gamma$ -complex, as a result both subunits can activate their own specific signals and events. Most cellular effects which have been described to be elicited by muscarinic receptors involve the α -subunit and the different α -subunits of the G-proteins are known to mediate distinct cellular signaling by coupling differentially with the different muscarinic receptors. The odd numbered muscarinic receptor subtypes, $M_1/M_3/M_5$, are coupled to the PTX-insensitive $G\alpha_q$ protein, while the even numbered subtypes of muscarinic receptors M_2/M_4 coupled to the PTX-sensitive $G\alpha_{i/o}$ protein (Figure 1). Recently many $\beta\gamma$ -subunits have been identified playing a functional role in the transduction of muscarinic signals eliciting more investigations in their structure and functions (74). The agonist-induced receptor phosphorylation by G-protein receptor kinases (75, 76) by this controlling of the functional state of the receptors, targeting of ion channels, phospholipase C_β , some isoforms of adenylyl cyclase or phosphoinositide-3-kinase and through this the MAP kinase cascade have been attributed to the functional $\beta\gamma$ -subunit of the G-proteins.

Figure 1 Schematic representation of signal transduction via G-protein coupled receptors in smooth muscle cells. M₁, M₂ and M₃ muscarinic receptors, PLC phospholipase C, DAG diacylglycerol, IP₃ inositol 1,4,5-triphosphate. (adapted after revision from Eglen RM et al 1994)



1.4.1 Adenylyl Cyclase

The decrease in the adenylyl cyclase activity induced by muscarinic receptor activation has been well documented (44). The expression of the M₂ and M₄ receptors in cell lines displayed coupling to adenylyl cyclase inhibition (44, 64, 77, 78, 79, 80). In addition, G-protein reconstitution experiments showed that the G_i subtype coupled to the muscarinic acetylcholine receptors is responsible for this response (81). Adenylyl cyclase catalyzes the breakdown of ATP into cAMP, which in turn can activate cAMP-dependent protein kinases (PKA). Some studies have shown that the expressed M₁ subtype can weakly couple to adenylyl cyclase inhibition through a PTX-sensitive mechanism like in RAT-1 cells (82), while on the other hand previous reports have shown that the endogenous M₃ subtype can cause an accumulation of cAMP in several other cell types (83, 84, 85). Also the $\beta\gamma$ -subunits of the G-proteins coupled to the M₁ and the M₅ muscarinic receptors can also weakly stimulate adenylyl cyclase (86, 87). The

coupling of muscarinic receptors to adenylyl cyclase activation can also be regulated through calcium and protein kinase mechanisms (88, 89). cAMP production may occur through calcium/calmodulin sensitive (type I and type III) or insensitive (type II, IV, V and VI) adenylyl cyclases. The adenylyl cyclase type coupled to the muscarinic receptors is dependent on the cell line in which they are expressed. Nevertheless, the accumulation of cAMP may actually be the result of muscarinic receptors mediated phosphodiesterase inhibition as observed in a variety of cell types (90).

1.4.2 Phospholipase C

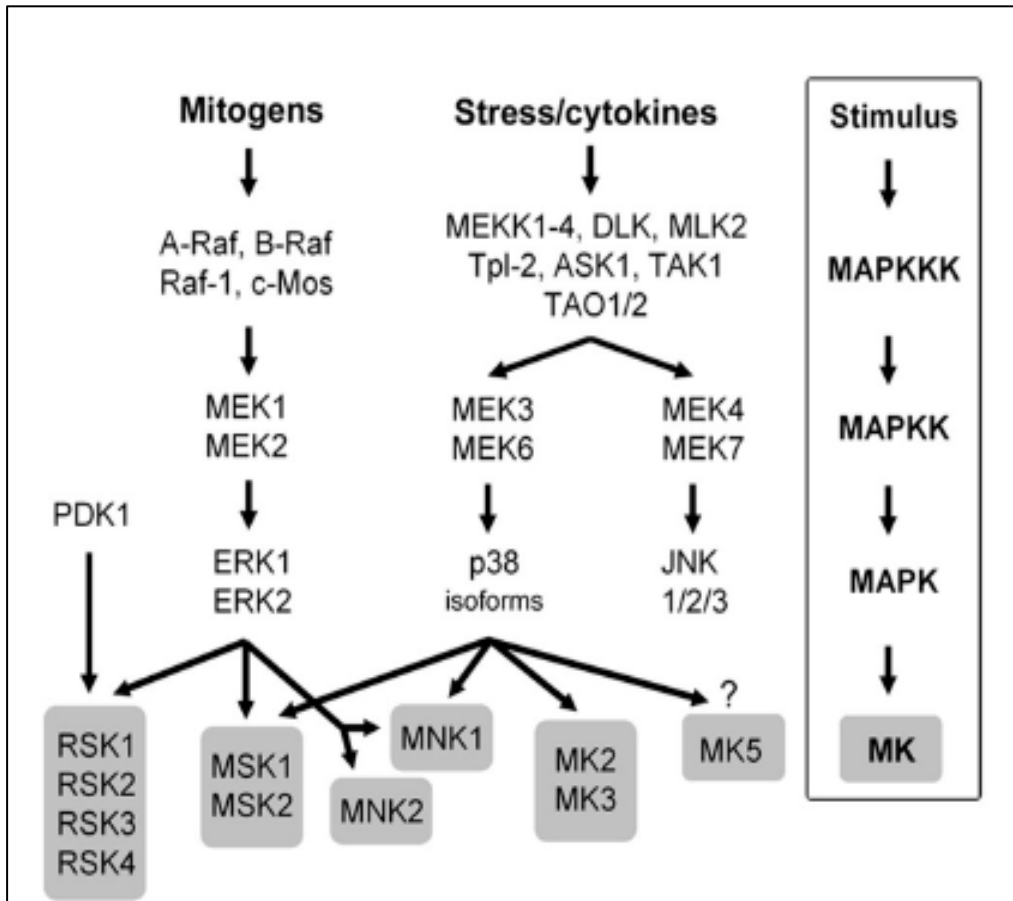
The phospholipid isoenzymes of particular interest with regard to muscarinic acetylcholine receptor signaling pathways are the phospholipases C, A and D (PLC, PLA and PLD). The family of PLC enzymes is grouped into three classes β , γ , and δ , with subtypes within each group (91). The receptor-mediated activation of the PLC lead to the hydrolysis of the phosphatidylinositol-4,5-bisphosphate (PIP₂) to inositol triphosphate (IP₃) and diacylglycerol (DAG), which in turn mediate the activation of intracellular calcium release and protein kinase C activation respectively. Phosphoinositide breakdown by acetylcholine has been well studied and linked to M₁/M₃/M₅ muscarinic receptors through the coupling of G_{q/11} protein, while M₂ and M₄ subtypes have been reported to weakly activate PLC (92). In the case of M₁ subtype, the phosphoinositide breakdown is mediated by PLC β ₁ through G_{q/11} alpha subunits (93, 94, 95). On the other hand, the M₅ subtype has been linked to the activation PLC β and PLC γ . PLC γ activation is normally stimulated by tyrosine kinase-dependent phosphorylation, a mechanism induced by M₅ mediated calcium influx that activates voltage-independent calcium channels and subsequent tyrosine kinase phosphorylation (96). However the M₂ subtype did not stimulate the phosphorylation of PLC γ or mediation of calcium influx. Later studies have shown, though, that the M₂ and M₄ receptors can also stimulate with lower efficiency phospholipase C through a PTX-sensitive G-protein, namely through G α ₂ and G α _{i3} (86, 97). Also $\beta\gamma$ -subunits were shown to couple M₂ receptors and phospholipase C β ₂ (98). In another

study it was observed that protein kinase C (PKC) seemed to play a regulatory role in the muscarinic acetylcholine receptor mediated accumulation of inositol triphosphate (99). IP₃ can act on its respective receptor in the endoplasmic reticulum (an IP₃-sensitive calcium channel), releasing calcium from its intracellular store, while DAG, can activate with cooperation of calcium and certain isoenzymes of PKC. PKC consist of three subgroups: the classical, which include α , β I, β II and γ isoenzymes that are activated by DAG and calcium, the novel, which include δ , ϵ , θ , η , μ , and are activated by DAG alone, the atypical, which include ζ , λ , L, and are independent of both calcium and DAG (100). It should be noted that certain isoenzymes are involved in stimulating proliferation (101), while others are involved in negatively regulating muscarinic acetylcholine receptor activity by phosphorylating sites on the i3 loop (60).

1.5 Mitogen Activated Protein Kinases

Mitogen-activated protein kinase (MAPK) pathways regulate diverse processes ranging from proliferation and differentiation to apoptosis. It is activated by both tyrosine kinase receptors as well as G-protein coupled receptors. The core of the MAPK cascade consists of an evolutionally conserved module of three sequentially activated protein kinases. The activation of the MAPK requires phosphorylation on conserved tyrosine and threonine residues localized to the so called activation loop, and is catalyzed by a dual specificity MAPK kinase (MAPKK). MAPKK, in turn, is under the control of a MAPKK kinase (MAPKKK), which in turn, is regulated by G-proteins and in some cases, by a MAPKKK kinase (MAPKKKK). Three of these modules are present in the mammalian cells: extracellular signal regulated kinases (ERK1 and ERK2) which are also known as p42^{MAPK} and p44^{MAPK}, N-terminal c-Jun kinases (JNKs) and p38MAPKs.

Figure II Schematic view of MAPK signaling pathways in mammalian cells.



ERKs, were the first to be cloned and their actions have been best examined in the context of growth factor signaling via receptor tyrosine kinases (RTKs). The archetypal ERK cascade involves the activation of small GTPase Ras upon agonist stimulation of the RTK receptors. This stimulation leads to the autophosphorylation of the RTK in tyrosine residues and recruitment of adaptor proteins bearing SH2 and SH3 motif (Shc and Grb2) that bind to an exchange factor for Ras, SOS. SOS allows nucleotide exchange dependent activation of the MAPKKK Raf-1. Raf-1 is a kinase with a serine/threonine specificity that catalyzes the activating phosphorylation of MEK1/2, which ultimately phosphorylates ERK1/2 on its activation loop (Figure II). Amplification via this signaling cascade is such that it is estimated that activation of solely 5% Ras molecules is sufficient to induce a full activation of ERKs (102). In resting cells, ERKs are anchored in the cytoplasm via association with MEK1/MEK2, but

following activation they dissociate from the cytoplasmatic anchoring complex and enter the nucleus, the site for signal termination (103).

The second group of MAPKs, JNK proteins, were first described as kinases that phosphorylate serine residues on the N-terminus c-Jun transcription factor following UV exposure. The third subgroup p38, were found to be activated in response to different forms of stress. Both JNK and p38 are given the more clarifying name SAPKs (stress activated protein kinases). Rho family members (Rho, Rac, Cdc42) are thought to be involved in SAPK activation in response to cytokines or cellular stress (104).

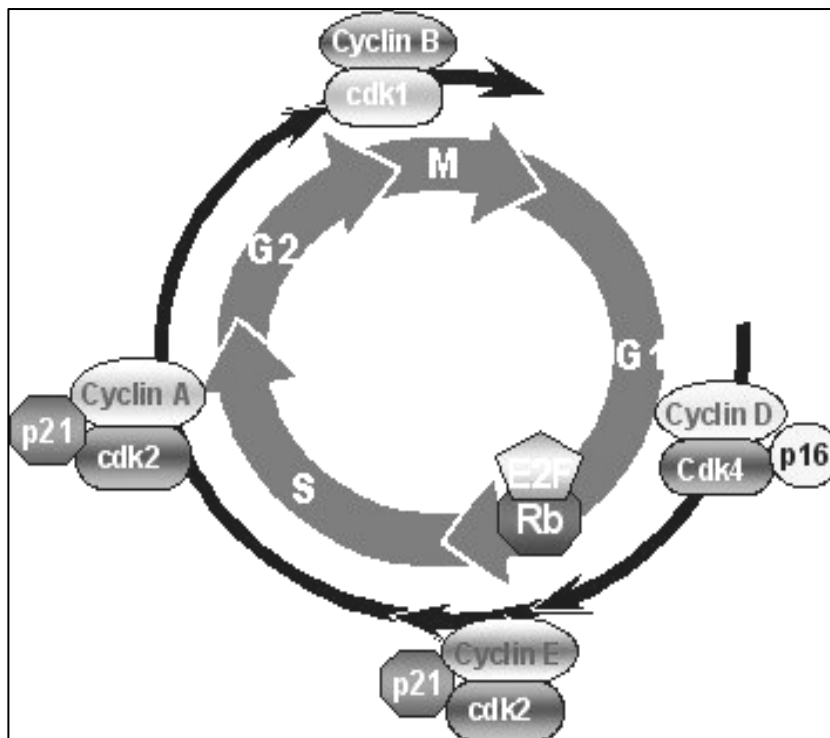
1.5.1 MAPKs in the Regulation of Cell Cycle

The cell cycle is controlled by a class of nuclear enzymes called cyclin-dependent kinases (CDKs), expressed constitutively but present in inactive form unless combined with their cyclin partners. The stimulatory effects of cyclins are counteracted by the inhibitory effects of CDK inhibitory proteins (CKIs), of which two families are well described: INK4 and Cip/Kip (p21) (105). Progression through G1 phase is especially affected by extracellular signals, and is regulated by CDK4/CycD, CDK6/CycD and CDK2/CycE complexes. Most studies indicate that integrins and growth factors, by activating MAPK pathways, typically control expression of Cyclin D1 and/or downregulate CKIs. In this regard, the activation of MAPK/ERK pathway has been linked to the induction of cyclin D1 transcription, since expression of dominant negative mutants of MEK and ERK prevented growth-factor dependent transcription of the Cyclin D1 gene (106). The formation of active CyclinD/CDK4 complex is considered rate-limiting for cell growth (107, 108). Recent studies indicate the critical determinant in the induction of Cyclin D1 is the duration of the ERK signal. Activation of ERK can be transient or sustained, depending on the stimulus. For example, serotonin induced a transient (10 min) stimulation of ERK in the CCL39 cells (Chinese hamster lung fibroblast cell line); while thrombin induced a far more sustained activation that peaks 3-4 hours after addition to cells (109). Some studies have observed a correlation between the strength of the mitogenic signaling and the

duration of ERK stimulation. While non-mitogenic factors induce a transient activation of ERKs (less than 15 mins) that does not lead to cell cycle entry, mitogens induce cell proliferation and sustained ERK activation (up to 6 hrs) (110).

From these studies, an important link between MEK/ERK pathway and cell cycle machinery was established, and furthermore, that sustained ERK activation was a common characteristic elicited by mitogens that would permit entry and progression through G1 phase of cell cycle (Figure III)

Figure III Cell cycle progression. ERKs phosphorylates transcription factors turning on the expression of target genes, including Cyclin D (CycD). Association of CycD with its cyclin dependent kinase partners (CDKs), results in phosphorylation of retinoblastoma protein (pRB). Its phosphorylation is required for progression through G1 phase of cell cycle. Other Cyclin/CDKs complexes (CycE/CDK2, CycA/CDK2) are required for progression through late G1 and S phases.



1.6 G-protein Coupled Receptor Signaling to MAPK

Activation of MAPKs mediated by G-protein-coupled receptors has been extensively studied, including investigation on bombesin, endothelin-1, adrenaline, somatostatin, thromboxane A₂, and muscarinic receptors. These receptors have been shown to couple to PTX-sensitive and PTX-insensitive G-proteins, thus signaling to MAPK using both G-proteins (G_{i/o} and G_{q/11}). To study the mechanism of activation of MAPK by G-protein-coupled receptors such as muscarinic acetylcholine receptors, transfected cell lines that express p^{42mapk} (labeled as MAPK in this text) together with muscarinic acetylcholine receptor subtypes were used (111). In transfected cell lines like COS-7 carbachol stimulation increased MAPK activity in a concentration dependent manner through M₁ and M₂ subtypes (112), whereby the M₁ mediated activation was PTX-insensitive, while the M₂ mediated activation displayed PTX-sensitivity. To elucidate the role of the α -subunits of G-proteins, studies were performed in transfected cells expressing wild-type or activated G-protein α -subunits, including G α_q and G α_{i2} which couple M₁ and M₂ subtypes respectively. However, these transfected cells did not exhibit elevated MAPK phosphorylating activity. As a result leading to speculations of molecules in addition to α -subunits of G-proteins playing a role in M₁ and M₂ mediated MAPK activation.

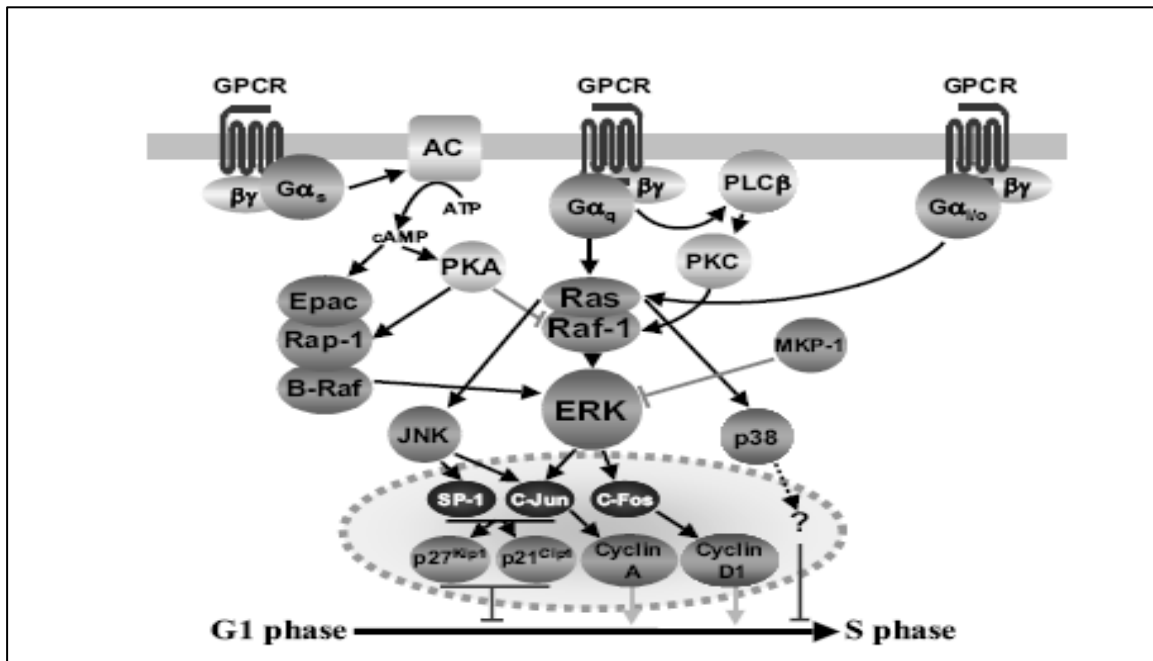
Recently available evidence has supported an active role for the G $\beta\gamma$ complex in signal transduction (113). Since α -subunits did not stimulate the activation of MAPK, studies investigating the role of G $\beta\gamma$ -subunits were performed. Indeed, transfecting cells with β_1 and γ_2 subunits and MAPK effectively elevated its phosphorylating activity demonstrating that the $\beta\gamma$ heterodimers directly elicits biochemical pathways leading to MAPK activation. Also, sequestration studies performed on $\beta\gamma$ complexes by overexpressing G α_i proteins abolished the M₂ and $\beta\gamma$ -mediated activation of MAPK, and reduced this response when elicited by M₁ stimulation. Therefore, these results indicate that M₁ signaling to MAPK involves $\beta\gamma$ -dependent and independent pathways; while M₂ mediated activation of MAPK appears to be strictly dependent on G $\beta\gamma$.

Mutant-Ras studies were performed to investigate whether signaling from M_1 and M_2 receptors or $\beta\gamma$ dimmers involves $p21^{ras}$ (Ras). These studies have shown that mutant Ras expression abolished the elevated MAPK activity in response to M_1 , M_2 and $\beta\gamma$ dimer overexpression (114, 115). Similar studies were done to elucidate the role of PKC, and the results suggested that signaling from M_1 receptors to MAPK involves a PKC-dependent and PKC-independent pathway, and both pathways converge at Ras. The PKC-independent pathway is mediated by the $G_{\beta\gamma}$ complex. On the other hand the M_2 -mediated MAPK activation is PKC-independent, and involves $G_{i\beta\gamma}$ dimmers, acting on a Ras-dependent pathway.

1.7 Intracellular Signaling Pathways Linking G-protein Coupled Receptors to MAPK

Activation of a given type of G-protein-coupled receptor (GPCR) triggers a limited set of signaling events in a very rapid and specific manner. The classical paradigm of GPCR signaling was rather linear and sequential. Emerging evidence, however, has revealed that this is only a part of the complex signaling mediated by GPCR. Propagation of GPCR signaling involves cross-regulation of many but specific pathways; including cross-talk between different GPCRs as well as with other signaling pathways and that the MAPK activation appears to be a common point of convergence for most of these pathways (Figure IV). A few of these signaling cascades relevant to the present study will be elucidated in this paper.

Figure IV GPCR mediated activation of MAPK regulated by generation of intracellular second messengers. GPCR activity leads to AC/cAMP (Adenylyl cyclase/cyclic adenosine monophosphate), and PLC β /PKC (Phospholipase C/Protein kinase C) second messenger pathways. cAMP directly, or via PKA (Protein kinase A), activates RAP-1/B-Raf/ERK pathway, and potentially inhibits Raf-1 activated ERK activity. The G α_q /PLC β /PKC promotes Ras/Raf-1/ERK activity, and it is likely that G α_q and G $\alpha_{i/o}$ coupled GPCRs can activate JNKs and p38. The result of the interplay between these pathways is either proliferative or antiproliferative, depending on the expression of GPCRs and signaling intermediates. Dashed indicators identify the probable involvement of multiple, unidentified intermediates. (New and Wong 2007)



1.7.1 The Ras Mediated Activation of MAPK Cascade via G-protein Coupled Receptors

Ras belongs to the family of small GTPases which exhibit high-affinity binding for GDP and GTP, and possess low intrinsic GTP hydrolysis and GDP/GTP exchange activities. The GDP/GTP cycling is controlled by two main classes of regulatory protein. Guanine-nucleotide-exchange factors (GEFs) promote formation of the active GTP-bound form (116), whereas GTPase-activating proteins (GAPs) accelerate the intrinsic GTPase activity to promote the formation of the inactive GDP-bound form. A second important biochemical feature of Ras proteins is their post-translational modification by lipids. The Ras proteins

terminate with a C-terminal CAAX (C=cysteine, A=aliphatic, X=any amino acid) tetrapeptide sequence (117). This motif, when coupled together with residues immediately upstream (e.g. cysteine residues modified by the fatty acid palmitate), comprises the membrane-targeting sequences that dictate interactions with distinct membrane compartments and subcellular locations. The CAAX motif is the recognition sequence for farnesyltransferase and geranylgeranyltransferase, which catalyze the covalent addition of a farnesyl or geranylgeranyl isoprenoid, respectively, to the cysteine residue of the tetrapeptide motif. These modifications are essential for facilitating membrane association and subcellular localization critical for biological activities. Ras proteins serve as signaling nodes activated in response to diverse extracellular stimuli. Activated Ras interacts with multiple, catalytically distinct downstream effectors, which regulate cytoplasmic signaling networks that control gene expression and regulation of cell proliferation, differentiation, and survival.

Lysophosphatidic acid (LPA) and thrombin were the first GPCR agonists shown to rapidly stimulate Ras-GTP accumulation in quiescent mammalian cells (118). However the best characterized Ras signaling pathway is activation of Ras by the epidermal growth factor receptor tyrosine kinase through the RasGEF Sos (119). Activated Ras binds to and promotes the translocation of the Raf serine/threonine kinase to the plasma membrane, where additional phosphorylation events promotes full Raf kinase activation. Raf phosphorylates and activates MEK1/2 dual specificity protein kinase, which phosphorylates and activates the ERK1/2 mitogen-activated protein (MAP) kinase. Activated ERK translocates to the nucleus, where it phosphorylates transcription factors leading to gene transcription and cell cycle progression. In quiescent fibroblast it was seen that LPA mediated Ras activation via pertussis toxin sensitive G_i protein (118) and also in certain cell type's α_2 adrenergic receptors could similarly activate Ras via G_i protein hence suggesting that Ras activation might be a common event in the action of G_i -coupled receptors (120). Furthermore in Rat 1a fibroblasts cells expressing the pertussis toxin-sensitive G-protein α subunits α_{i2} and α_{i3} but not α_o , muscarinic M_2 receptor stimulation resulted in activation of

Ras-Raf-MAPK, implicating the involvement of the G_i protein in this pathway (121). Various studies have shown that $G\alpha_i$ directly binds to and inhibits adenylyl cyclase, thereby lowering cytosolic cAMP levels and since the rise of cAMP levels inhibits the Ras-MAPK pathway, apparently at the level of Ras-Raf interaction (122, 123) it is conceivable that a $G\alpha_i$ mediated fall in cAMP levels may positively influence Ras-Raf coupling.

The classic $G\alpha_q$ -PLC- Ca^{2+} /PKC pathway can also mediate MAPK activation, either via Ras or independent of Ras. Certain Ras specific GEFs can activate Ras in response to PLC-generated messengers such as Ca^{2+} and DAG, which bind directly to these GEFs (124, 125, 126, 127). In cells expressing these GEFs, Ras can thus be activated by PLC activation in a Grb2-Sos-independent manner. Furthermore several PKC isoenzymes can phosphorylate and activate c-Raf independently of Ras (128, 129). PKC activation by phorbol ester leads to Ras activation in COS epithelial cells and in neonatal myocytes (130, 131), but this pathway apparently does not function in fibroblasts (118).

Raf proteins are the conserved signaling module that transducer signals from the cell surface to the receptor wherein the Ras family of small G-proteins are the upstream regulators in several cell types. However, it has been shown that activation of MAPK cascade can occur through Ras-independent mechanisms involving Raf for example, in rat C6 glioma cells activation of the purinergic $P2Y_{AC}$ -receptor a GPCR, by using specific agonist activated MAPK through a G_i -RhoA-PKC-Raf-MEK-dependent but a Ras and Ca^{2+} independent cascade (132). Another mechanism that has been suggested in the Ras-independent activation of Raf involves the activation of C-Raf by p21-activated kinases (PAK). PAKs are serine/threonine specific kinases that bind to and are activated by, the membrane bound Rho-family GTPases Cdc42 and Rac, and it has been proposed that these kinases lead to C-Raf activation in a Rac/Cdc42-and phosphatidylinositol-3-kinase (PI3K)-dependent manner. Although the physiological significance of this PAK-mediated C-Raf activation is not established, the PAK-dependent Ras-independent route to C-Raf activation might have an important role in C-Raf activation by integrins or when microtubules are disrupted (133).

1.7.2 Rho Mediated Activation of MAPK Cascade via G-protein Coupled Receptors

Like Ras, Rho proteins also serve as key regulators of extracellular-stimulus-mediated signaling networks that regulate actin organization, cell cycle progression and gene expression (134). Twenty members have been identified, RhoA, Rac and Cdc42 being the best studied. The guanine-nucleotide-exchange factors (GEFs) and GTPase-activating proteins (GAPs) control the activation of the small GTPases Rho, Rac and Cdc42. Once activated the GTPases bind to a spectrum of effectors to stimulate downstream signaling. Rho kinase 1 (ROCK1) and ROCK2 are key Rho effectors that have multiple substrates. Most GPCR agonist that regulate actin cytoskeletal responses, smooth muscle contraction, gene transcription, and cell growth through Rho-dependent pathways can couple to more than a single class of heterotrimeric G-protein. For example LPA and thrombin elicit cellular responses through both pertussis toxin-sensitive and insensitive G-proteins. Furthermore GPCR agonists have been also shown to mediate Rho activation through the $G\alpha_q$ and $G\alpha_{12/13}$ subtypes of the G-protein family (135). GPCRs including the thrombin receptor in platelets and LPA receptors in Swiss 3T3 cells have been shown to activate PI3K, and studies using C3 exoenzyme indicates this requires Rho function (136, 137). It has been shown that M_1 and M_2 muscarinic receptor stimulation can lead to phosphorylation and activation of a serine/threonine protein kinase Akt/PKB (138). Akt/PKB (protein kinase B) is regulated through PI3K and synthesis of PIP2 and PIP3 (139). Thus it is possible that GPCRs utilize Rho to regulate this cell survival pathway. Various studies have demonstrated that Rho-dependent signaling is required for transformation by oncogenic Ras (140, 141, 142). However, while Rho activation is known to promote the development of stress fibers and focal contact, Ras-transformed fibroblast generally exhibit a loss of these structural elements characteristic of Rho activity. These results have lead to the interpretation that Rho activity may be reduced in Ras-transformed cells. Accordingly, activated Rho can restore stress fibers in Ras transformed Rat1 fibroblasts, suggesting that Rho can be inactivated in these Ras-transformed

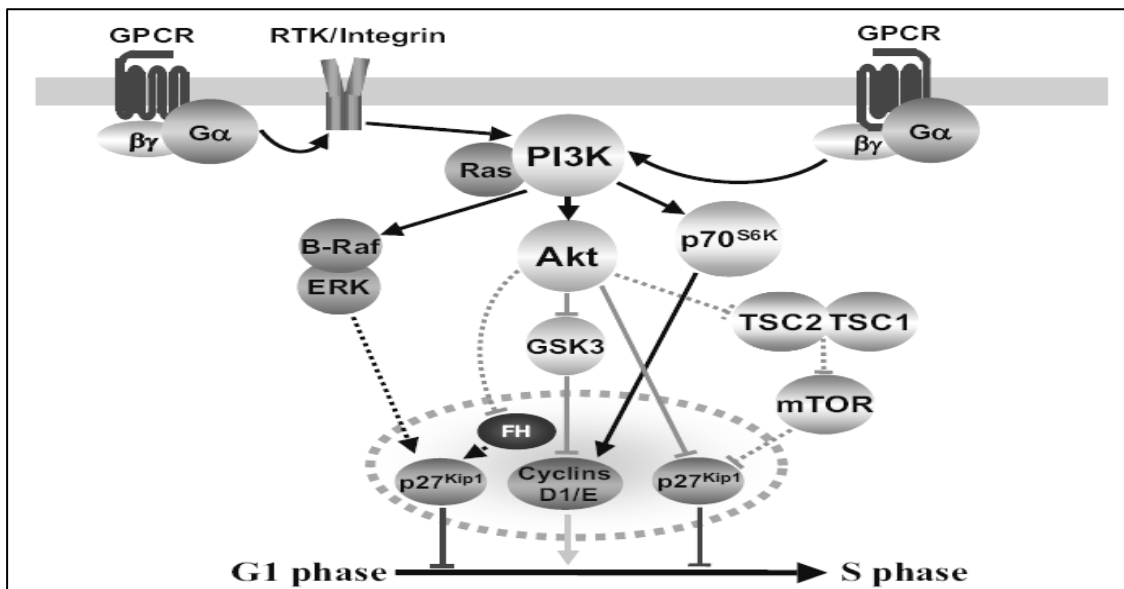
cells (143). By contrast, inhibition of Rho kinase was shown to block Ras transformation in NIH3T3 cells (144) and to attenuate invasive tumor cells (145). In another study done on vascular smooth muscle cells (VSMC) from rat aorta it was seen that thrombin stimulated DNA synthesis and migration were inhibited by exoenzyme C3 and Y27632 a Rho kinase inhibitor. Although thrombin activates RhoA, and Rho is necessary for thrombin-stimulated DNA synthesis in rat aortic VSM, adenoviral transfection of cells with activated RhoA was found not to be sufficient to induce DNA synthesis. Rather, for mitogenic signaling in VSMC, it appears that RhoA collaborates synergistically with Ras, such that DNA synthesis is activated only by agonists that stimulate both pathways (146). This supports studies indicating that activation of Rho is critical for Ras-induced cell cycle progression. Thus the relationship between Ras and Rho dependent signaling pathways during transformation is still unclear. A role for Rho in regulating cell proliferation was first suggested by studies in which it was demonstrated that C3 mediated inhibition of Rho caused fibroblasts to arrest in the G1 phase of the cell cycle (147). One downstream effect of Rho is to reduce expression of cell cycle inhibitor such as the cyclin-dependent kinase inhibitors p21^{Waf1/Cip1} and p27^{Kip1} in studies done on rat aortic VSMC it was demonstrated that adenoviral expression of a constitutively active form of RhoA reduced p27^{Kip1} protein levels. Direct activation of Rho with cytotoxic necrotizing factor-1 also decreases p27^{Kip1} and increases DNA synthesis in human smooth muscle cells (148). In another study it was shown that serotonin stimulation of bovine pulmonary artery VSMC leads to translocation of ERK to the nucleus, and this response is inhibited by treatment with either dominant negative RhoA or the Rho kinase inhibitor Y27632 (149). Furthermore it was reported that cyclin D1 expression is deregulated through a RhoA dependent mechanism that influences human lung fibroblast proliferation.

1.7.3 Phosphatidylinositol 3-Kinase (PI3K) Mediated Activation of MAPK Cascade via G-protein Coupled Receptors

Phosphoinositides (PIs) are rare lipids. Phosphoinositide 3-kinases (PI3Ks) are a family of related enzymes that are capable of phosphorylating the 3 position hydroxyl group of the inositol ring of phosphatidylinositol (PtdIns). PI3Ks are structurally diverse enzymes divided into three main classes. Each class exhibits distinct substrate specificity. Class IA PI3-kinases is a cytosolic heterodimer composed of a 110-kDa (p110 α , - β , or - δ) catalytic subunit and an 85-kDa (p85) adaptor protein. In response to growth factors stimulation, class IA PI3-kinases complex with activated receptor protein tyrosine kinases (through SH2 domains of the p85 subunit) or tyrosine-phosphorylated proteins. The class IB PI3-kinases- γ does not have an adaptor protein but instead is activated by the G $\beta\gamma$ subunits of the G-proteins (150). Class II PI3-kinases contain a COOH-terminal C2 domain that appears involved in regulation of this class by phospholipid and calcium (151). Recently Class III PI3-kinases have been also identified. It has been shown that receptor tyrosine kinase (RTK) and GPCR both can activate class I PI3Ks via phosphorylation steps which leads, through an adaptor molecule, to the recruitment of PI3K to the membrane. Once activated and localized to the membrane, PI3K phosphorylates phosphoinositol lipids on the D3 position of the inositol ring generating PtdIns-3-phosphates (PtdIns-3,4-P₂ and PtdIns-3,4,5-P₃). These specialized lipids serve to recruit pleckstrin homology (PH) domain-containing proteins such as the serine-threonine kinase Akt (protein kinase B) and PDK1 (phosphoinositide-dependent kinase 1) to the plasma membrane. After recruitment to the membrane Akt is phosphorylated and consequently activated, by PDK. In turn, Akt phosphorylates multiple proteins on serine and threonine residues. Through phosphorylation of these targets, Akt carries out its role as a key regulator of a variety of critical cell functions including glucose metabolism, cell proliferation and survival. Besides being a downstream effector of PI3-kinases, Akt may also be activated in a PI3-kinase-independent manner. Studies have suggested that cAMP-elevating agents could activate AKT through protein kinase A (PKA), although these studies are disputed and the

mechanism of action is unclear. The PI3K dependent Akt activation is regulated through PTEN which acts as a phosphatase to dephosphorylate PtdIns (3,4,5)P3 back to PtdIns(3,4)P2. This removes the membrane-localization factor from the Akt signaling pathway thus inhibiting downstream pathways dependent on Akt activation.

Figure V Activation of PI3K-dependent cell cycle regulation. The expression, stability and activity of cyclin and CDK inhibitors are regulated by the activity of several PI3K-dependent pathways. Numerous GPCRs activate PI3K isoforms either through $G_{\beta\gamma}$ subunits or via receptor tyrosine kinase (RTK) and integrin transactivation. PI3Ks activate ERK and Akt, leading to the transcriptional regulation of $p27^{Kip1}$. In addition Akt phosphorylates $p27^{Kip1}$, thereby affecting its nuclear localization. Acting through TSC1, TSC2 and mTOR (mammalian target of rapamycin), Akt can negatively affect the stability of $p27^{Kip1}$, although GPCR regulation of proliferation through mTOR has not been established (indicated by dashed line). PI3Ks may also promote proliferation by promoting cyclin expression (via $p70^{S6K}$). (New and Wong 2007)



Following direct or indirect GPCR-induced PI3K activation, cell cycle progression is regulated by the effects of PI3K activated kinases on the expression and stability of cell cycle proteins, or by the modulation of the activity of other signal transduction pathways (Figure V). For example, thrombin receptor activation in vascular smooth muscle cells lead to reduced levels of $p27^{Kip1}$ and increased proliferation (152), while in embryonic fibroblast the evidence suggests that

thrombin receptor activation of PI3K/Akt pathways promotes cyclin D1 accumulation, cyclin D1-CDK4 activity and cell cycle progression (153, 154). Furthermore, it has been postulated that thrombin receptor activation of ERK ultimately leads to enhanced translocation of CDK2 into the nucleus and fibroblast proliferation (155). In another study overexpression of phosphoinositide 3-kinase γ (PI3K γ) in COS-7 cells expressing M₂ muscarinic receptors, agonist induced G $\beta\gamma$ -subunit dependent MAPK activation via transactivation of tyrosine kinase receptors in a Sch-Grb2-Sos-Ras-Raf-MAPK manner. Expression of a catalytically inactive mutant of PI3K γ abolished this stimulation of MAPK by the G $\beta\gamma$ or in response to stimulation of muscarinic M₂ G-protein-coupled receptors. Indicating that, PI3K γ mediated G $\beta\gamma$ -dependent regulation of the MAPK signaling pathway (156).

1.7.4 Phospholipase C (PLC) Mediated Activation of MAPK Cascade via G-protein Coupled Receptors

The receptor-mediated activation of the PLC lead to the hydrolysis of the phosphatidylinositol-4,5-bisphosphate (PIP₂) to inositol triphosphate (IP₃) and diacylglycerol (DAG), which in turn mediate the activation of intracellular calcium release and protein kinase C activation respectively. Phospholipase C (PLC) is the principal effector of Gq-mediated signaling. Eleven different isoforms of PLC exist and exhibit distinct patterns of regulation; members of the PLC β subfamily tend to mediate the actions of activated Gq (157). It has been shown that activation of PKC isoforms by Gq/11-dependent regulation of phospholipase C β can also lead to MAPK activation through both Ras-dependent and Ras-independent mechanisms. In another study it was demonstrated that PKC α can apparently activate Raf-1 by direct phosphorylation thus activating the MAPK cascade (158). In cells of neuronal origin, Gq/11-dependent activation of the calcium and focal-adhesion-dependent focal adhesion kinase family member Pyk2, leads to Ras-dependent ERK activation (159). In this system, intracellular calcium, released as a result of PLC β -mediated inositol triphosphate production, triggers Pyk2 autophosphorylation, recruitment of nonreceptor tyrosine kinase c-

Src, tyrosine phosphorylation of Sch, and Ras-dependent ERK activation (160, 161). Activation of ERK1/2 by M₁, M₃ and M₅ muscarinic receptors typically involves PKC activation following Gq/11 activation of the PLC pathway with production of DAG. For example, in human neuroblastoma SK-N-BE2(C) cells activation of ERK1/2 by M₃ muscarinic receptors was dependent on PKC ϵ as well as the guanine nucleotide exchange factor, Ras and the Raf family of serine-threonine kinases (162).

1.8 Transactivation of Classical Receptor Tyrosine Kinases by GPCRs

Receptor transactivation refers to the ability of a primary agonist, via binding to its receptor, to activate a receptor for another ligand via signaling events. Transactivation of various growth factor receptors, including the epidermal growth factor receptor (EGFR), and the platelet derived growth factor (PDGF), by G-protein-coupled receptors has been documented in multiple cellular model systems (163, 164, 165, 166, 167). Receptor transactivation can potentially occur through several different mechanisms. One mechanism is through activation of intracellular protein tyrosine kinase, such as c-Src and PKC (168, 169), which can phosphorylate the growth factor receptor and thereby promote its activation. GPCR-induced transactivation of the EGFRs has been studied in some detail. GPCR activation leads to cleavage of the pro-EGF (eg pro-heparin-binding-EGF) ligands from the membrane initiating the transactivation (168, 170, 171). Proteolysis of the HB-EGF precursor is thought to be mediated by members of the ADAM family of matrix metalloproteases (MMPs) (172). The step that is stimulated by GPCRs has not been identified. EGFR transactivation has been shown to occur primarily through shedding of HB-EGF from the membrane (173, 174). Transactivation of EGFR results in intracellular signaling that leads to growth, proliferation, and migration. In fibroblasts, both G_{i/o}-coupled and G_{q/11}-coupled receptors have been shown to stimulate HB-EGF release. For G_{i/o}-coupled receptor, such as the LPA (112), α 2A adrenergic (175) and M₂ muscarinic acetylcholine receptors (176), HB-EGF shedding and EGFR transactivation are mediated by the G $\beta\gamma$ subunits of the heterotrimeric G-proteins

(177). HB-EGF shedding in response to stimulation of the $G_{q/11}$ -coupled receptors, such as endothelin-1 and α -thrombin receptors (178), mediated by the $G_{q/11}\alpha$ -subunits (179, 180). The G-protein effectors that regulate ectodomain shedding remain unidentified, although PI3Ks (156) and Src family nonreceptor tyrosine kinases have each been proposed as early intermediates in the EGFR transactivation pathway (177, 181).

1.9 Apoptosis and G-protein Coupled Receptor Signaling Interaction

Apoptosis is defined as a genetically controlled mechanism of cell death involved in the regulation of tissue homeostasis and morphologically characterized by cell shrinkage, membrane remodeling and blebbing, chromatin condensation and DNA and cellular fragmentation into apoptotic bodies. Pro-apoptotic signaling may be mediated by the specific ligands and surface receptors, which are capable of delivering death signal from the microenvironment and can activate the execution of apoptosis in the cell cytoplasm and organelles. Apoptosis can also be activated from inside the cell through specific cell sensors residing in the cell nucleus and cytoplasm. Both these pathways of apoptosis signaling converge into a common pathway causing the activation of effectors termed caspases (182). Caspases are a family of cysteine proteases that cleave their substrates at aspartic acid residues (183). They are hierarchically stratified into upstream initiator caspases, namely procaspases 8, 9, 10 and downstream the effector caspases 3, 6, 7, caspase-3 activity in particular is the common effector of most apoptotic pathways. Besides the caspases, members of the Bcl-2 protein family are also critical for the regulation of apoptosis. Both anti-apoptotic (BCL-2, Bcl-w, Bcl-xL) and pro-apoptotic (Bax, Bak, Bad) Bcl-2 family members have been identified (184). Studies have shown that ERK family of the MAPKK may also have anti-apoptotic effects when activated by the growth factor receptors. The proposed pathway for ligand binding to growth factor receptors initiating an anti-apoptotic signaling is via the activation of Raf which in turn activates ERK1/2 which could phosphorylate Bcl-2 in a manner that stabilizes its anti-apoptotic activity. Another mechanism is via the activation of Rsk, which phosphorylates

the pro-apoptotic protein Bad leading to its inactivation thus promoting cell survival.

The repertoire of signaling pathways controlled by GPCRs has recently been extended by studies linking GPCRs to the regulation of apoptosis. Depending on the receptor subtypes and the cell type in which the receptor is expressed, GPCRs can either induce apoptosis or protect cells from apoptotic stimuli. For example β 1-adrenergic receptors in cardiac myocytes can induce apoptosis through a G_s -mediated pathway, whereas β 2-adrenergic receptors in the same cell type can protect cells through a G_i -mediated mechanism (185). Prominent among the GPCRs that protect cells from apoptotic stimuli are the subtypes of the muscarinic receptor family (186, 187). Previous studies have also shown that muscarinic receptors that couple to the $G_{q/11}$ protein (e.g. M_1 , M_3 and M_5) can protect cells from apoptosis following DNA damage whereas those coupled to the G_i -proteins (M_2 and M_4) have no protective properties (188). In a study done using CH (Chinese-hamster ovary) cells it was shown that the M_3 muscarinic receptor anti-apoptotic effect is independent of calcium/phospholipase C signaling but proceeds in a manner that involves both gene transcription and the up-regulation of the anti-apoptotic Bcl-2 protein.

2 Materials and Methods

2.1 Materials

2.1.1 Reagents

Agarose	Serva Roth
BSA	Bio-Rad
Bromophenol blue	Sigma-Aldrich
Chemiluminescence Blotting Substrate (POD)	Bio-Rad
Disodium hydrogen orthophosphate (Na ₂ HPO ₄)	Merck
Desoxynucleotide mixture	Sigma-Aldrich
DNA Smart-Ladder	Eurogene Tech
Developing Solution	Sigma-Aldrich
ECL Detection Kit	Boehringer Ingelheim
Ethidium Bromide	Sigma-Aldrich
Ficoll 400, Type 400	Sigma-Aldrich
Fixing Solution	Sigma-Aldrich
Fetal Calf Serum (FCS)	Seromed
Kaleidoscope Marker	Sigma-Aldrich
Leupeptin	Sigma-Aldrich
Lowry Kit	Bio-Rad
Lumasafe scintillation cockt	Lumac
MEM Non Essential Amino Acids (100 x) = NEAA	PAA
β-Mercaptoethanol	Sigma-Aldrich
(Methyl- ³ H)-Thymidine 37 mBq/ml	PerkinElmer
Nonidet P-40	Sigma-Aldrich
Oligo dT-Primer	MWG-Biotech
Omniscript RT Kit:	Qiagen
Penicillin / Streptomycin solution (10000 U/ml / 10 mg/ml)	Sigma-Aldrich
Platelet derived growth factor = PDGF	Sigma-Aldrich
Pepstatin A	Sigma-Aldrich

Phenylmethylsulphonylfluoride (PMSF)	Sigma-Aldrich
Ponceau S	Boehringer Ingelheim
RNase-Free DNase Set	Qiagen
RNase Inhibitor RNasin Plus 40 U/μl	Promega
RNeasy Mini Kit	Qiagen
RNeasy Tissue Kit	Qiagen
Roti-Load 1	Roth
Sodium chloride (NaCl)	Roth
Sodium hydroxide pellets (NaOH)	Merck
Sodium Pyrovate Solution = SPS (100mM)	PAA
Streptomycin	Sigma-Aldrich
TaqDNA Polymerase 5 U/μl	Invitrogen
Trichloro-acetic acid crystals (TCA)	Merck
Tris (Tris-(hydroxymethyl-aminomethane)	Roth
Tris-HCl (Tris-(hydroxymethyl)-aminomethane hydrochloride)	Boehringer Ingelheim
Triton x-100	Boehringer Ingelheim
Trypthan Blue (0,4 %)	Sigma-Aldrich
Trypsin EDTA 10	Sigma-Aldrich
Tween 20	Sigma-Aldrich

2.1.2 Test Drugs

Atropine sulphate (10 mM) Sigma-Aldrich

Stock solution prepared in sterile water, further dilutions were done with sterile water

Actinomycin D (1 mg/ml) Sigma-Aldrich

Stock solution prepared in DMSO, further dilutions were carried out with sterile carried

AF-DX 384 (10 mM) Boehringer Ingelheim
(5,11-dihydro-11-[[2-[(2-[(dipropylamin)methyl]-1-piperidinyl]ethyl)amino]carbonyl]-6H-pyrido(2,3-β) (1,4)benzodiazepine-6-one methanesulfonate)
Stock solution prepared in sterile water, further dilutions were done with sterile water

AQ-RA 741 (10 mM) Boehringer Ingelheim
(11-({4-[4-(diethylamino)butyl]-1-piperidinyl}acetyl)-5,11-dihydro-6H-pyrido(2,3-β) (1,4)benzodiazepine-6-one hydrochloride)
Stock solution prepared in sterile water, further dilutions were done with sterile water

Carbachol (10 mM) Sigma-Aldrich
(Carbamylcholine chloride)
Stock solution prepared in sterile water, further dilutions were done with sterile water

Cycloheximide (1 mg/ml) Sigma-Aldrich
Stock solution prepared in sterile water, further dilutions were done with sterile water

4-DAMP (10 mM) Sigma-Aldrich
(4-diphenylacetoxy-N-methylpiperidine methoiodide)
Stock solution prepared in sterile water, further dilutions were carried out with sterile water

FTI-277 (10 mM) Calbiochem

(Methyl{N-[2-phenyl-4-N[2(R)-amino-3-mecaptopropylamino]benzoyl]}-methionate, TFA)

Stock solution prepared in DMSO, further dilutions were performed with sterile water

GW 5074 (20 mM) Tocris

(3-(3,5-Dibromo-4-hydroxy-benzylidene)-5-iodo-1,3-dihydro-indol-2-one)

Stock solution prepared in DMSO, further dilutions were done with sterile water

Himbacine (10 mM) Sigma-Aldrich

Stock solution prepared in ethanol, further dilutions were performed with sterile water

Hexamethonium Bromide (10 mM) Sigma-Aldrich

(Hexane-1,6-bis(trimethylammoniumbromide)N,N,N,N',N',N'-Hexamethylhexamethylenediammonium dibromide)

Stock solution prepared in sterile water, further dilutions were done with sterile water

Manumycin A (10 mM) Calbiochem

Stock solution prepared in DMSO, further dilutions were done with sterile water

Nicotine hydrogen tartrate salt (10 mM) Sigma-Aldrich

Stock solution prepared in sterile water, further dilutions were done with sterile water

Oxotremorine sesquifumerate (10 mM) Sigma-Aldrich

Stock solution prepared in sterile water, further dilutions were done with sterile water

PD-98059 (10 mM) Sigma-Aldrich

(2-(2'-amino-3'-methoxyphenyl)-oxanaphthalen-4-one)

Stock solution prepared in DMSO, further dilutions were done with serum-free medium for human lung fibroblast

Pirenzepine (10 mM) Boehringer Ingelheim

Stock solution prepared in sterile water, further dilutions were done with sterile water

PDGF (1 µg/ml) Sigma-Aldrich

Stock solution prepared with 4 mM HCl in 0.1% BSA further dilutions were done with the serum-free medium for human lung fibroblast

Pertussis Toxin (10 µg/ml) Sigma-Aldrich

Stock solution prepared in sterile water, further dilutions were done with sterile water

Tiotropium Bromide monohydrate (10 mM) Boehringer Ingelheim

Stock solution prepared in sterile water, further dilutions were performed with sterile water

TNF alpha Human recombinant (0.1 mg/ml) Sigma-Aldrich

Stock solution prepared in sterile water, further dilutions were done with sterile water

Tryphostin AG1295 (5 mM) Sigma-Aldrich

Stock solution prepared in DMSO, further dilutions were done with sterile water

U73122 (10 mM) Sigma-Aldrich

(1-[6-(((17β)-3-Methoxyestra-1,3,5[10]-trien-17-yl)amino)]-1H-pyrrole-2,5-dione)

Stock solution prepared in DMSO, further dilutions were done with sterile water

Wortmannin (10 mM) Calbiochem

Stock solution prepared in DMSO, further dilutions were done with sterile water

Y27632 (10 mM) Tocris

(trans-4-[(1R)-1-Aminoethyl]-N-4-pyridinylcyclohexanecarboxamide dihydrochloride)

Stock solution prepared in 1X PBS (sterile), further dilutions were done with sterile water

2.1.3 Buffers and Reagents for Cell Culture

Culture medium for human fibroblast without FCS

Basismedium EARLE`S MEM

Penicillin/Streptomycin 100 U/ml / 100 µg/ml

Non Essential Amino Acids = NEAA 1x

Sodium Pyrovate Solution = SPS 1 mM

Culture medium for human fibroblast with 10% FCS

Basismedium EARLE`S MEM

FCS 10% (v/v)

Penicillin/Streptomycin 100 U/ml / 100 µg/ml

Non Essential Amino Acids = NEAA 1x

Sodium Pyrovate Solution = SPS 1 mM

10x PBS (Phosphate buffered saline) pH 7.4-7.5

KCl 27 mM

KH₂PO₄ 15 mM

NaCl 1,38 M

Na₂HPO₄ x H₂O 81 mM

Distilled water

1x PBS-Buffer pH 7.4-7.5

10x PBS, 1:10 dilution with distilled water

1x Trypsin-EDTA-solution

10x Trypsin-EDTA, 1:10 dilution with 1x sterile PBS-Buffer

0.15% (w/v) Trypthan blue staining dye

0.4% Trypthan Blue Stain, 3:8 dilution with 1x PBS-Buffer

2.1.4 Solutions and Buffers for Proliferation Assay

10% Trichloro-acetic acid

Trichloro-acetic acid crystals 10% (w/v)

Distilled water

5% Trichloro-acetic acid

Trichloro-acetic acid crystals 5% (w/v)

Distilled water

0,1 N Sodium hydroxide

Sodium hydroxide pellets 0.1N

Distilled water

1 M Tris-HCl pH 7,4

Tris-HCl 1 M

Distilled water

Adjust to pH 7.4 with HCl

2.1.5 Reagents for Protein Determination using the Lowry method

BSA-Standard solution

BSA	4 mg/ml
0.1% Tris/Triton X100 solution	

1% Tris/TritonX100 solution

1 M Tris-HCl-solution pH 7.4	100 mM
Triton x-100	1% (v/v)
Distilled water	

Reagent A'

Reagent S	1% (v/v)
Starting Reagent A	99% (v/v)

RIPA Lysis Buffer

50 mM Tris-HCl pH 7.5
150 mM NaCl
0.5% Sodium deoxycholat
1% Nonidet P-40
0.1% SDS

Protein Lysis Buffer with Protease and Phosphatase Inhibitors

RIPA Lysis Buffer	
0.1 M EDTA pH 8	2 Mm
125 µg/ml Pepstatin A	0.7 µg/ml (1 µM)
100 mM PMSF	170 µg/ml (1 mM)
10 µg/ml Leupeptin	0.5 µg/ml (1 µM)
1.75 mM NaF	35 mM
20 mM Na ₃ VO ₄	1 mM

2.1.6 Primers for Polymerase Chain Reaction

The PCR for β actin were done using the oligonucleotide pair of β actin-s (Sigma-Aldrich) and h β actin-as (MWG Biotech). All the muscarinic and nicotinic receptor expression PCR's were carried out using primers provided by MWG Biotech.

Human

h β actin-s 5'-TTC TAC AAT GAG CTG CGT GTG GC-3'

Human

h β actin-as 5'-CTC GTC ATA CTC CTG CTT GC-3'

Human Muscarinic Receptor primers

hM₁-s 5'-CAG GCA ACC TGC TGG TAC TC-3'

hM₁-as 5'-CGT GCT CGG TTC TCT GTC TC-3'

hM₂-s 5'-CTC CTC TAA CAA TAG CCT GG-3'

hM₂-as 5'-GGC TCC TTC TTG TCC TTC TT-3'

hM₃-s 5'-GGA CAG AGG CAG AGA CAG AA-3'

hM₃-as 5'-GAA GGA CAG AGG TAG AGT GG-3'

hM₄-s 5'-ATC GCT ATG AGA CGG TGG AA-3'

hM₄-as 5'-GTT GGA CAG GAA CTG GAT GA-3'

hM₅-s 5'-ACC ACA ATG CAA CCA CCG TC-3'

hM₅-as 5'-ACA GCG CAA GCA GGA TCT GA-3'

Human Nicotinic Receptor primers

α_1 -hnAChR-s 5'-CAT CAA GTA CAT CGC AGA GA-3'

α_1 -hnAChR-as 5'-TTC TCT GCT CTG GTA GGT TC-3'

α_3 -hnAChR-s 5'-AGG CCA ACA AGC AAC GAG-3'

α_3 -hnAChR-as 5'-TTG CAG AAA CAA TCC TGC TG-3'

α_5 -hnAChR-s 5'-TCA ACA CAT AAT GCC ATG GC-3'

α_5 -hnAChR-as 5'-CCT CAC GGA CAT CAT TTT CC-3'

α_7 -hnAChR-s 5'-CTT CAC CAT CAT CTG CAC CAT C-3'

α_7 -hnAChR-as 5'-GGT ACG GAT GTG CCA AGG ATA T-3'

α_9 -hnAChR-s 5'-ATC CTG AAA TAC ATG TCC AGC G-3'

α_9 -hnAChR-as 5'-AAT CGG TCT ATG ACT TTC GCC-3'

β_1 -hnAChR-s 5'-TGT ACC TGC GTC TAA AAA GG-3'

β_1 -hnAChR-as 5'-TCA ACC CTC CAG TCT TC-3'

β_4 -hnAChR-s 5'-TGT GAG CAT TGG CCA TCA AC-3'

β_4 -hnAChR-as 5'-AAT GCC AAG CCT CTG AGC TG-3'

2.1.7 Buffers and Solutions for RT/PCR

DEPC-Water

DEPC

0.2% (v/v)

Sterile water

Oligonucleotide Primers

The oligonucleotide primer stocks were prepared with DEPC water to 100 μ M and further diluted in a 1:10 concentration with DEPC water to get a working 10 μ M concentration

Gelelectrophoresis

5x TBE-Buffer

Tris	0.45 M
Boric acid	0.44 M
EDTA	0.012 M
Distilled water	

Agarose-Gel 1.2%

Agarose	1.2%
0.5x TBE-Buffer	
Ethidium bromide solution (10 mg/ml)	5 μ l

Ethidiumbromide-solution 1%

Ethidiumbromide	1%
Distilled water	

PCR loading Buffer

Ficoll 400	15% (w/v)
1% Bromophenolblue-solution	0.25% (w/v)
5x TBE-Buffer	0.5x
Distilled water	

2.1.8 Human Lung Fibroblast Cells

MRC-5

MRC-5 human lung fibroblast cell line was developed from the lung of a 14 week old human fetus. The cumulative population doublings to senescence is 42-46. American Type Culture Collection number CCL-171.

Primary Human Lung Fibroblasts

Primary human lung fibroblasts (phLFb) were established from histologically normal areas of surgically resected lung tissue, which was obtained from lung cancer patients after thoracotomy. The protocol for obtaining human tissue was approved by the local ethics review board for human studies (Ethics Committee, Medical Faculty, University of Bonn, Bonn, Germany), and informed consent was obtained from the patient.

Primary human lung fibroblast cultures (phLFbOH.1, phLFb.4, phLFb.5, phLFb.6, phLFb.8, phLFb.9, phLFb.11, phLFb.12) were similarly established from histologically normal areas of surgically resected lung tissue from lung cancer patients wherein, phLFb.4, phLFb.6, phLFb.8, phLFb.11, phLFb.12 were from the central and phLFb.5, phLFb.9 were from the peripheral region of the lung.

2.1.9 Buffers and Reagents for Protein Gel Electrophoresis and Immunoblot

NuPAGE MOPS SDS Running Buffer 1X

NuPAGE MOPS SDS Running Buffer 20X	5% (v/v)
Distilled water	

Laemmli (Running) Buffer 5X

Tris	125 mM
Glycine	7.2%
SDS	5%
Distilled water	

Transfer Buffer

Tris	25 mM
Glycine	192 mM
Methanol	20% (v/v)
Distilled water	

Ponceau S solution

Ponceau S	0.2% (w/v)
Tris-HCl	3% (w/v)
Distilled water	

Tris Buffered Saline (TBS) solution pH 7.5

Tris	50 Mm
NaCl	150 mM
Distilled water	

TBST (TBS + Tween 20)

Tween 20	0.1% (v/v)
TBS	

5% Blocking solution

Dried milk powder	5 gm
Distilled water	100 ml

Chemiluminescence solution

Starting solution	1% (v/v)
Blotting substrate	

0.2% (w/v) Sodium Hydroxide solution

NaOH	0.2% (w/v)
Distilled water	

Developing solution

Developing stock solution	20% (v/v)
Distilled water	

Fixing solution

Fixing stock solution	20% (v/v)
Distilled water	

2.1.10 Antibodies

Anti-mAChR M2 (H-170)	Santa Cruz Biotechnology
Anti-mAChR M3 (H-210)	Santa Cruz Biotechnology
Anti-Phospho-p44/42	Cell Signaling Technology
Anti-ERK-2 IgG	Santa Cruz Biotechnology

2.1.11 Reagents and Solutions for Caspase-3 Fluorimetric Assay

Caspase-3 Fluorimetric Assay was performed using the kit provided by Sigma-Aldrich, all reagent stocks and working solutions were prepared as per the manufacturer's instructions with the materials provided along with the kit unless otherwise specified.

5X Lysis Buffer

HEPES	250 mM
(4-(2-hydroxyethyl)-1-piperazineethanesulphonicacid)	
CHAPS	25 mM
(3-[(3-Cholamidopropyl)dimethylammonio]-1-propanesulphonate)	
DTT	25 mM
((D, L)-1, 4-Dithiothreitol)	
pH adjusted to 7.4	

10X Assay Buffer

HEPES	200 mM
CHAPS	1%
DTT	50 mM
Ethylenediaminetetraacetic acid (EDTA)	20 mM
pH adjusted to 7.4	

1X Assay Buffer

10X Assay Buffer, 1:10 dilution with 17 megohm water

1X Lysis Buffer

5X Lysis Buffer, 1:5 dilution with 17 megohm water

1X Lysis Buffer with Protease Inhibitors

0.1 M EDTA pH 8	2 mM
125 µg/ml Pepstatin A	0.7 µg/ml
200 µg/ml Aprotinin	2 µg/ml
Volume made up with 1X Lysis Buffer	

Caspase-3 Substrate Solution

Caspase-3 Substrate (Ac-DEVD-AMC)	10 mM
DMSO	2.5 mg
	370 µl

Caspase-3 Inhibitor Solution

Caspase-3 Inhibitor (Ac-DEVD-CHO)	2 Mm
DMSO	0.5 mg
	500 µl

Caspase-3 Inhibitor Assay solution

Caspase-3 Inhibitor Solution, 1:10 dilution with 1X Assay Buffer	200 µM
--	--------

<u>Caspase-3 Positive Control Solution</u>	100 µg/ml
Caspase-3 Positive Control	5 µg
17 Megohm Water	50 µl

<u>Caspase-3 Positive Control Assay Solution</u>	1 µg/ml
Caspase-3 Positive Control Solution, 1:100 dilution with 1X Assay Buffer	

Reaction Mixture, 400 µl per reaction for 96 well plate assay

10 mM AC-DEVD-AMC	12.5 µl
1X Assay Buffer	7.5 ml

<u>7-Amino-4-methylcoumarin (AMC) Standard Solution</u>	10 mM
AMC	1 mg
DMSO	0.57 ml

2.1.12 Equipment

Mycycler Thermal Cycler System	Bio-Rad
Photometer	DU-64 spectrophotometer
Liquid Scintillation Analyzer	Tri-Carb2100 TR, Packard
Fluorescence Microplate Reader Fluorometer	Fluostar OPTIMA, BMG

2.1.13 Tools for Statistical Analysis

GraphPad Software

GraphPad InStat 3.01 program was used to calculate statistical significance of differences using ANOVA, followed by Dunnet's or Bonferroni's test. All values are mean±SEM of n experiments. A P value of < 0.05 was accepted as significant. All graphical representations were generated using the GraphPad Prism software.

Microsoft Excel 5.0 and Excel 97

This program was used for calculation of means and SEM's from individual experimental data and summarizing these values for a particular set.

RFLPscan 2.01

Optical density of bands from PCR and western blot experiments were semiquantitatively measured using the RFLPscan software.

2.2 Methods

2.2.1 Culture of Human Lung Fibroblast

The MRC-5 cell line was derived from normal lung tissue of a 14-week-old male fetus (189). Cryogenically preserved MRC-5 human lung fibroblast culture was thawed for 1 minute at room temperature followed by thawing at 37°C on a water bath. The contents of the vial were then transferred to 75 cm² pre-incubated culture flask containing human fibroblast medium supplemented with 10% FCS in a humidified incubator at 37°C and 5% CO₂. After 24 hours of incubation the medium was changed to remove the cryoprotective agent DMSO, to prevent cell damage. The cells were then allowed to grow, with the medium being changed twice per week. Upon confluence cells were passaged further.

For this purpose the cells were washed with warm sterile 1X PBS followed by addition of warm sterile 1X Trypsin/EDTA solution just enough to cover the cell surface to facilitate the detachment of the cell from the surface of the flask. Trypsin is a proteolytic enzyme which helps in breaking cell-cell adhesion whereas EDTA is a chelator that binds divalent cations such as calcium and magnesium present between the cells allowing trypsin access to the cell-cell and cell-substrate bonds. The cells were incubated for 45 seconds after which the trypsin was aspirated out. Then the cells were re-suspended in medium with 10% FCS and centrifuged at 1000RMP for 5 minutes. The supernatant was discarded and the cell pellet was re-suspended in the 10% FCS medium. Cell count was carried out using trypan blue (20µl of cell suspension plus 80µl of the stain) in a Neubauer counting chamber. Required amount of cells were seeded further in a 175 cm² culture flask with medium containing 10% FCS and an aliquot was re-suspended in a vial containing medium with 10% FCS and 5% DMSO and frozen to -80°C before being stored in liquid nitrogen.

Primary human lung fibroblasts were established from histologically normal areas of surgically resected lung tissue, which was obtained from lung cancer patients after thoracotomy. Tissue was sliced into tiny pieces, treated with pronase (1mg/ml) at 37°C for 30 minutes, placed in cell culture plates, and incubated in human fibroblast medium with 15% FCS. After 2 weeks, fibroblasts had grown

out from the tissue and were passaged by standard trypsinization protocol as mentioned in the case of MRC-5 cells.

2.2.2 RNA Preparation

Total RNA isolation was done using RNeasy tissue kit provided by Qiagen as per the manufacturer's instructions.

The RNeasy procedure for RNA purification combines the selective binding properties of a silica based membrane with the speed of microspin technology. A specialized high salt buffer system assists the binding of RNA to the silica based membrane.

Cells were seeded in a 55mm dish and grown to 85% confluence prior to being used for RNA isolation. The medium was aspirated out and the cell surface was washed with 1X PBS followed by addition of the RLT lysis buffer (350µl). The cell lysate was homogenized by centrifugation with the QIA shredder for 2 minutes at 13000 RPM and the filtrate was collected in 1.5ml Eppendorf tubes. Ethanol (70%) was added to the filtrate to provide appropriate binding conditions and the sample was then applied to an RNeasy spin column, centrifuged at 10000 RPM for 15 seconds. The flow-through was discarded and the spin column was placed on a new collection tube. The wash buffer RW1 (700µl) was added on the spin column and centrifuged for 15 seconds at 10000 RPM. The flow-through was discarded and the spin column was placed on a new collection tube. The muscarinic receptor genes are intronless, and contamination of RNA preparation by genomic DNA would cause false-positive PCR results; hence an additional DNase treatment step was carried out by adding 80µl DNase (10µl DNase + 70µl RDD buffer) on the spin column and incubating it at room temperature for 15 minutes. After incubation, the spin column was centrifuged and the flow-through discarded. Buffer RPE was added on the spin column and centrifuged at 10000 RPM for 15 seconds. The RPE buffer wash step was repeated with an extended centrifugation time for 2 minutes. The flow-through was discarded and the RNeasy column was spun dry at 10000 RPM for 15 seconds. The elution was

done using 40µl of RNase free water at 10000 RPM for 15 seconds twice to get a total volume of 80µl of eluate collected into a sterile tube.

The RNA concentration in the sample was measured photometrically at a wavelength of 260nm in a 1:40 dilution with RNase free water and the sample preparation was stored at -80°C.

Note: - All the steps involved in this protocol were performed in RNase free conditions using RNase free pipette tips to prevent degradation of the sample.

2.2.3 Reverse Transcription

Reverse transcription also known as “first strand reaction,” is a process wherein complementary DNA (cDNA) is made from an mRNA template using dNTP’s and an enzyme called reverse transcriptase.

RNA is susceptible to degradation hence care was taken to prevent any contamination by using RNase free pipette tips and all reactions were carried out on ice. Total RNA concentration was calculated and amount equivalent to 1µg of RNA was used as a starting template, making up the volume to 12.5µl with DEPC water. The RT-Master mix containing oligodT primer in a reverse transcriptase buffer was added to this probe making up the volume to 20µl/probe and incubated at 37°C for 1 hr. The reverse transcription was terminated by incubation at 93°C for 5 minutes. Following which the probes were centrifuged and 80µl of sterile water were added per probe. The synthesized cDNA were stored at -20°C or 5µl of this cDNA was used as template for further PCR reactions.

$A_{260\text{ nm}} \times 40 \times \text{Dilution Factor} = \text{RNA concentration in } \mu\text{g/ml}$

RT-Master-Mix

<u>Reagents</u>	<u>Quantity per probe</u>
10 µM Oligo dT-Primer	2 µl
5 mM dNTP-Mix	2 µl
10x RT-Buffer	2 µl
10 U/µl RNase Inhibitor RNasin Plus (1:4 dilution with 1x RT-Buffer)	0.5 µl
Omniscript Reverse Transcriptase	1 µl
Total volume	7.5µl

2.2.4 Polymerase Chain Reaction (PCR)

The polymerase chain reaction (PCR) is a technique for "amplifying" a specific DNA sequence.

To beware of any contamination all the apparatus used was autoclaved and sterile pipette tips were used. For the PCR 5µl of cDNA was used as the template mixed with the PCR-Master mix and run on a PCR thermal cycler set to the following parameters;

<u>Function</u>	<u>Temperature</u>	<u>Time</u>
Initial Denaturation	94°C	3 mins
23 -35 Cycles of:-		
-Denaturation	94°C	45 s
-Annealing	53°C to 60°C	30 s
-Elongation	72°C	1 min
Final Elongation	72°C	10 mins one time

PCR-Master-Mix

<u>Reagents</u>	<u>Quantity per probe</u>
Water	32.5µl
10X PCR Reaction Buffer	5 µl
50 mM MgCl ₂	1,5 µl
10 mM Desoxynucleotide-Mix	1 µl
10µM sense-Primer	2.5µl
10µM antisense-Primer	2.5µl
5 U/µl TaqDNA Polymerase	0,5 µl
Total volume	45µl

2.2.5 Agarose Gel-Electrophoresis

At the end of the PCR reaction 5µl of a PCR buffer was added per probe and mixed well with a pipette. For the purpose of electrophoresis, a 1.2% agarose gel was used and 30µl per probe was loaded onto the gel and run at a constant current of 72 mA for 1 hour. A 100bp DNA ladder was also loaded onto the gel as a marker. Then the gel was placed under UV light; causing the ethidium bromide intercalated into the DNA to fluoresce. Gel photos were taken using a digital camera. Optical density of bands was quantified by RFLPscan software, corrected for β-actin, and referred to the respective amplification of genomic DNA to normalize for variations in PCR effectiveness.

2.2.6 DNA Preparation

Genomic DNA from MRC-5 cell line was used as a positive control for the receptor expression studies carried out on human lung fibroblasts using polymerase chain reaction. The genomic DNA for this purpose was isolated using the DNeasy tissue kit provided by Qiagen as per the manufacturer's instructions. The basic principle involved here, is that the cells are lysed with Proteinase K which inactivates the DNases with the buffering conditions being adjusted to provide optimal DNA binding conditions when the lysate is loaded onto the DNeasy Mini spin column.

Cells in culture medium were centrifuged at 1750RPM for 5 minutes; the pellet was resuspended in 200µl of 1XPBS, 20µl of Proteinase K and 200µl Buffer AL. The reaction tube was mixed thoroughly by vortexing and then incubated at 70°C for 10 minutes. Ethanol 200µl (96%) was added to the sample and homogenized by vortexing. The homogenized sample was then pipetted into the DNeasy spin column placed in a 2ml collection tube and centrifuged at 800RPM for 1 minute. The flow-through was discarded and the spin column was placed on a new collection tube. Buffer AW1 (500 µl) was added and the tube was centrifuged at 800RPM for 1 minute. Then another wash step with Buffer AW2 was carried out at 14000RPM for 3 minutes to dry the DNeasy membrane. The DNeasy spin column was thereafter placed on a new 1.5ml microcentrifuge tube and 200µl of Buffer AE was added directly onto the DNeasy membrane, incubated for 1 minute at room temperature, and centrifuged at 8000RPM for 1 minute to elute. The DNA concentration was measured photometrically at 260nm.

2.2.7 Protein Preparation

Cells were seeded in 55mm culture dishes and grown in a humidified incubator at 37°C and 5% CO₂ with the last 24 hours under serum free conditions. Upon reaching 80-85% confluence the medium was aspirated out. The cells were then washed with 1XPBS (cold) and cellular proteins were extracted using 150-300µl (per dish) of the RIPA buffer (50mM Tris-HCl [pH 7.5], 150 mM NaCl, 0.5% sodium deoxycholat, 1% Nonidet P-40, 0-1% [wt/vol] SDS, 2mM EDTA [Ph 8.0]) containing protease inhibitors PMSF (1 mM), pepstatin A (0.7 µg/ml), leupeptin (0.5 µg/ml) and phosphatase inhibitors sodium fluoride (35 mM) and sodium orthovanadate (1 mM). Phosphatase inhibitors were added to lysis buffer in the case of protein extracts being immunoblotted to test for activated phospho-proteins. The cell suspension was then transferred to a sterile 1.5ml microcentrifuge tube and centrifuged at 14000RPM at 4°C for 15 minutes; the supernatant was used for total protein determination. Care was taken to perform all the above mentioned steps on ice to prevent sample degradation.

2.2.8 Protein Determination

Protein determination was carried out using the Protein Assay kit which is a colorimetric assay for protein concentration following detergent solubilization based on the reaction of protein with an alkaline copper tartrate solution, and the subsequent reduction of the Folin reagent by the copper treated protein giving rise to a characteristic blue colour which can be detected colorimetrically by absorbance at 750 nm.

For the assay 5 μ l of the supernatant previously extracted was mixed with 45 μ l of 0.1% Tris-Triton-X 100. Then 100 μ l of Working Reagent A' was added to the probe followed by 800 μ l of Reagent B. Similarly 50 μ l BSA standards in the concentrations of 50, 100, 300, 700, 1100 and 1500 μ g/ml in 0.1% Tris-Triton-X100 were mixed with 100 μ l of Working Reagent A' and 800 μ l of Reagent B was added to each probe. For the blank reading 5 μ l of the lysis buffer was treated in a similar fashion. The probes were later vortexed and incubated at room temperature for 15 minutes. The absorbance was measured spectrophotometrically at 750 nm, and a regression analysis was then performed with the help of the absorbance values obtained for the standards to calculate the concentration for the sample probe.

2.2.9 Protein Gel-Electrophoresis and Immunoblot

Protein gel electrophoresis was performed using the Novex Mini Cell along with the X Cell Sure Lock while the immunoblot was done using X Cell II Blot Module. The equipments required were provided by Invitrogen and experiments were performed as per the manufacturer's instructions.

2.2.9.1 Protein Gel-Electrophoresis

The electrophoretic separation of proteins is based on the principle of the sodium dodecyl sulphate polyacrylamide gel electrophoresis (SDS-PAGE) wherein the proteins are separated on the basis of their molecular weight. SDS is an anionic detergent which denatures secondary and non disulphide linked tertiary structures of the proteins, and applies a negative charge to each protein in

proportion to its mass enabling them to migrate towards the positive pole when run through a polyacrylamide gel placed in an electric field.

Cellular proteins were extracted in RIPA buffer as previously described in 3.17. Totals of 50-100µg protein equivalents for receptor expression studies or 20-50µg protein equivalents for MAPK activation studies were mixed with Roti-Load 1, a reducing protein loading buffer and heated at 70°C for 10 minutes which further denatures the proteins by reducing the disulphide linkages, thus overcoming some forms of tertiary protein folding, and breaking up quaternary protein structure. The XCell II mini cell apparatus was set up as per instructions and 500 µl of anti oxidant was added to the running buffer in the upper chamber which helps keep the sample reduced while the gel runs. Kaleidoscope marker proteins (5µl) were loaded as molecular size standards and the gel run was carried out at 200 V constant at approximately 80-90 mA current for 90 minutes. For the muscarinic receptor expression studies the samples were separated on 10% acrylamide Tris glycine precast gels (Mirador, Montreal, PQ, Canada) using the Laemmli buffer system (5% SDS, 125 mM Tris, 7.2% glycine whereas, a 4-12% Nu PAGE Bis-Tris Gel using the 1X MOPS-SDS buffer system was utilized for cell signaling studies.

2.2.9.2 Immunoblot

Prior to the completion of the gel run, equilibration of the polyvinylidene difluoride (PVDF) membrane was done by soaking it in methanol for 30 seconds followed by washing with distilled water for 1-2 minutes and 20 minutes in transfer buffer. Filter paper and blotting pads were pre soaked in transfer buffer prior to being used. After the completion of the gel run, the gel was removed from the gel cassette and equilibrated in transfer buffer for 10-15 minutes. At the end of the equilibration period a sandwich assembly of the membrane, gel, filter paper and blotting pads was prepared and transferred to the X Cell II Blot Module apparatus as instructed in the manual. The inner and outer chambers were then filled with transfer buffer and the unit was run at a constant current of 250 mA (100 V) for 90 minutes.

Once the blotting step was over the PVDF membrane was transferred onto a tray on a rocker and stained using Ponceau S (0.2% w/v) to ensure the quality of the blot and the lanes were marked. After the lanes were marked the stain was removed by washing twice with water followed by a TBS wash step for 3 minutes. The membrane was then blocked using 10 ml of 5% blocking solution (dried milk powder in 0.05% TBT) overnight at 4°C.

The blocking solution was then discarded and 10 ml of the primary antibody solution prepared in 3% blocking solution to appropriate dilution was added onto the membrane and left to incubate for 90 minutes at room temperature on the rocker. The membrane was then washed thrice for 10 minutes with 0.1% TBST and blocked with 3% blocking solution twice for 10 minutes. This was followed by addition of 10 ml of secondary antibody linked with a reporter enzyme diluted to optimal concentration in a 3% blocking solution over the membrane and incubated for 45 minutes on a rocking platform. After the end of the incubation period with the secondary antibody the membrane was washed for 15 minutes four times with 0.1% TBST.

During the time of final wash steps of the protocol the chemiluminescence detection solution was prepared employing BM chemoluminescence blotting substrate peroxidase (POD) kit and kept at room temperature. At the end of the final wash step the membrane was taken to the photo laboratory. The excess buffer from the washed membrane was drained and it was placed on a piece of two fold transparent film (protein side up). Then the detection solution was added on the protein side of the membrane for 1 minute following which a sandwich was prepared of the membrane with a new plastic wrap by closing the membrane with the second fold of the film. Care was taken to remove any trapped air bubbles by gently pressing the membrane wrap sandwich. The membrane wrap sandwich was then transferred to an autoradiographic cassette and exposed to an X-ray film for anywhere between 15 seconds to 5 minutes depending on the intensity of the signal. The film was then placed in a developing solution for 3-5 minutes, washed in water for 3 minutes and finally in a fixing solution for 5 minutes. Based on the intensity of the signal a second film was developed to optimal exposure

time. The developed films were then scanned and RFLPscan software was employed to quantify the optical density of the protein bands.

2.2.9.3 Membrane Stripping

Stripping of the membrane was done to make sure the loading of the samples were consistent by re-probing the membrane with another antibody. For this purpose the membrane was soaked in methanol and washed with distilled water. Then 0.2% NaOH solution was added onto the membrane for 5 minutes over a rocking platform followed by washing the membrane for 5 minutes with distilled water. Finally the membrane was blocked with a 5% blocking solution overnight at 4°C. This was followed by the addition of another primary antibody in a 3% blocking solution and the remaining protocol for the immunoblotting was similar to as described previously.

2.2.10 (³H)-Thymidine Incorporation Proliferation Assay

Human lung fibroblasts cells were cultured as previously described in 3.11. Cells were then trypsinized, harvested, and seeded into 12-well dishes at a density of 7.5×10^4 or 1.5×10^5 cells per well depending on the protocol being implemented. Four different sets of protocols were tested to find conditions under which cholinergic effects might be particularly prominent. In the first set, cells were initially cultured for 24 hours in the presence of 10% FCS, followed by an additional 48 hours under FCS-free conditions. Test drugs were either added at the onset of the FCS-free period or 24 hours later. (³H)-Thymidine (37kBq) was present during the last 24 hours of the 3-d culture period. In another series of experiments, fibroblasts were cultured for 30 or 48 hours under FCS-free conditions from the onset. Test drugs were present from the beginning, and (³H)-Thymidine during the last 24 hours. In experiments of 48 hour duration or longer, medium was renewed after 24 hours to ensure the presence of active drugs during the entire culture period. After the end of the incubation period the cells were washed with ice-cold 1X PBS, followed by a denaturation in 10% trichloroacetic acid (TCA) for 10 minutes at 37°C. The TCA was then aspirated

out and the cells were washed once again with ice cold 1X PBS and DNA was extracted during incubation for 1 hour in 0.1mol/l NaOH at 37°C. Samples of the supernatant solution (300 µl portions) were neutralized with 200 µl of Tris HCl (pH 7.4), combined with the scintillation cocktail, and the radioactivity was measured by liquid scintillation spectrometry in a Packard 2100 liquid scintillation analyzer. A blank reading was also performed correct for counting efficiency. In a further set of experiments cells were FCS-deprived and drugs were applied from the onset of the test culture period and the cells were incubated for 6 hours prior to the addition of (³H)-Thymidine, for a total of 30 hours. At the end of the incubation period the cells were washed with ice-cold PBS and denatured with 5% TCA as mentioned before and DNA was extracted by incubating the cells with 0.1mol/l NaOH at 4°C overnight. The radioactivity was then determined as described above. These conditions were held for subsequent experiments with subtype preferring muscarinic receptor antagonist and for elucidating the intracellular signaling pathways.

2.2.11 Caspase-3 Fluorimetric Assay

The assay was performed using the Caspase-3 Fluorimetric Kit provided by SIGMA as per the manufacturer's instructions.

Caspase-3 is an intracellular cysteine protease that exists as a proenzyme, becoming activated during the sequence of events associated with apoptosis. The caspase-3 fluorimetric assay is based on the hydrolysis of the peptide substrate acetyl-Asp-Glu-Val-Asp-7-amido-4-methylcoumarin (Ac-DEVD-AMC) by caspase-3, resulting in the release of the fluorescent 7-amino-4-methylcoumarin (AMC) moiety which when excited by light at 360 nm wavelength emits fluorescence at 460nm wavelength. The level of caspase enzymatic activity in the cell lysate being directly proportional to the fluorescence signal detected with the fluorescent microplate reader.

Stock solutions were prepared and diluted for assay use as per the instructions provided. Cells were seeded into a 24-well dish at density of 4×10^4 cells per well in the presence of 10% FCS in a humidified incubator at 37°C and 5% CO₂.

Upon reaching 80-85% confluence the medium was aspirated out and the cells were treated with various apoptosis inducers in the presence or absence of a muscarinic agonist under serum free conditions and incubated a further 4 hours. At the end of the incubation period the plate was kept on ice and the medium aspirated out, following which 50 μ l of 1X Lysis Buffer was added onto each well and the plate was left to incubate on ice for 15-20 minutes. Then 400 μ l of 1X Assay Buffer containing the substrate was added to each well and mixed well by pipetting. Readings were calculated in duplicates for each well by transferring 200 μ l to a fluorimeter multi well plate. Two wells for substrate blank, two for caspase positive control and two for caspase positive in combination with the caspase inhibitor were also prepared. Parallely an AMC standard curve analysis was performed over a concentration range 0.02, 0.1, 0.2, 0.4 and 0.8 nM of AMC in 200 μ l of 1X Assay Buffer. The fluorescence was read in a kinetic mode every 10 minutes over a period of 1 hour using FLUOstar OPTIMA (BMG LABTECH) microplate reader set to optimal parameters. The enzyme activity was calculated using the AMC standard curve.

AMC Standard Curve

AMC Solution	Nmol AMC in200 μ l	AMC Working Solution (10 μ M)	1X Assay Buffer
100 nM	0.02	3 μ l	297 μ l
500 nM	0.1	15 μ l	287 μ l
1 μ M	0.2	30 μ l	270 μ l
2 μ M	0.4	60 μ l	240 μ l
4 μ M	0.8	120 μ l	180 μ l

Representation of the Pipetting Scheme followed for the Caspase-3 Assay

Sample	Apoptosis Inducers	Muscarinic Agonist	Caspase Inhibitor	Caspase positive
Blank				
1	I _i + I _{iii}			
2	I _i + I _{iii}		+	
3	I _{ii} + I _{iii}			
4	I _{ii} + I _{iii}		+	
5		C		
6	I _i + I _{iii}	C		
7	I _i + I _{iii}	C	+	
8	I _{ii} + I _{iii}	C		
9	I _{ii} + I _{iii}	C	+	
10				+
11			+	+

Actinomycin D 200 ng/ml (I_i), Cycloheximide 10 µg/ml (I_{ii}) , TNF alpha H 10 ng/ml (I_{iii}) , Carbachol 10µM (C), Caspase-3 positive control 0.05 µg/ml, Caspase-3 inhibitor 2 µM,

3. Results

3.1 Muscarinic Receptor Expression in Human Lung Fibroblasts

3.1.1 Muscarinic Receptor Expression in MRC-5 Human Lung Fibroblasts

Semi-quantitative RT-PCR's were performed to determine the expression pattern of the mRNA encoding for the different muscarinic receptors subtypes in MRC-5 fibroblast cell line. Total RNA was isolated as described previously in 3.1.2 and first-strand cDNA was synthesized using Omniscript reverse transcriptase. Then the PCR amplification was carried out using specific oligonucleotide primers for human muscarinic receptors (M_1 - M_5) or β -actin in a programmable thermal cycler set to 23 cycles for β -actin and 35 cycles for muscarinic receptors.

Positive controls were performed for every PCR using genomic DNA (gDNA) isolated for MRC-5 cells and one PCR lacking template DNA was regularly performed as a negative control. Table A, shows the PCR product size and the specific annealing temperature for the primers pairs employed.

As shown in Figure 1, MRC-5 fibroblasts express mRNA encoding different muscarinic receptor subtypes. The most prominent expression was found for mRNA encoding M_2 receptor, followed by M_3 receptor transcripts. Lower but still detectable expression for M_4 receptor was observed, while only traces of M_5 receptor encoding mRNA were detected, and no transcript for M_1 receptor was detected. The expression pattern for the mRNA encoding the muscarinic receptors was found to be consistent under the culture conditions, as a similar pattern was found in different passages (passages 1-13).

Western blot analysis using specific commercially available polyclonal antibodies for M_2 and M_3 receptors were performed which confirmed the expression of the M_2 and M_3 receptors at protein levels (Figure 1.C). A single band somewhat larger than 80 kDa was observed for the immunoblot for M_2 receptor. A band of similar size was also observed for the M_3 receptor, but here two additional products, with a lower molecular weight, were also detected. These probably reflect the cellular degradation products which are still recognized by the antibody. An immunoblot performed with proteins extracted from rat lung tissue is also shown in Figure 2 for comparison purposes.

Table A

Receptor	Primer pair	Product size (bp)	Annealing temperature °C
hM ₁	hM ₁ -s/hM ₁ -as	538	58
hM ₂	hM ₂ -s/hM ₂ -as	654	53
hM ₃	hM ₃ -s/hM ₃ -as	560	60
hM ₄	hM ₄ -s/hM ₄ -as	498	58
hM ₅	hM ₅ -s/hM ₅ -as	751	57

Figure 1. Expression of human muscarinic receptors (M1-M5) in MRC-5 Human Lung Fibroblasts.

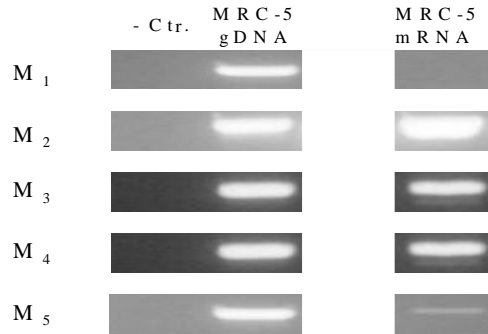
A. Samples of RT-PCRs of human muscarinic receptors (M₁-M₅) on RNA isolated from MRC-5 human lung fibroblasts. Cells were grown in 55-mm culture dishes to confluence, total RNA was isolated, treated with DNase, and used for RT-PCR with primers specific for the human muscarinic receptors or β -actin. To control effectiveness of primer pairs, PCRs were also performed on genomic DNA (gDNA) isolated from MRC-5 cells. One PCR lacking template DNA was regularly performed to account for any contamination (negative control, -Ctr.). PCR products were separated on a 1.2% agarose gel.

B. Densitometric evaluation of a series of experiments. Given are mean values (+SEM) of three experiments performed with cells of passages 1-13. Values were normalized first for β -actin to correct for quality of cDNA preparation and second for the respective amplification products obtained on gDNA to correct for effectiveness of the respective primer pairs.

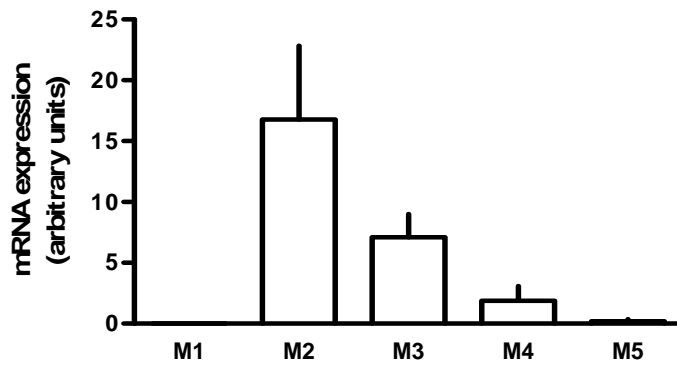
C. Immunoblot analysis of protein extracts of MRC-5 cells for comparison of rat lung tissue using commercially available antibodies against M₂ and M₃ receptor protein. Given are the representative samples of SDS-PAGE.

Figure 1.

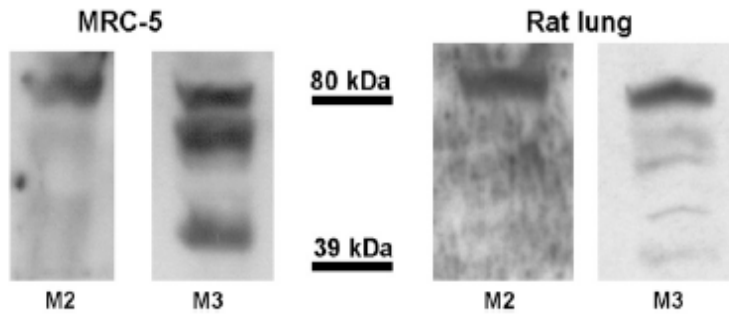
A.



B.



C.



3.1.2 Muscarinic Receptor Expression in Primary Human Lung Fibroblasts

Primary human lung fibroblasts cultures (phLFb) were obtained from patients with lung cancer and total RNA was isolated, followed by the first-strand DNA synthesis and amplification using PCR as described previously. As shown in Figure 2, mRNA encoding muscarinic receptors was detected. The expression of mRNA encoding the M₂ receptor transcript was most dominant, followed by mRNA encoding M₁ and M₃ receptors, whereas only traces of mRNA for M₄, and none for M₅, were observed at different passages.

To explore the regional expression pattern of mRNA encoding for muscarinic receptors M₂ and M₃ a wider pool of primary human lung fibroblasts cultures was obtained from lung cancer patients wherein, c/phLFb.4, c/phLFb.6, c/phLFb.8, c/phLFb.11, c/phLFb.12 were from the central and p/phLFb.5, p/phLFb.9 were from the peripheral region of the lung was obtained. Total RNA was isolated, followed by the first-strand-DNA synthesis and amplification using PCR as described previously. As Figure 2C shows, mRNA encoding muscarinic receptors M₂ and M₃ were detected, consistent with the results depicted in Figure 2A+B implicating that; there was no significant difference in the expression pattern of mRNA encoding for M₂ and M₃ muscarinic receptors in primary human lung fibroblast from different regions of the lung.

Figure 2. Muscarinic receptor expression in Primary Human Lung Fibroblasts

A. Samples of RT-PCRs of the five human muscarinic receptors (M₁-M₅) on RNA isolated from primary human lung fibroblasts (phLFb). Cells were grown in 55-mm culture dishes to confluence, total RNA was isolated, treated with DNase, and used for RT-PCR with primers specific for the human muscarinic receptors or β -actin. To control effectiveness of primer pairs, PCRs were also performed on genomic DNA (gDNA) isolated from MRC-5 cells. One PCR lacking template DNA was regularly performed to account for any contamination (negative control, -Ctr.). PCR products were separated on a 1.2% agarose gel.

B. Densitometric evaluation of a series of experiments. Data are means (+SEM) of three experiments performed on cells of passages 1, 5, and 10. Values were normalized first for β -actin to correct for quality of cDNA preparation and second for the respective amplification products obtained on gDNA to correct for effectiveness of the respective primer pairs.

C. Samples of RT-PCRs of human muscarinic receptors (M_1 and M_2) on RNA isolated from primary human lung fibroblasts obtained from different regions of the lung. Cells were grown in 55-mm culture dishes to confluence, total RNA was isolated, treated with DNase, and used for RT-PCR with primers specific for the human muscarinic receptors or β -actin. To control effectiveness of primer pairs, PCR were also performed on genomic DNA (gDNA) isolated from MRC-5 cells. One PCR lacking template DNA was regularly performed to account for any contamination. PCR products were separated on a 1.2% agarose gel.

D. Densitometric evaluation of a series of experiments. Data are means (+SEM) of three experiments performed of passages 0, 1, and 2. Values were normalized for β -actin to correct for quality of cDNA preparation and second for the respective amplification products obtained on gDNA to correct for effectiveness of the respective primer pairs.

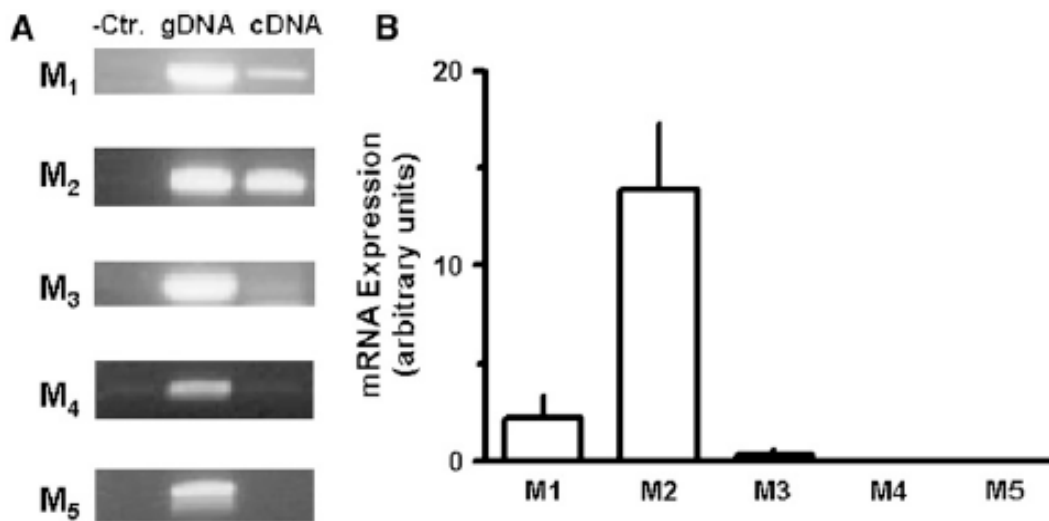
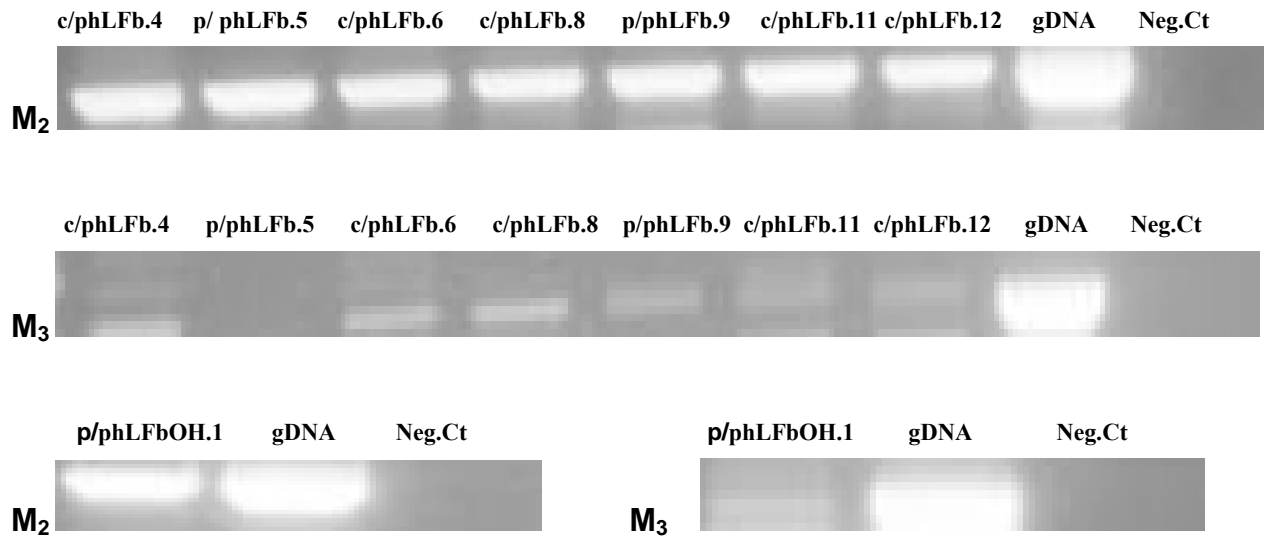
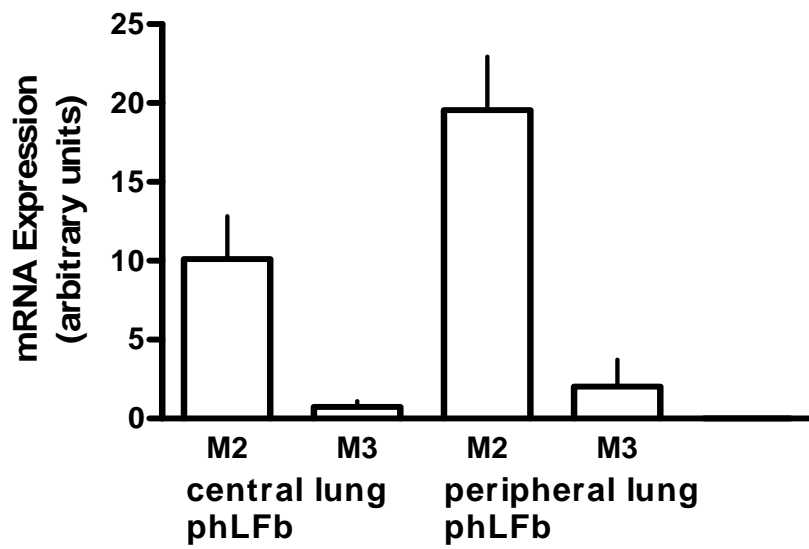


Figure 2.

C.



D.



3.2 Muscarinic Stimulation of Proliferation of Human Lung Fibroblasts

3.2.1 Muscarinic Stimulation of Proliferation of MRC-5 Human Lung Fibroblasts

Various experimental conditions were tested in order to determine optimal parameters for the (³H)-thymidine incorporation assay. The purpose being to test whether putative muscarinic effects on fibroblast proliferation were dependant on culture conditions and exposure time. In the first set of experiments, cells were cultured for 24 hours in the presence of 10% FCS, followed by 24 hours under FCS-free conditions in the presence of (³H)-thymidine and in the absence or presence of increasing concentrations of carbachol. Under control conditions (absence of drugs), (³H)-thymidine incorporation amounted to 7.281 ± 548 d.p.m (disintegration per minute) (n=52). Carbachol induced an increase in (³H)-thymidine incorporation by $38 \pm 18\%$ at 10 μ M in a concentration-dependent manner (Figure 3A). As shown in Figure 3A, this effect was abolished in the presence of 1 μ M atropine which alone did not have an effect on (³H)-thymidine incorporation. In spite of the fact that the stimulatory effect of carbachol was clearly significant, the magnitude of the effect showed considerable variation.

In a second set of experiments, cells were again cultured for 24 hours in the presence of 10% FCS, followed by 48 hours FCS-free conditions in the absence or presence of carbachol (10 μ M) with (³H)-thymidine present for the last 24 h. Under these conditions, carbachol caused an increase in (³H)-thymidine incorporation by $52 \pm 10\%$ (Figure 3B). Here again the proliferative effect of carbachol was inhibited by atropine and also by the long-acting muscarinic antagonist tiotropium (Figure 3B). Furthermore, oxotremorine also caused a similar increase (by 61%), an effect also prevented by atropine (Figure 3B). For comparison, when FCS (1 or 10%) was present instead of muscarinic agonist during the last 48 hours, (³H)-thymidine incorporation was enhanced by $69 \pm 17\%$ (n = 6) and $216 \pm 30\%$ (n = 9), respectively, compared to FCS-free conditions.

In the third protocol, cells were FCS-deprived and drugs were applied from the onset of the test culture period. Under these conditions, 10 μ M carbachol or oxotremorine increased (³H)-thymidine incorporation by $64 \pm 8\%$ and $100 \pm 26\%$,

respectively, when present 24 hours before (^3H)-thymidine, for a total of 48 hours. These effects were again shown to be atropine sensitive (Figure 3C).

In a further set of experiments carbachol was applied 6 hours before (^3H)-thymidine, for a total of 30 hours, (^3H)-thymidine incorporation was increased by $76 \pm 4\%$ ($n = 80$). These conditions were held for the subsequent interaction experiments with subtype-preferring muscarinic receptor antagonists.

As shown in Figure 4 when 1% FCS was present from the onset of the test culture period (6 hours before (^3H)-thymidine, for a total of 30 hours), (^3H)-thymidine incorporation was increased by 450%. Additional presence of 10 μM carbachol or oxotremorine induced a further significant increase in (^3H)-thymidine incorporation, by about 300% and 240% respectively, relative to the FCS-free controls (Figure 4). This corresponds to an increase of 54 and 43% respectively, when expressed in relation to FCS-containing control experiments.

Figure 3. Effects of muscarinic agonists and antagonists on (^3H)-thymidine incorporation in MRC-5 Human Lung Fibroblasts

7.5×10^4 cells were seeded in 12 well dishes in the absence or presence of 10 % FCS as indicated. In each series (^3H)-thymidine (37 kBq) was present for the last 24 h.

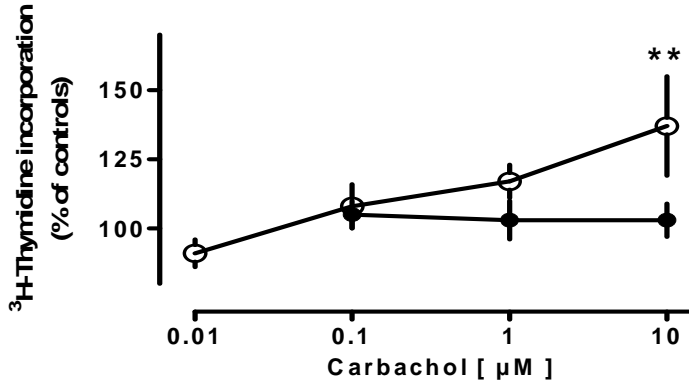
A. Effects of carbachol, at concentrations indicated by the abscissa, in absence (open symbols) or presence (filled symbols) of 1 μM atropine. Test drugs were added together with (^3H)-thymidine.

B and C. Carbachol (C, 10 μM), oxotremorine (O, 10 μM) and/or atropine (A, 1 μM) and/or tiotropium (T, 0.1 μM) were present already 24 h prior to (^3H)-thymidine until the end of the protocol. Data are means ($\pm\text{SEM}$) of $n=3-12$ (mostly $n \geq 6$). ** $P < 0.01$; *** $P < 0.001$ vs. controls; + $P < 0.05$, ++ $P < 0.001$, +++ $P < 0.001$ vs. the respective value in the absence of antagonists.

Figure 3.

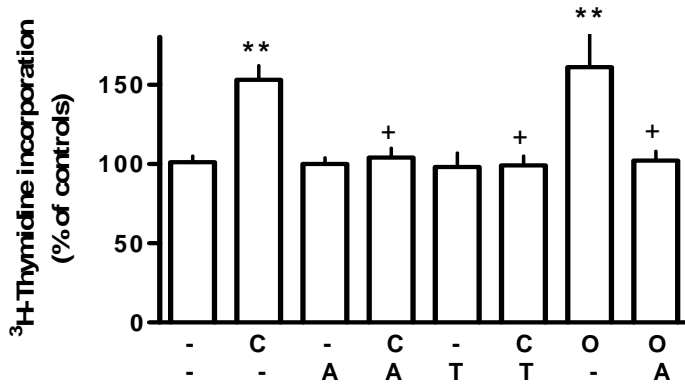
A.

24h 10 % FCS → 24 h FCS-free → 24 h FCS-free + test drugs



B.

24h 10 % FCS → 48 h FCS-free ± test drugs



C.

48 h FCS-free ± test drugs

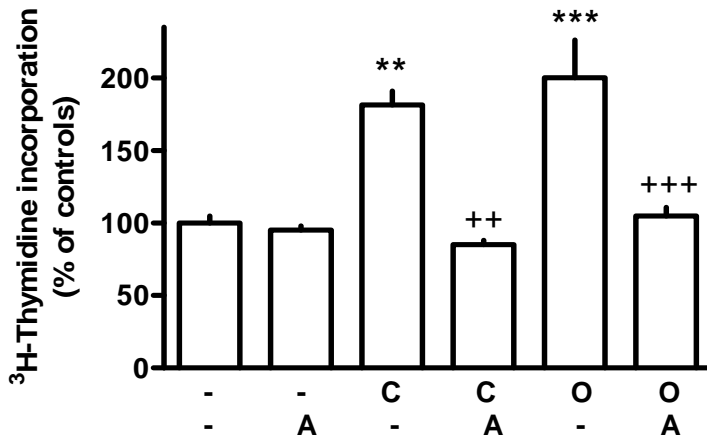
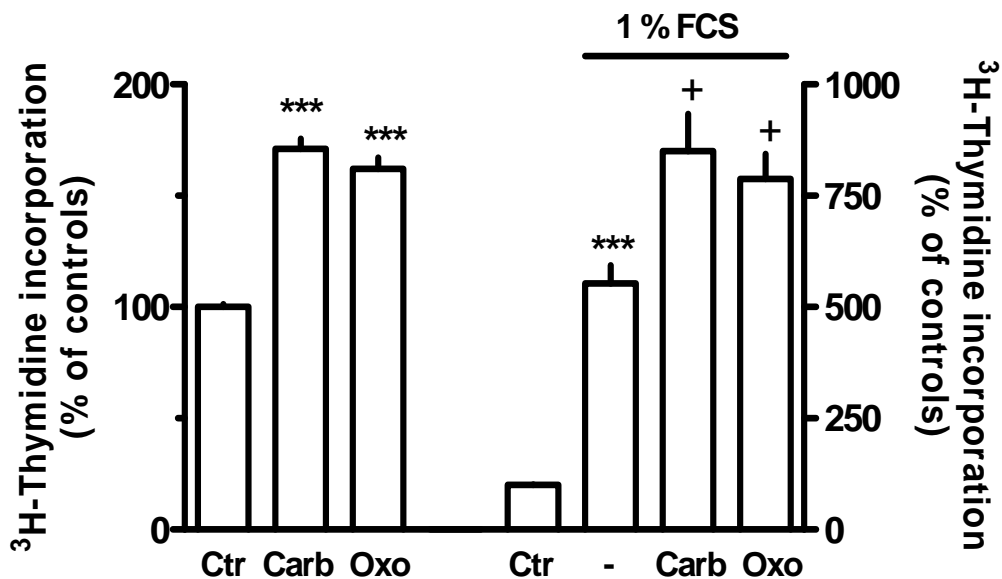


Figure 4. Comparison of the effects of carbachol and oxotremorine on (³H)-thymidine incorporation in MRC-5 human lung fibroblasts in absence and presence of FCS. 7.5 x 10⁴ cells were seeded in 12 well dishes and cultured under FCS-free conditions or in the presence of 1% FCS. Carbachol (Carb, 10 μM) or oxotremorine (Oxo, 10 μM) was added from the onset of incubation for a total of 30 h, (³H)-thymidine (37 kBq) was present for the last 24 h. Data are means (±SEM) of n=3-12. *** P < 0.001 vs. controls (Ctr); + P < 0.01 vs. the respective value in the presence of FCS alone.



3.3 Characterization of Muscarinic Receptor Sub-Type

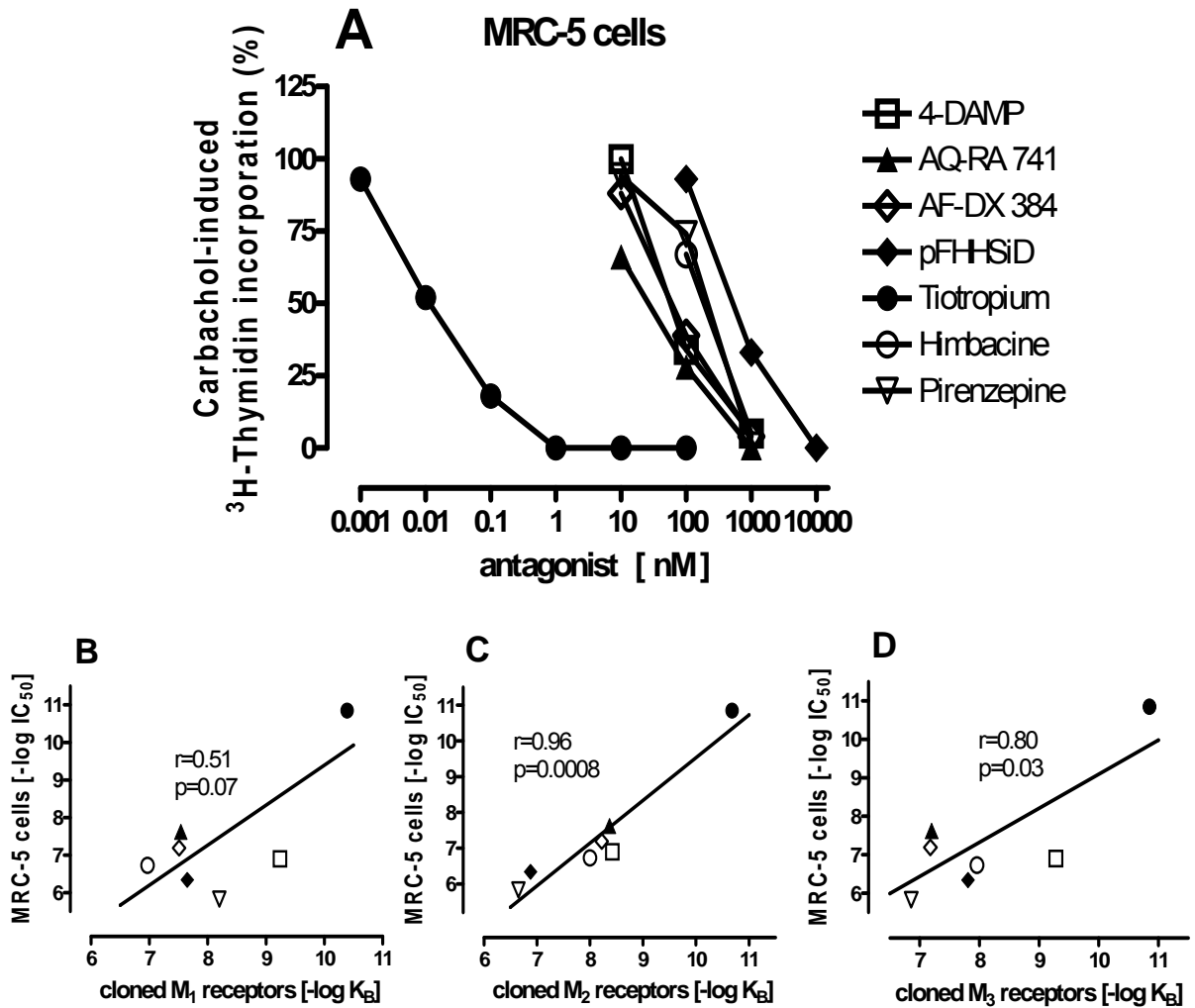
3.3.1 Inhibition of Muscarinic Proliferation using Receptor Sub-Type Specific Antagonists in MRC-5 Human Lung Fibroblasts

Receptor sub-type characterization studies were performed to determine the functional receptor/receptors involved in the muscarinic stimulation of proliferation in MRC-5 human lung fibroblasts using different selective muscarinic antagonists. As summarized in Figure 5, all muscarinic receptor antagonists tested inhibited the stimulatory effect of carbachol on (³H)-thymidine incorporation in a concentration dependent manner. Tiotropium was by far the most potent drug, with an IC₅₀ value of 14 pM. The M₂/M₄, receptor-preferring

antagonists, AQ-RA 741, AF-DX 384, and himbacine, showed IC_{50} values of 24, 64, and 187 nM, respectively, whereas, for the M_3/M_1 receptor-preferring antagonists, 4-DAMP and p-FHHSiD, IC_{50} values of 127 and 452 nM were determined. Pirenzepine a M_1/M_4 receptor-preferring antagonist was found to have an IC_{50} value of 1.5 μ M. None of the antagonists at any of the concentrations studied significantly affected (3 H)-thymidine incorporation on its own. When the potencies of these antagonists as determined here were correlated to their reported affinity constants to cloned human muscarinic receptors, the best and highly significant correlation was obtained for the M_2 receptor. Figures 5B-5D present only the correlations for M_1 , M_2 , and M_3 receptors, as affinity data of tiotropium for cloned M_4 and M_5 receptors have not yet been published. For these two receptors, the respective correlations calculated on the basis of the remaining six antagonist failed to be statistically significant, with $r = 0.60$ and 0.27 for M_4 and M_5 receptors, respectively. Furthermore when correlation significance was calculated as described previously for the various muscarinic receptors in the absence of tiotropium, M_2 muscarinic receptor showed the best and highly significant correlation with $r = 0.89$ as compared to M_3 ($r = 0.10$), M_1 ($r = 0.17$), M_4 ($r = 0.60$) and M_5 ($r = 0.27$).

Figure 5. A. Inhibitory effects of different muscarinic receptor antagonists on carbachol-induced stimulation of (3 H)-thymidine incorporation in MRC-5 human lung fibroblasts. A total of 7.5×10^4 cells were seeded in 12-well dishes under FCS-free conditions. Carbachol (10 μ M) was added from the onset of incubation for a total of 30 h, of which (3 H)-thymidine (37 kBq) was present for the last 24 h. In the absence of antagonists, carbachol enhanced (3 H)-thymidine incorporation by $98 \pm 10\%$ ($n = 53$). Antagonists were applied immediately before addition of carbachol at the concentrations given by the abscissa. Ordinate: stimulatory effect of carbachol in the presence of antagonist, expressed as percent of mean stimulatory effect of carbachol in the absence of antagonists, as observed in the respective series of experiment. Data are means of $n = 3-12$ (mostly $n \geq 6$); SEM, 6-12%.

Figure 5. B-D. Correlation between the potencies of the antagonists, as determined in the present experiments (ordinate), and the reported affinity constants, as determined on cloned human muscarinic receptors (abscissa). *Open squares*, 4-DAMP; *closed triangles*, AQ-RA741; *open diamonds*, AF-DX384; *closed diamonds*, p-FHHSiD; *closed circles*, tiotropium; *open circles*, himbacine; *open inverted triangles*, pirenzepine.



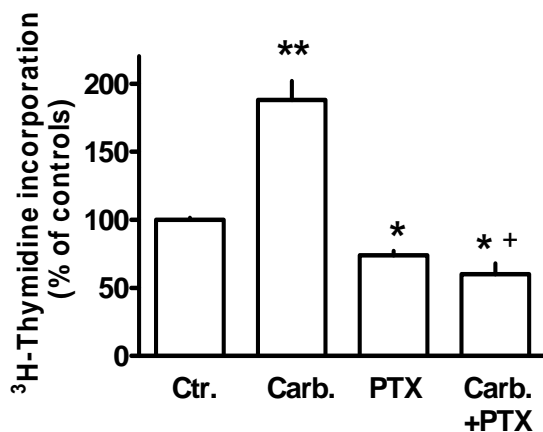
3.3.1.2 Effect of Pertussis Toxin on Muscarinic Stimulation of Proliferation of MRC-5 Human Lung Fibroblasts

Pertussis toxin (PTX) has been widely used as a reagent to characterize the involvement of heterotrimeric G-proteins in signalling. This toxin catalyses the ADP-ribosylation of specific G-protein subunits of the G_i family, and this modification prevents the occurrence of the receptor–G-protein interaction. As shown in Figure 6, pretreatment of the fibroblasts with PTX resulted in a slight reduction in (^3H)-thymidine incorporation, and abolished the stimulatory effect of carbachol. In order to test the specificity of PTX, the effects of this toxin were also studied on the proliferative effect of PDGF, which is known to act via a different class of receptors. Pretreatment of the cells with PTX, as described in Figure 6, did not inhibit the PDGF-induced stimulation of (^3H)-thymidine incorporation (increase by $219 \pm 40\%$ [$n = 6$] and $283 \pm 40\%$ [$n = 3$] in absence and presence of PTX, respectively).

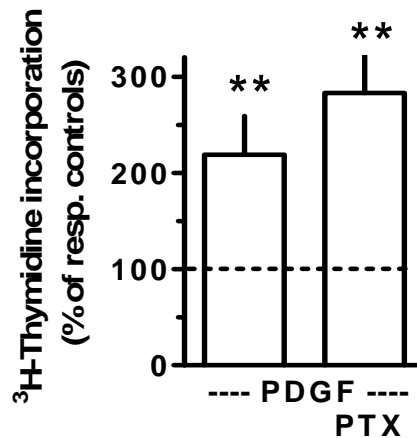
Figure 6. Effects of carbachol and/or pertussis toxin (PTX) on (^3H)-thymidine incorporation in MRC-5 Human Lung Fibroblasts

(A + B) 7.5×10^4 cells were seeded in 12 well dishes and cultured under FCS-free conditions. PTX (0.1 $\mu\text{g/ml}$) was present from the onset of incubation. Carbachol (Carb., 10 μM), PDGF 100 ng/ml) were added 3 h after PTX. Finally, (^3H)-thymidine (37 kBq) was added 6 h later and present for 24 h. Data are means ($\pm\text{SEM}$) of $n=3-12$ (mostly $n \geq 6$). * $P < 0.01$ and ** $P < 0.001$ vs. controls (Ctr); *, + $P < 0.01$ vs. Ctr, and ** $P < 0.001$ vs. Carb, alone.

A.



B.

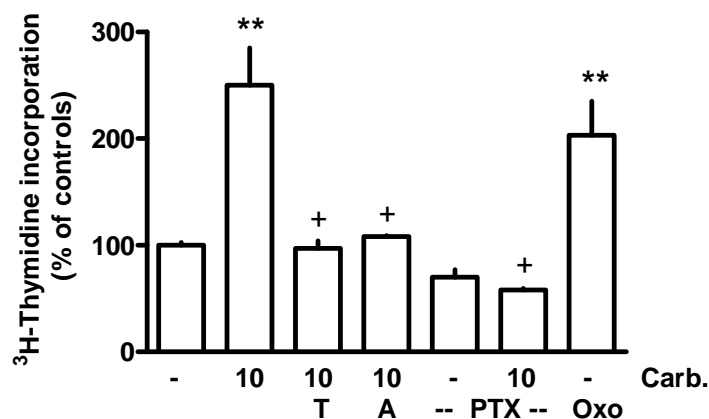


3.3.1.3 Muscarinic Stimulation and Effect of Pertussis Toxin on Proliferation in Primary Human Lung Fibroblasts (pHLFb)

(³H)-thymidine incorporation experiments were performed with primary human lung fibroblasts to confirm the muscarinic stimulation mediated proliferation using 10 μM carbachol or oxotremorine, in the presence of tiotropium or atropine, as well as pretreatment with PTX. It was observed that the stimulatory effect in the presence of the muscarinic agonists carbachol and oxotremorine were abolished in the presence of tiotropium or atropine and PTX. These results were in line with those seen for the MRC-5 cell line. Also, in the primary human lung fibroblasts, PTX pretreatment failed to inhibit the proliferative effect of 100 ng/ml PDGF (increased by 403 ± 49% [n = 12] and 487 ± 80% [n = 3] in the absence and presence of PTX, respectively).

Figure 7. Effects of carbachol and/or pertussis toxin (PTX), tiotropium or atropine on (³H)-thymidine incorporation in Primary Human Lung Fibroblasts.

7.5 x 10⁴ cells were seeded in 12 well dishes and cultured under FCS-free conditions. Cells were incubated for 30 h with carbachol (Carb, 10 μM) and/or tiotropium (T, 0.1 μM), atropine (A, 1 μM) or oxotremorine (Oxo, 10 μM) as indicated. (³H)-thymidine (37 kBq) was added 6 h after onset of exposure to these drugs. In the respective experiments PTX (0.1 μg/ml) was already present 3 h before carbachol. Data are means (±SEM) of n=3-12. ** P < 0.001 vs. controls; + P < 0.01 vs. carbachol alone.

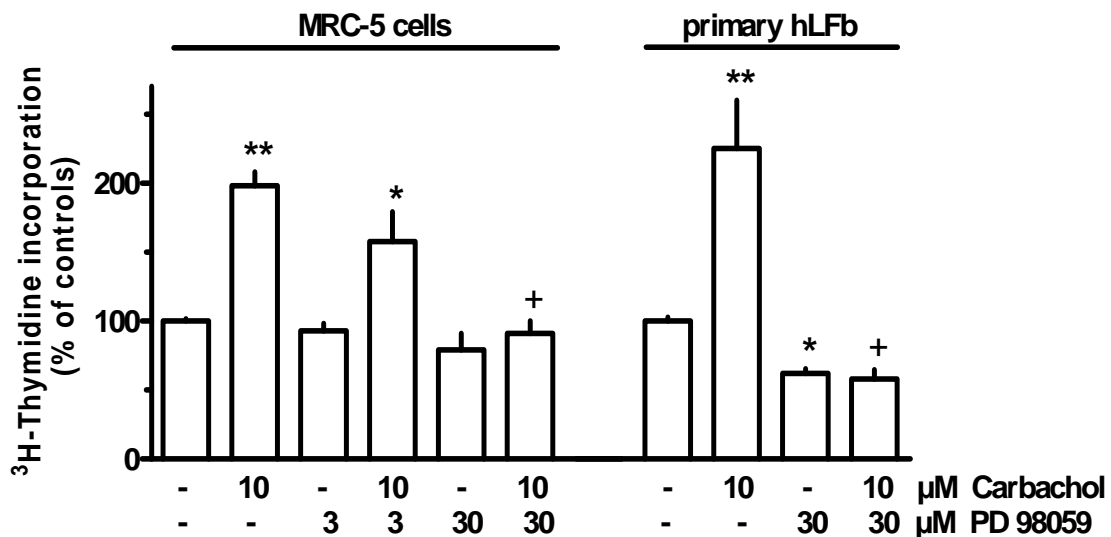


3.4 Muscarinic Stimulation Mediated Activation of MAPK Pathway in Human Lung Fibroblasts

3.4.1 Muscarinic Receptor Stimulation and Activation of p-42/44 MAPK Pathway in Proliferation of Human Lung Fibroblast

The preceding results confirm the presence of muscarinic receptors and its involvement in mediating proliferative effects in both the MRC-5 and the primary human lung fibroblasts. The next aspect to look into was to study the cellular transduction mechanism involved in the muscarinic stimulation of lung fibroblast proliferation. Since activation of MAPK cascade has been shown to be an essential transduction mechanism of many mitogens and growth factors, (³H)-thymidine incorporation assay was performed. Early passage MRC-5 cells were used for this purpose and for all experiments; primary cells were used before their 7th passage. Cells were disseminated in a 12-well dish at a density of 7.5×10^4 per well and cultivated in the absence of FCS for 30 hours in combination with the test drugs. (³H)-thymidine (37kBq) was applied for the last 24 hours. As shown in Figure 8, muscarinic receptor agonist carbachol (10 μ M) exerted a marked proliferative effect in both, MRC-5 cells and primary human lung fibroblasts as indicated by about 2-fold increase in (³H)-thymidine incorporation. Preceding results show this effect was inhibited by different muscarinic receptor antagonist like atropine and tiotropium proving that proliferation is mediated via specific muscarinic receptors. Figure 8, further shows that in both MRC-5 fibroblasts as well as in primary human lung fibroblasts the stimulatory effect of carbachol could be blocked by PD98059, a specific inhibitor of MAPK-activating enzyme (MEK), implicating that MAPK cascade is crucially involved in the proliferative response of human lung fibroblasts to cholinergic stimulation.

Figure 8. Effects of carbachol in absence and presence of PD 98059 on the (³H)-thymidine incorporation in Primary Human Lung Fibroblast (hLFb) and the Human Lung Fibroblast cell line MRC-5. 7.5 x 10⁴ cells were disseminated in 12-well dishes in the absence of FCS and cultured for 30 h in the absence and presence of test drug as indicated. The cells were pretreated with the PD 98059 drug for 30 min before the addition of the carbachol. (³H)-thymidine was applied for the last 24 h. Given are means ± SEM of n = 3-12 (mostly ≥ 6). Significance of differences; from controls, *P < 0.05; **P < 0.01; from carbachol, +P < 0.05.

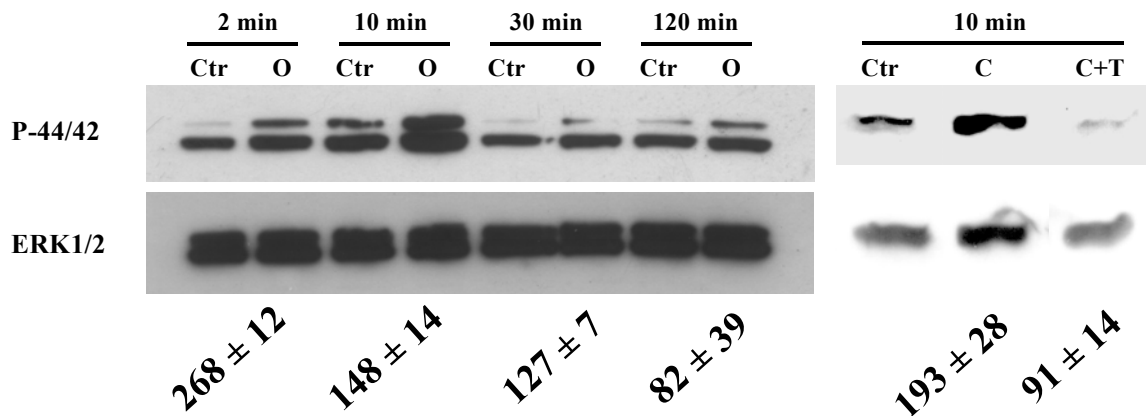


3.4.1.2 Western Blot Analysis of p42/44 MAPK (ERK1, ERK2) Activation in MRC-5 Human Lung Fibroblast

Western blot analysis was performed to confirm the activation of the MAPK cascade in response to the muscarinic stimulation induced proliferation in the MRC-5 fibroblasts at the protein levels. Western blot analysis conducted after a two to 120 minute stimulation of serum-starved MRC-5 fibroblasts with carbachol or oxotremorine (Figure 9) demonstrated activation of p42/44 MAPK (ERK1, ERK2). The effects of both oxotremorine and carbachol revealed to be counteractable by the muscarinic receptor antagonists atropine (1 μM, data not shown) and tiotropium (0.1 μM, exemplary shown for stimulation by carbachol in

Figure 9). Finally, similar activation patterns were observed in primary human lung fibroblasts (10 μ M carbachol enhanced p42/44 MAPK to $189 \pm 12\%$ of controls after 10 minutes ($n = 6$), data not shown).

Figure 9. Western blot analysis of p42/44 MAPK (ERK1, ERK2) activation in MRC-5 Human Lung Fibroblasts. Cells were cultured in a 55 mm² dishes to nearly confluence, serum-starved for 24 h and exposed to 10 μ M oxotremorine (Oxo), carbachol (C) in absence or presence of 0.1 μ M tiotropium or vehicle (Ctr) for 2-120 min as indicated. Cell lysates were prepared and 20-50 μ g were separated in 10-20% acrylamide Tris-glycine gels, immobilised to PVDF membranes and detected by antibodies specific for phosphorylated MAPK (P-44/42) and unphosphorylated MAPK (ERK1/2). Densitometrical quantification of the p-44/42 bands was performed and values (arbitrary units) in presence of agonists expressed as % of the the respective control. Given are means \pm SEM of $n = 3-6$ independent Western blots.



3.5 Effect of Kinase Inhibitors on Muscarinic Stimulation of MRC-5 Human Lung Fibroblast Proliferation

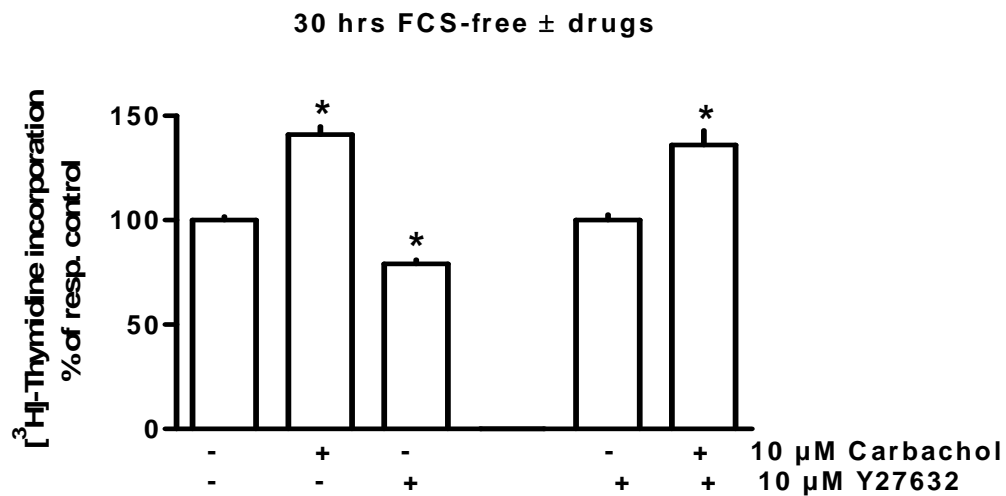
3.5.1 Effects of the Rho-kinase Inhibitor Y27632 on Muscarinic Stimulation of MRC-5 Human Lung Fibroblast Proliferation

The results previously indicated the muscarinic stimulation of proliferation in human lung fibroblast is mediated via the classical MEK-ERK MAPK cascade pathway. To elucidate the detailed transduction of how muscarinic receptor stimulation results in MAPK activation (³H)-thymidine incorporation proliferation assays were performed with various antagonists specific to signalling molecules, most likely to be involved in this G protein receptor coupled activation of MAPK pathway.

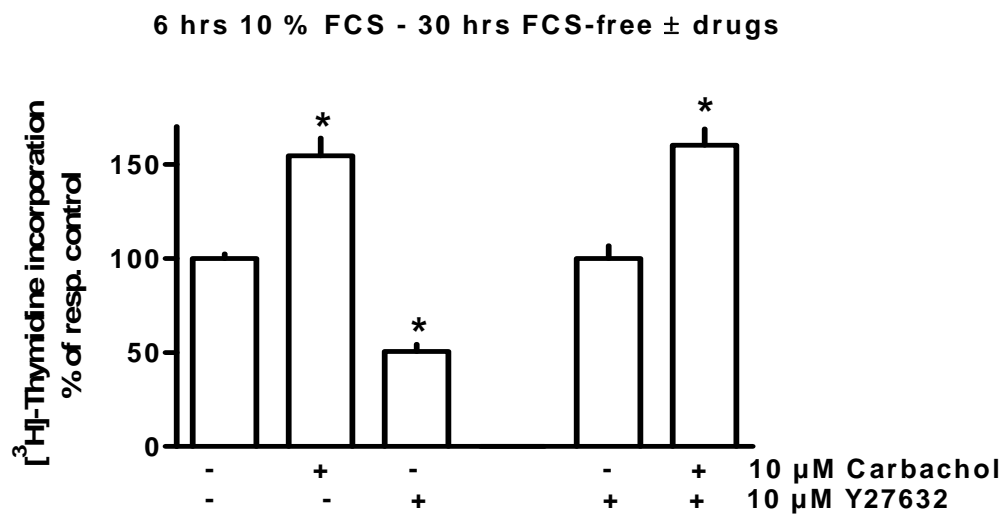
Rho a member of the family of small G-proteins has been shown to mediate cell cycle progression and proliferation via the activation of the MAPK cascade. To test if Rho was indeed involved in the muscarinic stimulation of proliferation of MRC-5 human lung fibroblast (³H)-thymidine incorporation assay was performed. Cells were seeded (1.5×10^5 cells/well) in a 12 well dish in the presence or absence of FCS and cultured for 30 hours with or without the test drugs. Passage numbers 1-10 were chosen for these experiments. The Rho-kinase inhibitor Y27632 (10 μ M) was added 30 minutes prior to addition of carbachol (10 μ M). As shown in Figure 10 (A + B) using the 30 hours FCS-free or the 6 hours 10% FCS followed by the FCS-free period protocols prior to addition of the drugs, carbachol enhanced the (³H)-thymidine incorporation to $141 \pm 4\%$ and $155 \pm 10\%$ while the Rho-kinase inhibitor Y27632 reduced the (³H)-thymidine incorporation to $79 \pm 2\%$ and $50 \pm 4\%$ with respect to the control. However the Y27632 Rho-kinase inhibitor did not inhibit the carbachol induced stimulation of (³H)-thymidine incorporation (increase to $136 \pm 7\%$ and $160 \pm 9\%$ respectively in the presence of Y27632).

Figure 10 A + B. Effects of the Rho-kinase inhibitor Y27632 on muscarinic stimulation of MRC-5 human lung fibroblast proliferation. MRC-5 cells (1.5×10^5 per well) were disseminated in 12 well dishes in the absence or presence of FCS and cultured for 30 h with or without test drugs as indicated. The cells were pre-treated with the Rho-kinase inhibitor Y27632 for 30 min before the addition of carbachol. (^3H)-thymidine was applied for the last 24 h. Given are means \pm SEM of n=9-18. Significance of differences: from respective controls, *P<0.01.

A.



B.

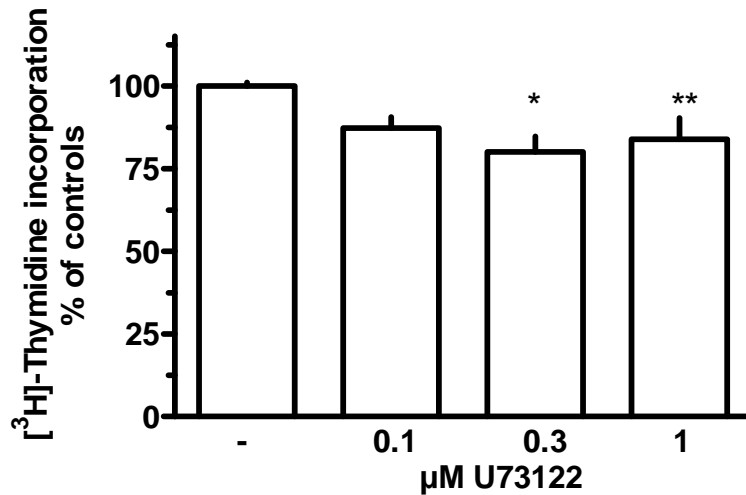


3.5.1.2 Effects of the Phospholipase C Inhibitor U73122 on Muscarinic Stimulation of MRC-5 Human Lung Fibroblast Proliferation

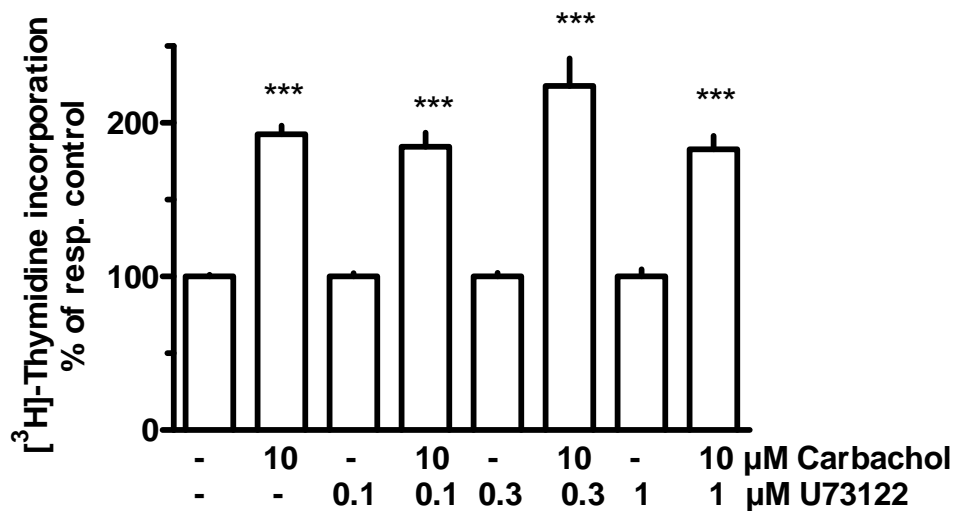
Previous studies have demonstrated the muscarinic stimulation induced activation of the MAPK pathway mediated via the Phospholipase C (PLC) in pertussis toxin sensitive G-proteins. In order to elucidate the involvement of PLC on the muscarinic stimulation of MRC-5 human lung fibroblast proliferation (^3H)-thymidine incorporation assays were performed. Cells in early passages were used in these experiments. Cells were disseminated (1.5×10^5 cells per well) in 12 well dishes in the absence of FCS and cultured for 30 hours with or without the test drugs. The PLC-inhibitor U73122 was added 30 minutes prior to the addition of carbachol ($10 \mu\text{M}$) in concentrations of 0.1, 0.3 and $1 \mu\text{M}$. As shown in Figure 11 (A + B), carbachol caused an increase in the (^3H)-thymidine incorporation by $193 \pm 6\%$ whereas the Phospholipase C inhibitor U73122 reduced the (^3H)-thymidine incorporation significantly to $80 \pm 5\%$ and $84 \pm 7\%$ at 0.3 and $1 \mu\text{M}$ concentrations relative to the control. However the PLC inhibitor U73122 did not inhibit the carbachol induced stimulation of (^3H)-thymidine incorporation (increase to $224 \pm 18\%$ [$n = 9$] and $183 \pm 9\%$ [$n = 9$] respectively in the presence of U73122 at 0.3 and $1 \mu\text{M}$).

Figure 11 A + B. Effects of the Phospholipase C inhibitor U73122 on muscarinic stimulation of MRC-5 human lung fibroblast proliferation. Cells (1.5×10^5 cell/well) were disseminated in 12 well dishes in the absence of FCS and cultured for 30 h with or without test drugs as indicated. The cells were pre-treated with the phospholipase C inhibitor U73122 for 30 min before the addition of carbachol. (^3H)-thymidine was applied for the last 24 h. Given are means \pm SEM of n=9-18. Significance of differences: from their respective controls, *P<0.05; **P<0.01; ***P<0.01.

A.



B.

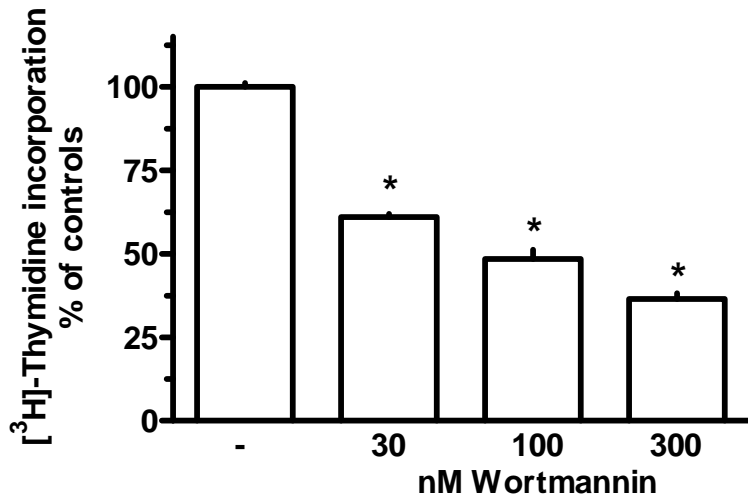


3.5.1.3 Effects of the PI3-kinase Inhibitor Wortmannin on Muscarinic Stimulation of MRC-5 Human Lung Fibroblast Proliferation

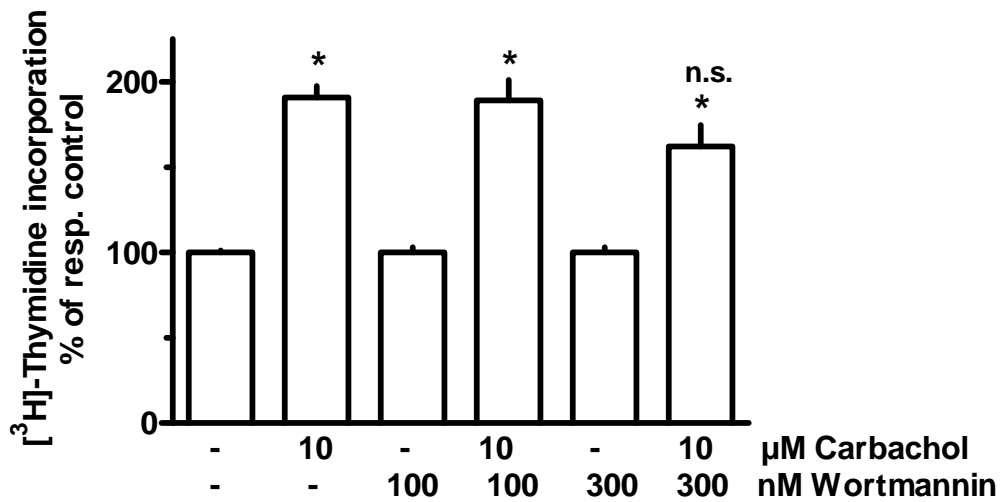
Phosphoinositide 3-kinases (PI3-kinases or PI3Ks) are a family of related enzymes that are capable of phosphorylating the 3 position hydroxyl group of the inositol ring of phosphatidylinositol. Several studies have documented the activation of the MAPK via PI-3 kinase. To investigate the role of PI-3 kinase in the muscarinic stimulation of proliferation in MRC-5 human lung fibroblasts (^3H)-thymidine incorporation assays were performed using the PI3-kinase inhibitor wortmannin. Cells in early passages were used in these experiments. Cells were disseminated (1.5×10^5 cells per well) in 12 well dishes in the absence of FCS and cultured for 30 hours with or without the test drugs. The PI3-kinase inhibitor wortmannin was added 30 minutes prior to the addition of carbachol ($10 \mu\text{M}$) in concentrations of 30, 100 and 300 nM. As shown in Figure 12 (A + B) carbachol caused an increase in the (^3H)-thymidine incorporation by $191 \pm 7\%$ whereas the PI3-kinase inhibitor wortmannin reduced the (^3H)-thymidine incorporation significantly to $61 \pm 1\%$, $48 \pm 3\%$ and $37 \pm 2\%$ at 30, 100 and 300 nM concentrations relative to the control. However the PI3-kinase inhibitor wortmannin did not inhibit the carbachol induced stimulation of (^3H)-thymidine incorporation (increase to $189 \pm 12\%$) in the presence of U73122 (100 nM). The effect of wortmannin (300 nM) on the carbachol induced proliferation could not be considered as a consistent result since the magnitude of the effect showed considerable variation and was not significantly different from respective value in the absence of wortmannin.

Figure 12 A + B. Effects of the PI3-kinase Inhibitor Wortmannin on Muscarinic Stimulation of MRC-5 Human Lung Fibroblast Proliferation. Cells (1.5×10^5 cell/well) were disseminated in 12 well dishes in the absence of FCS and cultured for 30 h with or without test drugs as indicated. The cells were pre-treated with PI3-kinase inhibitor wortmannin for 30 min before the addition of carbachol. (^3H)-thymidine was applied for the last 24 h. Given are means \pm SEM of n=9-18. Significance of differences: from controls, *P<0.01; n.s., not significantly different from respective value in absence of wortmannin.

A.



B.

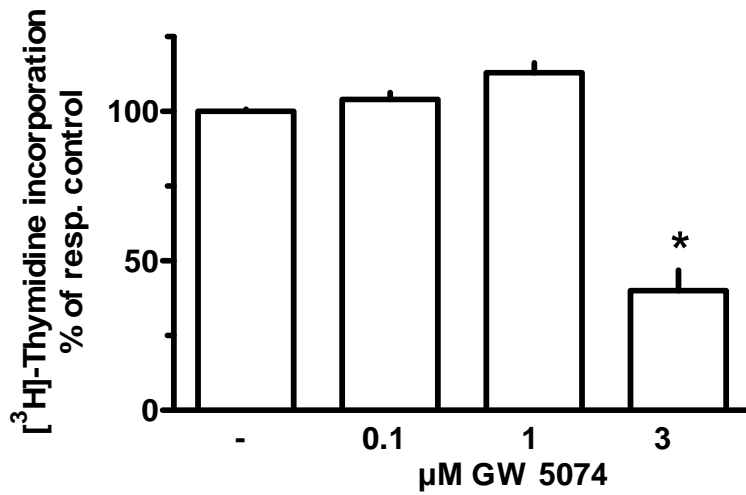


3.5.1.4 Effects of the Raf-1 Inhibitor GW5074 on Muscarinic Stimulation of MRC-5 Human Lung Fibroblast Proliferation

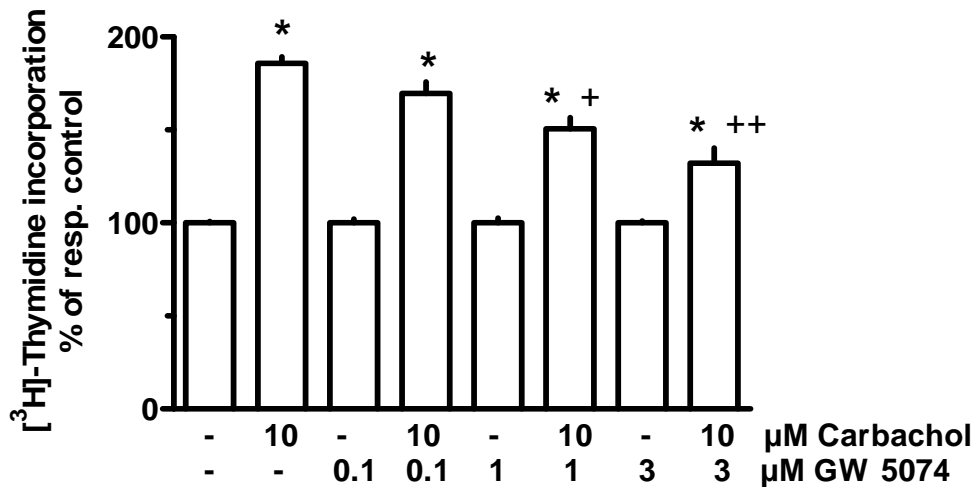
The RAS/RAF/MEK/ERK signal transduction pathway is a conserved pathway that regulates cell growth and signaling. Previous studies have shown the involvement of Ras and Raf in the G_i-coupled acetylcholine muscarinic M₂ receptor activation of MAPK, also Ras-independent activation of MAPK mediated via the Raf-MEK-MAPK have been reported. To study the role of Raf in the muscarinic stimulation of proliferation in MRC-5 human lung fibroblasts (³H)-thymidine incorporation assay was employed using the Raf-1 inhibitor GW5074. Early passages of MRC-5 cell up to passage 10 were used for the purpose of these experiments. Cells were disseminated (1.5×10^5 cells per well) in 12 well dishes in the absence of FCS and cultured for 30 hours with or without the test drugs. The Raf-1 inhibitor GW5074 was added 30 minutes prior to the addition of carbachol (10 μM) in concentrations of 0.1, 1 and 3 μM. as indicated in Figure 13 A +B. carbachol induced a proliferative stimuli, increasing the (³H)-thymidine incorporation to $167 \pm 6\%$ with respect to the control. The Raf-1 inhibitor GW5074 did not affect the basal proliferation rate at 0.1 and 1 μM although at a 3 μM concentration it inhibited the (³H)-thymidine incorporation to $40 \pm 7\%$ relative to the control. It was also observed that the carbachol induced muscarinic stimulation of proliferation was significantly inhibited by GW5074 at 1 and 3 μM as shown by the reduction in the (³H)-thymidine incorporation to $151 \pm 6\%$ and $132 \pm 8\%$ in the presence of the drug respectively.

Figure 13 A + B. Effects of the Raf-1 inhibitor GW 5074 on muscarinic stimulation of MRC-5 Human Lung Fibroblast proliferation. Cells (1.5×10^5 cell/well) were disseminated in 12 well dishes in the absence of FCS and cultured for 30 h with or without test drugs as indicated. The cells were pre-treated with Raf-1 inhibitor GW5074 for 30 min before the addition of carbachol. (^3H)-thymidine was applied for the last 24 h. Given are means \pm SEM of n=9-27. Significance of differences: from controls, *P<0.01; from the respective value in absence of GW5074, +P<0.05; ++P<0.01.

A.



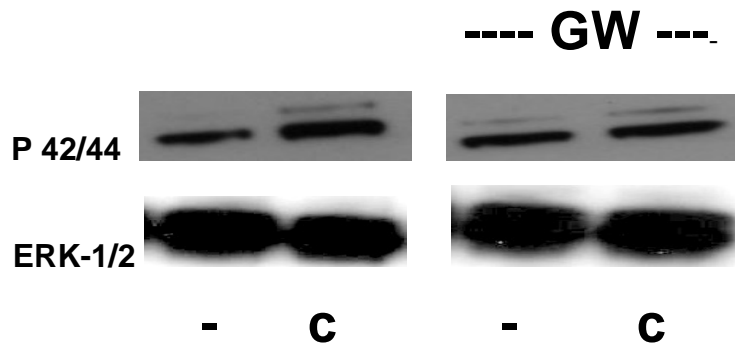
B.



3.5.1.5 Effects of the Raf-1 Inhibitor GW5074 (GW) on Muscarinic Stimulation of the ERK-MAP Kinase in MRC-5 Human Lung Fibroblasts

Western blot analysis was performed to confirm the inhibitory effect of the Raf-1 inhibitor GW5074 on the activation of the MAPK cascade in response to the muscarinic stimulation induced proliferation in the MRC-5 fibroblasts at the protein levels. Western blot analysis conducted after a two minute stimulation of serum-starved MRC-5 fibroblasts with carbachol (10 μ M) demonstrated activation of p42/44 MAPK (ERK1, ERK2). Densitometrical quantification of the p-44/42 bands was performed and values (arbitrary units) revealed that carbachol (10 μ M) enhanced p-44/42 MAPK to $249 \pm 61\%$ (n =3) while GW5074 by itself did not appear to affect the MAPK activation with respect to the control, the carbachol enhanced p-44/42 MAPK was reduced to $186 \pm 36\%$ (n = 3) in the presence of the Raf-1 inhibitor.

Figure 14. Effects of the Raf-1 inhibitor GW5074 (GW) on muscarinic stimulation of the ERK-MAP kinase in MRC-5 Human Lung Fibroblasts. Cells were cultured in a 55 mm² dishes to nearly confluence, serum-starved for 24 h and exposed to 10 μ M carbachol (C) in absence or presence of 3 μ M GW5074 or vehicle (Ctr) for 2 minutes. Cell lysates were prepared and 20-50 μ g were separated in 10-20% acrylamide Tris-glycine gels, immobilised to PVDF membranes and detected by antibodies specific for phosphorylated MAPK (P-44/42) and unphosphorylated MAPK (ERK1/2).

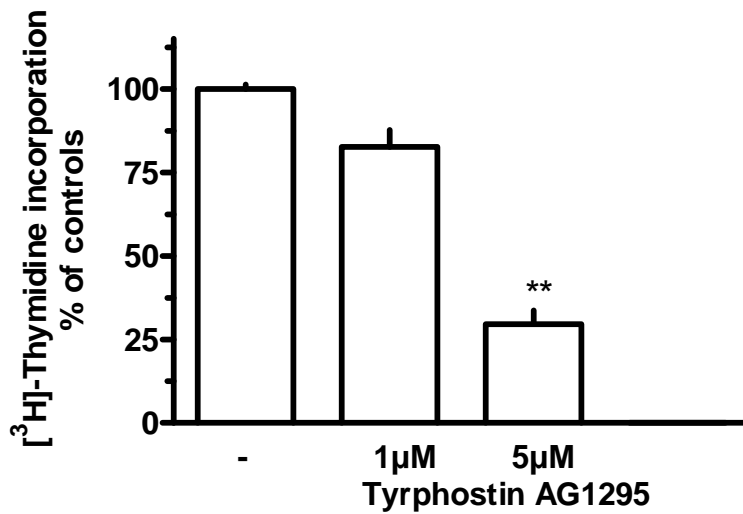


3.5.1.6 Effects of the Tyrosine-Kinase Inhibitor Tyrphostin AG1295 on Muscarinic Stimulation of MRC-5 Human Lung Fibroblasts

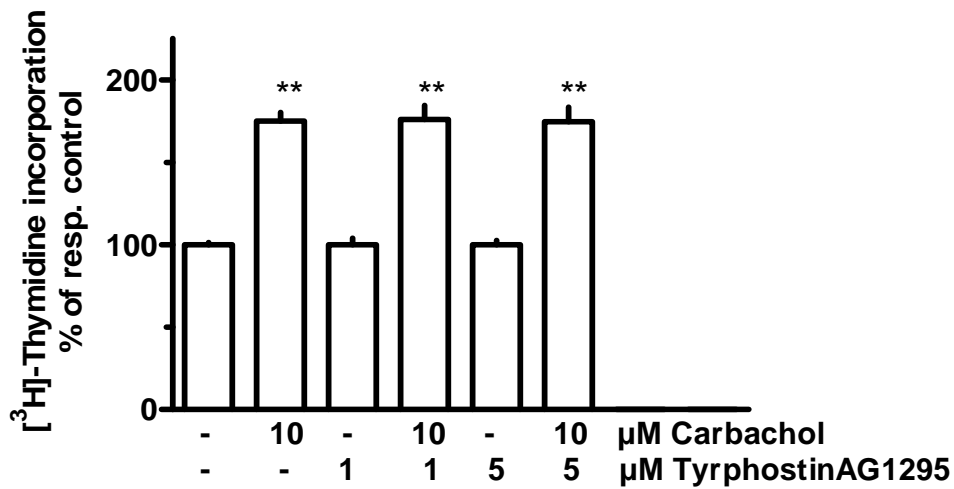
Protein tyrosine kinases (PTKs) play a key role in normal cell and tissue development. Enhanced PTK activity is intimately correlated with cell proliferation. Numerous studies have shown that GPCRs may utilize receptor tyrosine kinases (RTKs) such as platelet derived growth factor receptor (PDGF) or epidermal derived growth factor receptor (EGFRs) as intermediate signaling proteins thereby mimicking the signaling pathways downstream leading to activation of MAPK cascade. To investigate whether muscarinic stimulation of MRC-5 human lung fibroblast lead to the transactivation of PDGF receptor, (³H)-thymidine incorporation assays were performed in the presence or absence of tyrphostin AG1295 a specific tyrosine kinase inhibitor for PDGF receptors. As shown in Figure 15 A + B. carbachol (10 μM) caused an increase in the (³H)-thymidine incorporation to 175 ± 5% while tyrphostin AG1295 (5 μM) inhibited (³H)-thymidine incorporation to 29 ± 4% with respect to the control. However the tyrphostin AG1295 the tyrosine kinase inhibitor did not inhibit the carbachol induced stimulation of (³H)-thymidine incorporation (increase to 175 ± 9%) in the presence of tyrphostin AG1295 (5 μM). In a further set of control experiments (data not shown [n = 3]) it was observed that the PDGF (10 ng/ml) induced increase in (³H)-thymidine incorporation in MRC-5 human lung fibroblast was unimpeded in the presence of tiotropium (1 μM), confirming its selectivity in inhibition of carbachol induced muscarinic proliferation of MRC-5 human lung fibroblast.

Figure 15 A + B Effect of tyrosine-kinase inhibitor tyrphostin AG1295 on muscarinic stimulation of MRC-5 human lung fibroblast. Cells (1.5×10^5 cell/well) were disseminated in 12 well dishes in the absence of FCS and cultured for 30 h with or without test drugs as indicated. The cells were pre-treated with tyrosine kinase inhibitor AG1295 for 30 min before the addition of carbachol. (^3H)-thymidine was applied for the last 24 h. Given are means \pm SEM of n=9-18. Significance of differences: from controls, **P<0.01

A.



B.



3.6 Muscarinic Stimulation of proliferation of MRC-5 Human Lung Fibroblast and Anti-apoptotic effects

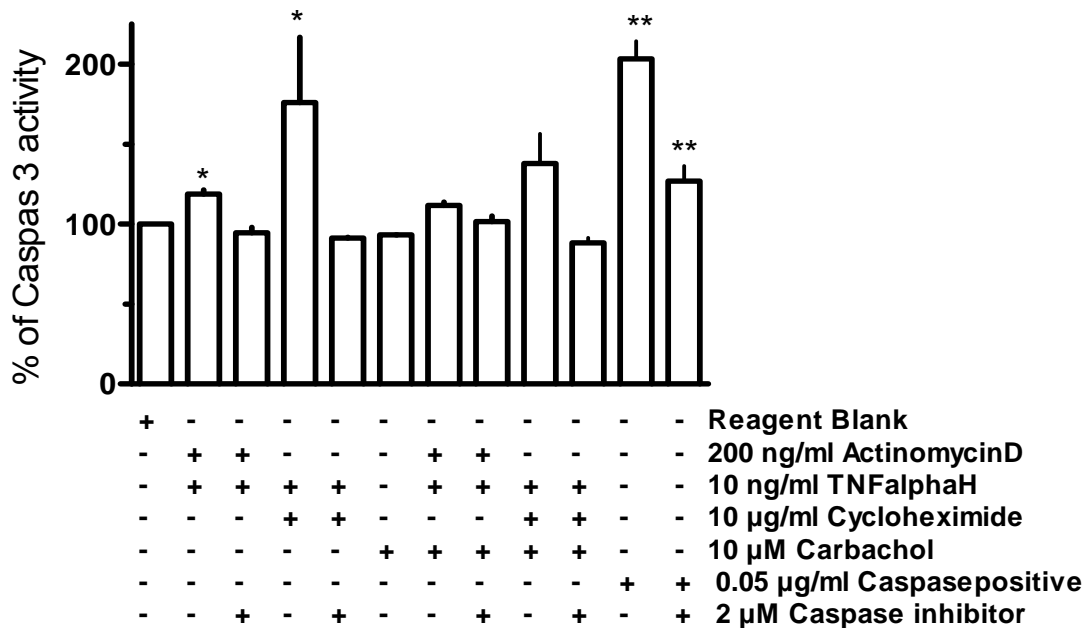
Apoptosis represents a multi-step process for elimination and subsequent removal of cells in response to environment insults or as part of organismal development. The caspases are a family of proteins that are one of the main executors of the apoptotic process. They belong to a group of enzymes known as cysteine proteases which can be activated following the occupation of certain cell surface 'death' receptors (e.g. tumor necrosis factor) or by agents that induce stress or DNA damage (e.g. actinomycin D, cycloheximide). A member of this family, caspase-3 has been identified as being a key mediator of apoptosis of mammalian cells. The previous experiments that were performed clearly indicated the functional role of the muscarinic receptors in the carbachol induced proliferation of the MRC-5 human lung fibroblasts cells. Various studies performed in the past have confirmed the anti-apoptotic effects of the G-protein coupled muscarinic receptor activation

The next aspect that was explored was whether the proliferative stimuli mediated via the muscarinic receptors in the MRC-5 fibroblasts were augmented by an anti-apoptotic effect concomitantly. For this purpose caspase-3 fluorimetric assays were performed using a combination of apoptosis inducers like TNF α , actinomycin D and cycloheximide in the presence or absence of the muscarinic agonist carbachol. MRC-5 cells (4×10^4 cells/well) were disseminated in 24-well dishes in the presence of 10% FCS, upon confluence the medium was aspirated out cells were treated with apoptosis inducers in the presence or absence of carbachol (10 μ M) as indicated in Figure 16, and incubated further for 4 hours under serum-free conditions followed by lysis and treatment with the substrate. Two wells for substrate blank, two for caspase positive control and two for caspase positive in combination with the caspase inhibitor were also prepared for every experiment. As shown in Figure 16, actinomycin D in presence of TNF α and cycloheximide in combination with TNF α enhanced caspase-3 activity to $119 \pm 2\%$, $176 \pm 40\%$ respectively relative to the control. The positive control showed an increased caspase-3 activity to $203 \pm 11\%$ which was reduced to $127 \pm 10\%$

with respect to the control in the presence of the caspase inhibitor. Nonetheless it was observed that carbachol (10 μ M) did not significantly affect the level of caspase-3 activity in the presence of the either of the two combinations of the apoptosis inducers. Although these results seem to suggest that the carbachol induced muscarinic proliferation of MRC-5 human lung fibroblasts is unaided by anti-apoptotic mechanisms the magnitude of the effect showed considerable variations hence could not be considered conclusive.

Figure 16. Effects of various apoptosis inducers on muscarinic stimulation of MRC-5 Human Lung Fibroblast using caspase-3 fluorimetric assay.

Cells (4×10^4 cell/well, passages 14, 15 and 16)) were disseminated in 24 well dishes in the presence of 10% FCS upon confluence the medium was changed to serum free with the addition of TNF α (TNF α H) 10 ng/ml, Actinomycin D 200 ng/ml, Cycloheximide 10 μ g/ml, Carbachol 10 μ M, Caspase positive 0.05 μ g/ml and Caspase inhibitor 2 μ M as indicated and incubated for 4 h followed by lysis and substrate addition. Given are means \pm SEM of n = 6 for 3 sets of experiments. Significance of differences: from controls, *P<0.05, **P<0.01 (paired t-test).



3.7 Nicotinic Receptor Expression and Function in MRC-5 Human Lung Fibroblasts

Semi-quantitative RT-PCR's were performed to determine the expression pattern of the mRNA encoding for the different nicotinic receptors subunit subtypes in MRC-5 fibroblast cell line. Total RNA was isolated as described previously and first-strand cDNA was synthesized using Omniscript reverse transcriptase. Then the PCR amplification was carried out using specific oligonucleotide primers for human nicotinic receptors (α_1 - α_7 , α_9 , α_{10} and β_1 - β_4) or β -actin in a programmable thermal cycler set to 23 cycles for β -actin and 35 cycles for nicotinic receptors. Positive controls were performed for every PCR using genomic DNA (gDNA) isolated for MRC-5 cells and one PCR lacking template DNA was regularly performed as a negative control. Table B, shows the PCR product size and the specific annealing temperature for the primers pairs employed.

As shown in Figure 17 A + B, MRC-5 fibroblasts express mRNA encoding different nicotinic receptor subunit subtypes. The most prominent expression was found for mRNA encoding α_1 subunit, followed by α_7 , α_5 subunit transcripts respectively. Slightly lower expression of mRNA encoding for α_3 and β_1 subunit was also observed. The expression pattern for the mRNA encoding the nicotinic receptors subunit subtypes was found to be consistent under the culture conditions, as a similar pattern was found in different passages (passages 5-7). Studies conducted previously have implicated α_7 nicotinic receptors subunits increased expression associated with lung fibroblast proliferation. To explore the possibility of a cross talk between the muscarinic and nicotinic receptors expressed in the MRC-5 fibroblast cells (^3H)-thymidine incorporation assays were performed using nicotinic agonist and antagonist in the presence or absence of carbachol. Nicotine did not appear to either affect proliferation by itself nor in the presence of carbachol (data not shown) although there was some indication that the muscarinic agonist carbachol induced increase in (^3H)-thymidine incorporation was supplemented in the presence of hexamethonium a nicotinic antagonist, but the extent of the effect showed considerable variation over a range of experiments making it impossible to be considered as a true effect.

Table B

Receptor	Primer pair	Product size (bp)	Annealing temperature °C
$\text{h}\alpha_1$	α_1 -hnAChr-s α_1 -hnAChr-as	233	55
$\text{h}\alpha_3$	α_3 -hnAChr-s α_3 -hnAChr-as	419	52
$\text{h}\alpha_5$	α_5 -hnAChr-s α_5 -hnAChr-as	324	64
$\text{h}\alpha_7$	α_7 -hnAChr-s α_7 -hnAChr-as	308	55
$\text{h}\beta_1$	β_1 -hnAChr-s β_1 -hnAChr-as	455	51.9

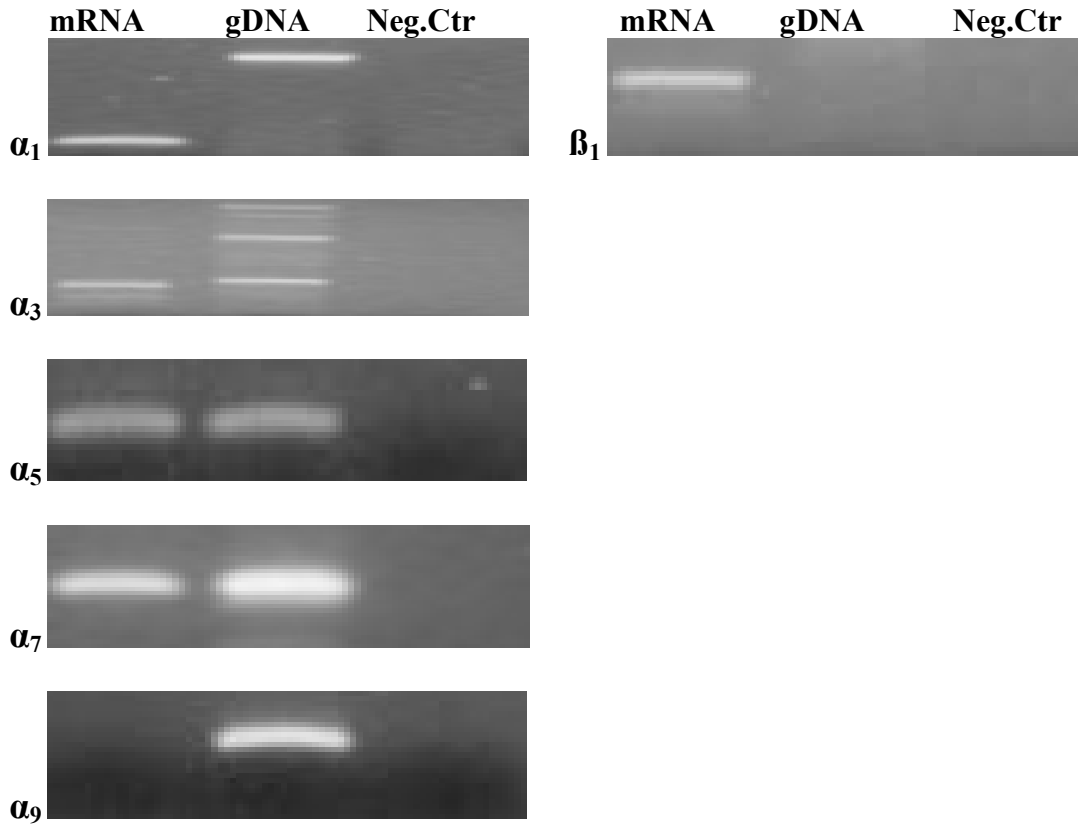
Figure 17. Expression of human nicotinic receptors in MRC-5 Human Lung Fibroblasts.

A. Samples of RT-PCRs of human nicotinic receptors on RNA isolated from MRC-5 human lung fibroblasts. Cells were grown in 55-mm culture dishes to confluence, total RNA was isolated, treated with DNase, and used for RT-PCR with primers specific for the human nicotinic receptors or β -actin. To control effectiveness of primer pairs, PCRs were also performed on genomic DNA (gDNA) isolated from MRC-5 cells. One PCR lacking template DNA was regularly performed to account for any contamination (negative control, -Ctr.). PCR products were separated on a 1.2% agarose gel.

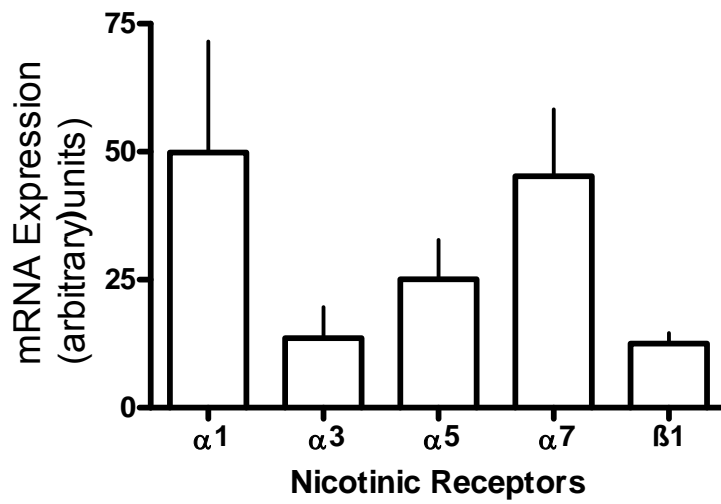
B. Densitometric evaluation of a series of experiments. Given are mean values (+SEM) of three experiments performed with cells of passages 5-7. Values were normalized for β -actin to correct for quality of cDNA preparation

Figure 17.

A.



B.



4. Discussion

4.1 Muscarinic Receptor Expression in Human Lung Fibroblasts

Almost every cell type in the lung and airways expresses cholinceptors, but expression of muscarinic receptors in lung fibroblasts has not been characterized yet. For this purpose semi-quantitative RT-PCR's were performed using both the MRC-5 as well as the primary human lung fibroblasts. Our results demonstrated that muscarinic receptors were expressed in both MRC-5 and primary human lung fibroblasts. In both, the cell line and primary cells the strongest mRNA expression was observed for M₂ receptor, whereas some gradual differences were found with regard to the other muscarinic receptors. In MRC-5 cells the levels of mRNA encoding M₃ receptor appeared to be higher than in the primary cells, which on the other hand seem to express a clear message for M₁ receptor. As mentioned before the genes of muscarinic receptors are intronless. Therefore, the RNA preparations were treated with DNase prior to the RT reaction to exclude any contamination with genomic DNA. The differential expression pattern observed in the present study, in particular the lack of PCR products accounting for M₁ and M₅ receptors in MRC-5 and primary lung fibroblasts, respectively, argues against an artefact. Moreover, in MRC-5 cells the expression of M₂ and M₃ receptors could be confirmed at the protein level by Western blot analysis. Finally to confirm the regional expression pattern of mRNA encoding for muscarinic receptors M₂ and M₃ semi-quantitative RT-PCRs were performed using primary fibroblast cultures obtained from peripheral and distal region of the human lung and our results showed that again in this case mRNA encoding M₂ receptor subtype was dominantly expressed followed by a slightly lower expression of mRNA encoding for M₃ receptor subtype.

4.2 Muscarinic Stimulation of Proliferation of Human Lung Fibroblasts

Subsequent to our findings that human lung fibroblasts expressed muscarinic receptors we investigated further to see if these receptors did play a part in mediating proliferative response. For this purpose proliferation studies were performed using a range of protocols to determine the optimal parameters which

then could be set as a standard for the remaining proliferation studies that would ensue. The proliferation of lung fibroblasts in vitro largely depends on the presence of FCS which obviously contains a cocktail of diverse factors promoting fibroblast growth. Consequently, the effects of muscarinic agonists were first tested in FCS-deprived conditions, i.e. in absence of other mitogenic stimuli. Under these conditions carbachol and oxotremorine caused an increase in (³H)-thymidine incorporation in MRC-5 cells and primary human lung fibroblasts. In both cell types, the proliferative effects of carbachol or oxotremorine were blocked by the muscarinic antagonist atropine and the long acting muscarinic antagonist tiotropium at concentrations at least 10- and 100-fold lower than those of the agonists, proving the involvement of specific muscarinic receptors. The antagonists had no effect on their own, which excludes significant effects of non-neuronal acetylcholine under the present culture conditions.

In MRC-5 cells the muscarinic stimulation of proliferation was studied in more detail. The stimulatory effect of carbachol appeared to be somewhat more pronounced when the drug was added after dissemination isochronal to FCS-deprivation and when it was present already prior to the (³H)-thymidine exposure compared to conditions where the agonist was applied at the same time with (³H)-thymidine only for the last part of the incubation period. This may suggest that the muscarinic mitogenic stimulus is slowly developing, but long lasting. A mitogenic effect of muscarinic agonists has also been demonstrated on airway smooth muscle (10, 11), but in contrast to the present observations on fibroblasts, muscarinic agonists alone showed no proliferative effect in airway smooth muscle, but augmented the effect of other mitogenic stimuli such as platelet-derived growth factor (PDGF) or epidermal growth factor (EGF). The present experiments showing that the proliferative effects of carbachol and oxotremorine were basically the same in absence or presence of 1% FCS, indicate that in human lung fibroblasts the proliferative effects induced by muscarinic receptor activation may be additive to proliferative effects caused by other mitogenic stimuli.

4.3 Inhibition of Muscarinic Proliferation using Receptor Sub-Type Specific Antagonists in MRC-5 Human Lung Fibroblasts and Effect of Pertussis Toxin on Muscarinic Stimulation of Proliferation of Human Lung Fibroblasts

Our previous results indicate that human lung fibroblasts do express muscarinic receptors and that they mediated proliferative effects. Both, M_2 and/or M_3 receptors have been shown to mediate activation of the mitogen-activated protein kinase/extracellular signal-regulated kinase 1/2 pathway (188, 190, 191), which is known to mediate proliferative responses in various cell types (192, 193, 194). In order to characterize the muscarinic receptor subtype mediating the proliferative effect in MRC-5 fibroblasts the M_2/M_4 receptor preferring antagonists AF-DX 384, AQ-RA 741 and himbacine, the M_3/M_1 receptor preferring antagonists 4-DAMP and p-FHHSiD and the M_1/M_4 receptor preferring antagonist pirenzepine were tested in addition to tiotropium. It should be emphasized that the subtype selectivity of the currently available “selective” muscarinic receptor antagonists is rather limited. Usually they show a relatively high potency at least for two of the five muscarinic receptors and the potency difference to the other muscarinic receptors is only about one order of magnitude. Nonetheless, comparing the potency of a series of subtype preferring antagonists is an approach to deal with this problem (195). When the antagonist potencies as observed in the present experiments were correlated to their reported affinity constants on cloned human muscarinic receptors (71, 196), by far the best correlation was obtained for the M_2 receptor, supporting the assumption that this muscarinic receptor subtype may be essential in mediating the proliferative effects. This correlates well with the observation that at the mRNA level M_2 receptors represented the major muscarinic receptor subtype in these cells. In line with this conclusion is also the observation, that pertussis toxin abolished the effect of carbachol, since pertussis toxin is known to inhibit $G_{i/o}$, G proteins to which only M_2 and M_4 receptors couple (196). An unspecific antiproliferative action of the PTX may be excluded, as PTX did not inhibit the proliferative effect of PDGF, which is known to exert its effects via activation of a tyrosine kinase

receptor, a class of receptors different from G-protein-coupled receptors. Therefore, the PTX-induced reduction of baseline proliferation may reflect a background activation of G_i-mediated effects, possibly caused by paracrine mediators (as, for example, chemokines) released by the fibroblasts themselves. The long-acting muscarinic antagonist tiotropium was by far the most potent antagonist. The affinity constants of tiotropium are similar for M₁, M₂ and M₃ receptors, but the dissociation of the respective receptor complexes shows different kinetics, with the longest half-life for the M₃ receptor (196). This kinetic subtype selectivity of tiotropium may not be of significance in the present experiments, because they were performed under equilibrium conditions. Whether the kinetical subtype selectivity of tiotropium is of clinical importance is still debatable (197). Because the half-life of the tiotropium-M₂ receptor complex, although shorter than that of the M₃ receptor complex, is still 3.6 hours (196), it may be expected that tiotropium causes a significant blockade of M₂ receptors in the lung under clinical conditions.

Although detailed pharmacological experiments have only been performed on MRC-5 cells, the observations that pertussis toxin abolished the proliferative effect of carbachol also in primary human lung fibroblasts and that the M₂ receptor mRNA represented the predominant muscarinic receptor mRNA in these cells as well suggest that also in primary human lung fibroblasts M₂ receptors might mediate the proliferative stimulus.

4.4 Muscarinic Receptor Stimulation and Activation of p-42/44 MAPK Pathway in Proliferation of Human Lung Fibroblast

Our findings from the present study indicate that human lung fibroblasts do indeed express muscarinic receptors and that they mediate proliferation in pertussis toxin-sensitive manner. Mitogen-activated protein kinase (MAP kinase) / extracellular signal-regulated kinase 1/2 (ERK-1/2) is one of the classical pathways mediating proliferative responses induced by various stimuli including activation of G-protein coupled receptor (192, 193, 194, 198), and also muscarinic receptors (both, M₂ and M₃) have been shown to be able to activate

this pathway (188, 190, 191). Therefore to probe if muscarinic receptor stimulation in human lung fibroblasts leads to the activation of MAPK pathway functional studies were performed using PD98059 a specific inhibitor for MAPK-activating enzyme (MEK). Our results demonstrated that the carbachol induced muscarinic proliferation in human lung fibroblasts was completely inhibited by PD98059, moreover in Western blot analysis carried out with MRC-5 human lung fibroblasts it was observed that the carbachol and oxotremorine induced activation of p-42/44 MAPK was blocked by muscarinic receptor antagonists tiotropium and atropine. These observations strongly support the conclusion that muscarinic stimulation of proliferation in human lung fibroblasts is mediated via the classical MEK-ERK MAPK cascade.

4.5 Intracellular Signaling Mechanism Involved in Muscarinic Stimulation Mediated Activation of MAPK Cascade in MRC-5 Human Lung Fibroblast Proliferation

4.5.1 Effects of the Rho-kinase Inhibitor Y27632 on Muscarinic Stimulation of MRC-5 Human Lung Fibroblast Proliferation

Our previous results demonstrated that the muscarinic stimulation of proliferation in human lung fibroblasts is mediated via the classical MEK-ERK MAPK cascade in a pertussis toxin sensitive manner. Rho a member of the family of small G-proteins has been shown to mediate cell cycle progression and proliferation via the activation of the MAPK cascade. Rho kinase, a key Rho effector has been implicated in the activation of MAPK pathway. In a previous study it was shown that inhibition of Rho kinase blocked the Ras transformation in NIH3T3 cells (144). Furthermore serotonin stimulation of bovine pulmonary artery VSMC lead to the translocation of ERK to the nucleus, and this response was inhibited by treatment with either dominant negative RhoA or the Rho kinase inhibitor Y27632 (149). Therefore to investigate the role of Rho in muscarinic stimulation mediated proliferation in MRC-5 human lung fibroblasts we performed (³H)-thymidine proliferation assay using the selective Rho kinase inhibitor Y27632. In both the protocols that were tested be it the 6 hours 10% FCS period prior to addition of

drugs or the one with the FCS free conditions for the duration of the assay it was observed that carbachol induced more than 2-fold increase in (³H)-thymidine incorporation and the Rho kinase inhibitor Y27632 by itself inhibited the basal proliferation level but failed to inhibit the carbachol induced (³H)-thymidine incorporation. These results indicate that although Rho does mediate proliferative signals in these cells, it is not involved in the muscarinic stimulation mediated activation of MAPK in MRC-5 human lung fibroblast cells.

4.5.1.2 Effects of the Phospholipase C Inhibitor U73122 on Muscarinic Stimulation of MRC-5 Human Lung Fibroblast Proliferation

The receptor mediated activation of PLC leads to the generation of two second messengers, inositol1,4,5-triphosphate (IP₃) and diacylglycerol (DAG). It has been well established that IP₃ can cause an increase in the concentration of intracellular calcium as a result of intracellular storage mobilization and DAG can activate the protein kinase C (PKC). The activation of the ERK1/2 pathway involving PKC activation following the activation of PLC pathway with production of DAG has been previously reported. Therefore we speculated a role for PLC and its generated second messengers in linking the activation of muscarinic acetylcholine receptors to downstream activation of MAPK in MRC-5 human lung fibroblast cells. To investigate the role of PLC, in the present study we performed (³H)-thymidine incorporation assays using U73122 a selective PLC inhibitor. Our results demonstrate that although the PLC inhibitor U73122 inhibited the basal level of (³H)-thymidine incorporation it failed to inhibit the carbachol induced increase in the (³H)-thymidine incorporation. Various studies have reported that PLC is the principal effector of G_q-mediated signaling. Activation of ERK1/2 by the odd numbered muscarinic receptors has been shown to typically involve PKC activation following G_{q/11} activation of PLC pathway with production of DAG. On the other hand M₂ and M₄ muscarinic receptors have been shown to produce only weak activation of PLC pathway (40, 41, 42, 199). Our previous results have indicated that the muscarinic stimulation mediated activation of MAPK in human lung fibroblasts follows a pertussis toxin sensitive mechanism via the G_{i/o} protein

which correlates well with our finding that PLC inhibition did not inhibit the carbachol induced (^3H)-thymidine incorporation in MRC-5 human lung fibroblast cells. The decrease in the basal level of (^3H)-thymidine incorporation in the presence of the PLC inhibitor U73122 could be explained possibly by the fact that U73122 could act on other sites in addition to PLC inhibition. Such mechanisms include the inhibition of both the intracellular calcium channels, which are activated by formation of IP_3 by PLC, and plasma membrane bound calcium channels (200). In the absence of carbachol stimulation, muscarinic receptor coupled PLC is inactive and thus intracellular calcium channels activated by IP_3 are closed. On the other hand plasma membrane bound calcium channels are independent of PLC activation and may play a role in transient calcium currents. Therefore, U73122 may antagonise plasma membrane calcium channels and as a result decrease the basal levels of (^3H)-thymidine incorporation.

4.5.1.3 Effects of the PI3-kinase Inhibitor Wortmannin on Muscarinic Stimulation of MRC-5 Human Lung Fibroblast Proliferation

Phosphoinositide 3-kinases (PI3-kinases or PI3Ks) are a family of related enzymes that are capable of phosphorylating the 3 position hydroxyl group of the inositol ring of phosphatidylinositol. Previously, Lopez-Illasaca et al. (1998) have demonstrated that the p42 MAPK activation by G-protein-coupled receptors can be mediated by PI3K through a process that requires G-proteins $\beta\gamma$ -subunits. The wortmannin-sensitive PI3K isoenzyme, PI3K γ , can be activated by both the α and the $\beta\gamma$ subunits of the heterotrimeric G-proteins (150). Several studies have reported on the regulation of different phosphatidylinositol kinases and phosphoinositide pools by muscarinic acetylcholine receptors. Hence to investigate whether the PI-3 kinase was crucially involved in the activation of the MAPK pathway, in the muscarinic stimulation of proliferation in MRC-5 human lung fibroblasts we performed (^3H)-thymidine incorporation assays using the PI3-kinase inhibitor wortmannin. Our results demonstrate that although PI3K is involved in mediating proliferative signals in these cells the carbachol induced

(³H)-thymidine incorporation is unaffected by the PI3K inhibitor wortmannin thus suggesting that PI3K may not be implicated in the carbachol mediated process.

4.5.1.4 Effects of the Raf-1 Inhibitor GW5074 on Muscarinic Stimulation of MRC-5 Human Lung Fibroblast Proliferation

The RAS/RAF/MEK/ERK signal transduction pathway is a conserved pathway that regulates cell growth and signaling. Previous studies have shown the involvement of Ras and Raf in the G_i-coupled acetylcholine muscarinic M₂ receptor activation of MAPK, also Ras-independent activation of MAPK mediated via the Raf-MEK-MAPK have been reported. Hence to elucidate the role of Raf in the muscarinic stimulation of proliferation in MRC-5 human lung fibroblasts we performed (³H)-thymidine incorporation using the Raf-1 inhibitor GW5074. Our results demonstrated Raf-1 inhibitor GW5074 did not affect the basal proliferation rate at 0.1 and 1 μM although at a 3 μM concentration it inhibited the (³H)-thymidine incorporation to 40 ± 7% relative to the control. It was also observed that the carbachol induced muscarinic stimulation of proliferation was significantly inhibited by GW5074 at 1 and 3 μM as shown by the reduction in the (³H)-thymidine incorporation to 151 ± 6% and 132 ± 8% in the presence of the drug respectively. Furthermore Western blot analysis carried out to confirm the inhibitory effect of the Raf-1 inhibitor on the activation of the MAPK cascade in response to the muscarinic stimulation induced proliferation in the MRC-5 fibroblasts at the protein levels showed that while GW5074 by itself did not appear to affect the MAPK activation, the carbachol induced increase in MAPK activity was inhibited in the presence of the Raf-1 inhibitor. These findings show that Raf-1 is indeed involved in the muscarinic stimulation mediated activation of MAPK cascade in MRC-5 human lung fibroblast cells and is a signal upstream of the MEK-ERK-MAPK cascade. Raf proteins are the conserved signaling module that transducer signals from the cell surface to the receptor wherein the Ras family of small G-proteins have been shown to be the upstream regulators in several cell types. One of the critical steps in the Ras-Raf-MEK cascade is the post translational lipid modification of Ras which aids the Ras protein to attach to

the cell membrane; this process involves the enzyme farnesyl transferase. Hence we performed (³H)-thymidine incorporation assays using farnesyl transferase inhibitors, however the inhibitor of Ras farnesyl transferase FTI-277 (up to 3 μM) did not affect carbachol-stimulated (³H)-thymidine incorporation, whereas manumycin, a chemically different Ras inhibitor, exerted large cytotoxic effects. Therefore making it impossible to draw any conclusions about the role of Ras in the muscarinic stimulation mediated activation of MAPK in MRC-5 human lung fibroblast cells.

4.5.1.5 Effects of the Tyrosine-Kinase Inhibitor Tyrphostin AG1295 on Muscarinic Stimulation of MRC-5 Human Lung Fibroblasts

Receptor transactivation refers to the ability of a primary agonist, via binding to its receptor, to activate a receptor for another ligand via signaling events. Transactivation of various growth factor receptors, including the epidermal growth factor receptor (EGFR), and the platelet derived growth factor (PDGF), by G-protein-coupled receptors has been documented in multiple cellular model systems (163, 164, 165, 166, 167). Studies have shown that GPCRs may utilize receptor tyrosine kinases (RTKs) such as platelet derived growth factor receptor (PDGF) or epidermal derived growth factor receptor (EGFRs) as intermediate signaling proteins thereby mimicking the signaling pathways downstream leading to activation of MAPK cascade. To explore the possibility of whether muscarinic stimulation of MRC-5 human lung fibroblast lead to the transactivation of PDGF receptor, (³H)-thymidine incorporation assays were performed using tryphostin AG1295 a specific tyrosine kinase inhibitor for the PDGF receptors. Our findings show that although tryphostin AG1295 inhibited the basal level of (³H)-thymidine incorporation it did not inhibit the carbachol induced (³H)-thymidine incorporation excluding transactivation of receptor tyrosine kinase as a signaling pathway mediated via the carbachol stimulated G-protein coupled stimulation of MRC-5 human lung fibroblast cells. Studies performed by other groups in our laboratory using human lung fibroblasts showed that PDGF (10 ng/ml) induced almost a one fold increase in the (³H)-thymidine incorporation confirming its strong

stimulatory effect on proliferation and this effect was potently inhibited by the tyrosine kinase inhibitor tyrphostin AG1295 (5 μ M). In a further set of control experiments it was observed that the PDGF induced increase in (3 H)-thymidine incorporation in MRC-5 human lung fibroblast was unimpeded in the presence of tiotropium confirming its selectivity in inhibition of carbachol induced muscarinic proliferation of MRC-5 human lung fibroblast.

4.6 Muscarinic Stimulation of Proliferation of MRC-5 Human Lung Fibroblast and Anti-apoptotic Effects

Apoptosis represents a multi-step process for elimination and subsequent removal of cells in response to environment insults or as part of organismal development. Pro-apoptotic signaling may be mediated by the specific ligands and surface receptors or can also be activated from inside the cell through specific cell sensors residing in the cell nucleus and cytoplasm. The caspases are a family of proteins that are one of the main executors of the apoptotic process. They belong to a group of enzymes known as cysteine proteases which can be activated following the occupation of certain cell surface 'death' receptors (e.g. tumor necrosis factor) or by agents that induce stress or DNA damage (e.g. actinomycin D, cycloheximide). A member of this family, caspase-3 has been identified as being a key mediator of apoptosis of mammalian cells. The repertoire of signaling pathways controlled by GPCRs has recently been extended by studies linking GPCRs to the regulation of apoptosis. Depending on the receptor subtypes and the cell type in which the receptor is expressed, GPCRs can either induce apoptosis or protect cells from apoptotic stimuli. Prominent among the GPCRs that protect cells from apoptotic stimuli are the subtypes of the muscarinic receptor family (186, 187). Previous studies have also shown that muscarinic receptors that couple to the $G_{q/11}$ protein (e.g. M_1 , M_3 and M_5) can protect cells from apoptosis following DNA damage whereas those coupled to the G_i -proteins (M_2 and M_4) have no protective properties (186). The previous experiments that were performed clearly indicated the functional role of the muscarinic receptors in the carbachol induced proliferation of the MRC-5

human lung fibroblasts cells. Hence we explored the possibility whether the proliferative stimuli mediated via the muscarinic receptors in the MRC-5 fibroblasts were augmented by an anti-apoptotic effect concomitantly. Our studies performed by means of the caspase-3 activity as a marker for the level of apoptotic signaling using a combination of apoptosis inducers in the presence or absence of muscarinic stimuli in MRC-5 human lung fibroblasts suggests that the muscarinic mediation of proliferation in these cells is unaided by anti-proliferative effects mediated via the muscarinic stimulation. These findings appear to correlate well with our previous findings that in MRC-5 human lung fibroblasts the muscarinic stimulation mediated proliferation is via the M₂ muscarinic receptor subtype and also literature which has attributed the anti-proliferative effects mediated via muscarinic receptors to the odd numbered muscarinic subtypes. However because of the considerably large variation in the magnitude of effects over a range of experiments it makes it difficult to positively conclude the relationship between the muscarinic stimuli mediated proliferation and its anti-apoptotic effects in MRC-5 human lung fibroblasts. We speculate that a study done on the regulation of pro/anti-apoptotic genes during muscarinic stimulation mediated proliferation in MRC-5 human lung fibroblasts might probably help shed more light on this interaction.

4.7 Nicotinic Receptor Expression and Function in MRC-5 Human Lung Fibroblasts

The α -7 nicotinic receptor subunit has been detected in many non-neuronal cells such as the bronchial epithelial cells, endothelial airway cells and airway fibroblasts (16). In vitro studies carried out on bronchial epithelial cells and pulmonary neuroendocrine cells indicated nicotinic receptor mediated activation of cell proliferation cascade (31, 32). Furthermore studies carried out on WI38 cells, a human embryonic pulmonary fibroblast cell line showed an expression of α -3 and α -7 nicotinic receptor subunits. Hence we performed semi-quantitative RT-PCRs to explore the expression pattern of nicotinic receptor subunits in MRC-5 human lung fibroblasts. Our results demonstrated the expression of α -1,

α_3 , α_5 , α_7 and β_1 nicotinic receptor subunits in MRC-5 human lung fibroblasts with the most dominant expression of α_1 subunit followed by α_7 subunit. Studies conducted previously have implicated an increased expression of α_7 subunit of nicotinic receptors with lung fibroblast proliferation. To explore the possibility of a cross talk between the muscarinic and nicotinic receptors expressed in the MRC-5 fibroblast cells we performed (^3H)-thymidine incorporation assays using nicotinic agonist and antagonist in the presence or absence of carbachol. Our results demonstrated that nicotine did not appear to either affect proliferation by itself nor in the presence of carbachol although there was some indication that the muscarinic agonist carbachol induced increase in (^3H)-thymidine incorporation was supplemented in the presence of hexamethonium a nicotinic antagonist, but the extent of the effect showed considerable variation over a range of experiments making it impossible to be considered as a true effect.

5. Conclusion

Fibrotic alteration and airway remodeling are pathological features associated with asthma and COPD and almost every cell type in the airways expresses cholinergic receptors. However, only fragmentary knowledge exists with regards to the expression and function of muscarinic receptors in pulmonary fibroblasts. To characterize the expression pattern of muscarinic receptors we performed semi-quantitative RT-PCR studies which showed that human lung fibroblasts indeed expressed muscarinic receptors with the most dominantly expressed subtype being the M_2 followed by the M_3 muscarinic receptor. Since confirming the expression of muscarinic receptors in human lung fibroblasts we explored its functional role in mediating proliferation using muscarinic agonists such as carbachol and oxotremorine and it was observed that the muscarinic stimulation indeed mediated proliferation in human lung fibroblast cells which was completely blocked in the presence muscarinic antagonist such as atropine or tiotropium. To further explore the muscarinic receptor subtype involved in mediating this proliferative response, receptor subtype characterization studies were performed using various muscarinic receptor subtype preferring antagonists. The pharmacological profile obtained by comparing the potency of several subtype preferring antagonists to inhibit the proliferative effect of carbachol with reported affinity constants of these antagonists at cloned muscarinic receptors indicated that muscarinic stimulation of proliferation of human lung fibroblasts was mediated via M_2 receptors. In line with this conclusion was the observation that pertussis toxin, known to inactivate $G_{i/o}$ proteins prevented the stimulatory effect of carbachol, both in MRC-5 cells and primary human lung fibroblasts. Mitogen-activated protein kinase (MAP kinase) / extracellular signal-regulated kinase 1/2 (ERK-1/2) is one of the classical pathways mediating proliferative responses induced by various stimuli including activation of G-protein coupled receptor and muscarinic receptors (both, M_2 and M_3) have been shown to be able to activate this pathway so we looked into this possibility. In our present study we demonstrated that in pulmonary human lung fibroblasts activation of muscarinic receptors indeed caused an increase in the

phosphorylated, i.e. activated form of the ERK-MAP kinase which was blocked by PD 98059 a specific inhibitor of the MAPK-activating enzymes (MEK) These observations strongly support the conclusion that muscarinic stimulation of proliferation in human lung fibroblasts is mediated via the classical MEK-ERK MAPK cascade. To illuminate further the signalling pathways, linking the muscarinic receptor stimulation and activation of MAPK cascade we explored several putative pathways that might be involved in this process and demonstrated the role of Raf-1 using GW5074 a specific Raf-1 inhibitor in activation of MAPK pathway in response to muscarinic stimulation in MRC-5 fibroblasts at a functional and protein level. Recently studies were carried out in our laboratory on pulmonary fibroblasts investigating whether muscarinic mechanisms were involved in collagen synthesis in turn contributing to the airway remodelling process. These studies confirmed that muscarinic stimulation indeed lead to increased collagen synthesis and activation of the MAPK cascade in a pertussiss toxin sensitive manner thus implicating a pivotal role for the M₂ muscarinic receptors in this process (201).

In conclusion, human lung fibroblasts express muscarinic receptors, which obviously mediate proliferative stimulus via a Gi/o-Raf-1-MEK-MAPK/ERK pathway, an effect which might contribute to structural changes known to occur in chronic obstructive airway diseases. Prolonged blockade of these receptors may contribute to the long term beneficial effects of anticholinergics, as observed for example, for the long-acting muscarinic antagonist, tiotropium, in COPD.

6. References

1. Saetta M, Finkelstein R, Cosio MG. Morphological and cellular basis for airflow limitation in smokers. *Eur Respir J* 1994; 7: 1505-1515.
2. Saetta M, Turato G. Airway pathology in asthma. *Eur Respir J* 2001; 18: Suppl. 34, 18s–23s.
3. Buist AS. Similarities and differences between asthma and chronic obstructive pulmonary disease: treatment and early outcomes. *Eur Respir J* 2003; 21: Suppl. 39, 30s–35s.
4. Jeffery PK. Remodeling in asthma and chronic obstructive lung disease. *Am J Respir Crit Care Med* 2001; 164: 28s–38s.
5. Barnes PJ. The role of anticholinergics in chronic obstructive pulmonary disease. *Am J Med* 2004; 20(117, Suppl. 12A): 24s–32s.
6. Kai-Michael Beeh, Tobais Welte, Roland Buhl. Anticholinergics in the treatment of chronic obstructive pulmonary disease. *Respiration* 2002; 69: 372–379.
7. Vincken W, van Noord JA, Greefhorst AP, Bantje TA, Kesten S, Korducki L, Cornelissen PJ. Improved health outcomes in patients with COPD during 1 yr's treatment with tiotropium. *Eur Respir J* 2002; 19: 209–216.
8. Anzuetto A, Tashkin D, Menjoge S, Kesten S. One-year analysis of longitudinal changes in spirometry in patients with COPD receiving tiotropium. *Pulm Pharmacol Ther* 2005; 18: 75–81.
9. Keam SJ, Keating GM. Tiotropium bromide. A review of its use as maintenance therapy in patients with COPD. *Treat Respir Med* 2004; 3(4): 247–68.
10. Krymskaya VP, Orsini MJ, Eszterhas AJ, Brodbeck KC, Benovic JL, Panettieri RA, Penn RB. Mechanisms of proliferation synergy by receptor tyrosine kinase and G protein-coupled receptor activation in human airway smooth muscle. *Am J Respir Cell Mol Biol* 2000; 23: 546–554.
11. Gosens R, Nelemans SA, Grootee Bromhaar MM, McKay S, Zaagsma J, Meurs H. Muscarinic M₃-receptors mediate cholinergic synergism of

- mitogenesis in airway smooth muscle. *Am J Respir Cell Mol Biol* 2003; 28: 257–262.
12. Gosens R, Bos IS, Zaagsma J, Meurs H. Protective effects of tiotropium bromide in the progression of airway smooth muscle remodeling. *Am J Respir Crit Care Med* 2005; 171: 1096–1102.
 13. Racké K, Matthiesen S. The airway cholinergic system: physiology and pharmacology. *Pulm Pharmacol Ther* 2004; 17: 181–198.
 14. Racké K, Juergens UR, Matthiesen S. Control by cholinergic mechanisms. *Eur J Pharmacol* 2006; 533: 57–68.
 15. Wessler I, Kirkpatrick CJ, Racké K. Non-neuronal acetylcholine, a locally acting molecule, widely distributed in biological systems: expression and function in man. *Pharmacol Ther* 1998; 77: 59–79.
 16. Carlisle DL, Hopkins TM, Gaither-Davis A, Silhanek MJ, Luketich JD, Christie NA, Siegfried JM. Nicotine signals through muscle-type and neuronal nicotinic acetylcholine receptors in both human bronchial epithelial cells and airway fibroblasts. *Respir Res* 2004; 5:27.
 17. Sekhon HS, Keller JA, Proskocil BJ, Martin EL, Spindel ER. Maternal nicotine exposure upregulates collagen gene expression in fetal monkey lung: association with $\alpha 7$ nicotinic acetylcholine receptors. *Am J Respir Cell Mol Biol* 2002; 26:31–41.
 18. Roman J, Ritzenthaler JD, Gil-Acosta A, Rivera HN, Roser-Page S. Nicotine and fibronectin expression in lung fibroblasts: implications for tobacco-related lung tissue remodeling. *FASEB J* 2004; 18:1436–1438.
 19. Catherine R, Gwilt, Louise E. Donnelly, Duncan F. Rogers. The non-neuronal cholinergic system in the airways: An unappreciated regulatory role in pulmonary inflammation? *Pharmacol Ther* (2007), doi: 10.1016/j.pharmthera.2007.05.007.
 20. Wessler I, Kirkpatrick CJ, Racké K. The cholinergic ‘pitfall’: acetylcholine, a universal cell molecule in biological systems, including humans. *Clin Exp Pharmacol Physiol* 1999; 26: 19196–19199.

21. Wessler I, Kilbinger H, Bittinger F, Kirkpatrick CJ. The biological role of non-neuronal acetylcholine in plants and humans. *Japanese Journal of Pharmacology* 2001a; 85, 2–10.
22. Wessler I, Panter H, Bittinger F, Kriegsmann J, Kirkpatrick CJ, Kilbinger H. Subcellular location of choline acetyltransferase (ChAT) and acetylcholine (Ach) in human placenta. *Naunyn-Schmiedeberg's Archives of Pharmacology* 2001b; 363, R23.
23. Kawashima K, Fujii T. The lymphocytic cholinergic system and its contribution to the regulation of immune activity. *Life Sciences* 2003; 74, 675–696.
24. Grando SA, Pittelkow MR, Schallreuter KU. Adrenergic and cholinergic control in the biology of epidermis: physiology and clinical significance. *Journal of Investigative Dermatology* 2006; 126 (9), 1948–1965.
25. Grando SA. Biological functions of keratinocyte cholinergic receptors. *Journal of Investigative Dermatology Symposium Proceeding* 1997; 2, 41–48.
26. Wessler IK, Kirkpatrick CJ. The non-neuronal cholinergic system: an emerging drug target in the airways. *Pulmonary, Pharmacology and Therapeutics* 2001; 14, 423–434.
27. Kawashima K, Fujii T. Extraneuronal cholinergic system in lymphocytes. *Pharmacology and Therapeutics* 2000; 86, 29–48.
28. Wessler I et al. Dysfunction of the non-neuronal cholinergic system in the airways and blood cells of patients with cystic fibrosis. *Life Sciences* 2007; doi: 10.1016/j.lfs.2007.01.042.
29. Conti-Tronconi BM, McLane KE, Raftery MA, Grando SA, Protti MP. The nicotinic acetylcholine receptor: structure and autoimmune pathology. *Crit Rev Biochem Mol Biol* 1994; 29:69–123.
30. Lukas RJ, Changeux JP, Le Novere N, Albuquerque EX, Balfour DJ, Berg DK, Bertand D, Chiappinelli VA, Clarke PB, Collins AC, Dani JA, Grady SR, Kellar KJ, Lindstorm JM, Marks MJ, Quik M, Taylor PW, Wonnacott S. *International Union of Pharmacology. XX. Current status of nomenclature*

for nicotinic acetylcholine receptors and their subunits. *Pharmacol Rev* 1999; 51:397–401.

31. West KA, Brognard J, Clark AS, Linnoila IR, Yang X, Swain SM, Harris C, Belinsky S, Dennis PA. Rapid Akt activation by nicotine and a tobacco carcinogen modulates the phenotype of normal human airway epithelial cells. *J Clin Invest* 2003; 111: 81–90.
32. Jull 3rd BA, Plummer HK, Schuller HM. Nicotinic receptor mediated activation by the tobacco-specific nitrosamine NNK of a Raf-1/MAP kinase pathway, resulting in phosphorylation of c-myc in human small cell lung carcinoma cells and pulmonary neuroendocrine cells. *J Cancer Res Clin Oncol* 2001; 127: 707–17.
33. Conti-Fine BM, Navaneetham D, Lei S, Maus AD. Neuronal nicotinic receptors in non-neuronal cells: new mediators of tobacco toxicity? *Eur J Pharmacol* 2000; 393: 279–94.
34. Zia S, Ndoye A, Nguyen VT, Grando SA. Nicotine enhances expression of α_3 , α_4 , α_5 , and α_7 nicotinic receptors modulating calcium metabolism and regulating adhesion and motility of respiratory epithelial cells. *Res Commun Mol Pathol Pharmacol* 1997; 97: 243–62.
35. Wang Y, Pereira EF, Maus AD, Ostlie NS, Navaneetham D, Lei S, Albuquerque EX, Conti-Fine BM. Human bronchial epithelial and endothelial cells express α_7 nicotinic acetylcholine receptors. *Mol Pharmacol* 2001; 60: 1201–9.
36. Rehan VK, Wang Y, Sugano S, Romero S, Chen X, Santos J, Khazanchi A, Torday JS. Mechanism of nicotine-induced pulmonary fibroblast transdifferentiation. *Am J Physiol Lung Cell Mol Physiol* 2005; 289: L667–L676.
37. Bonner TI. The molecular basis of muscarinic receptor diversity. *Trends Neurosci* 1989; 12: 148–51.
38. Hulme EC, Birdsall NJ, Buckley NJ. Muscarinic receptor subtypes. *Ann Rev Pharmacol Toxicol* 1990; 30: 633–73.

39. Caulfield MP, Birdsall NJM. International Union of Pharmacology. XVII. Classification of muscarinic acetylcholine receptors. *Pharmacol Rev* 1998; 50: 279–90.
40. Ashkenazi A, Peralta EG, Winslow JW, Ramachandran J, Capon DJ. Functionally distinct G proteins selectively couple different receptors to PI hydrolysis in the same cell. *Cell* 1989; Vol 56, 487–493.
41. Tietje KM, Goldman PS, Nathanson NM. Cloning and functional analysis of a gene encoding a novel muscarinic acetylcholine receptor expressed in chick heart and brain. *J Biol Chem* 1990; Vol 265. Issue 5, 2828–2834.
42. Tietje KM, Nathanson NM. Embryonic chick heart expresses multiple acetylcholine receptor subtypes. Isolation and characterization of a gene encoding a novel m₂ muscarinic acetylcholine receptor with high affinity for pirenzepine. *J Biol Chem* 1991; Vol 266, Issue 26, 17382–17387.
43. Katz A, Wu D, Simon MI. Subunits $\beta\gamma$ of heterotrimeric G protein activate β 2 isoform of phospholipase C. *Nature* 1992; 360: 686–689.
44. Felder CC. Muscarinic acetylcholine receptors: signal transduction through multiple effectors. *FASEB J* 1995; 9: 619–25.
45. Kubo T, Fukuda K, Mikami A, Maeda A, Takahashi H, Mishina M, Haga T, Haga K, Ichiyama A, Kangawa K, Matsuo H, Hirose T, Numa S. Cloning, sequencing and expression of complementary DNA encoding the muscarinic acetylcholine receptor. *Nature* 1986a; 323: 411–416.
46. Kubo T, Maeda A, Sugimoto K, Akiba I, Mikami A, Takahashi H, Haga T, Haga K, Ichiyama A, Kangawa K, Matsuo H, Hirose T, Numa S. Primary structure of porcine primary muscarinic acetylcholine receptor deduced from the cDNA sequence. *FEBS Lett* 1986b; 209: 367–372.
47. Bonner TI, Buckley NJ, Young AC, Brann MR. Identification of a family of muscarinic acetylcholine receptor genes. *Science* 1987; 237: 527–532.
48. Bonner TI, Young AC, Brann MR, Buckley NJ. Cloning and expression of the human and rat m₅ muscarinicacetylcholine receptor genes. *Neuron* 1988; 1: 403 – 410.

49. Peralta EG, Ashkenazi A, Winslow JW, Smith DH, Ramachandran J, Capon DJ. Distinct primary structures, ligand binding properties and tissue-specific expression of four human muscarinic acetylcholine receptors. *EMBO J* 1987; 6: 3923–3929.
50. Hall JM, Caulfield MP, Watson SP, Guard S. Receptor subtypes or species homologues: Relevance to drug discovery. *Trends Pharmacol Sci* 1993; 14: 376–383.
51. Eglen RM, Hedge SS, Watson N. Muscarinic receptor subtypes and smooth muscle function. *Pharmacol Rev* 1996; 48: 531–565.
52. Curtis CA, Wheatly M, Bansal S, Birdsall NJM, Eveleigh P, Pedder EK, Poyner D, Hume EC. Propylbenzilylcholine mustard labels an acidic residue in transmembrane helix 3 of the muscarinic receptor. *J Biol Chem* 1989; 264: 489–495.
53. Spalding TA, Birdsall NJM, Curtis CAM, Hulme EC. Acetylcholine mustard labels the binding site aspartate in muscarinic acetylcholine receptors. *J Biol Chem* 1994; 269: 4092–4097.
54. Baldwin JM, Schertler GF, Unger VM. An alpha-carbon template for the transmembrane helices in the rhodopsin family of G-protein-coupled receptors. *J Mol Biol* 1997; 272: 144–164.
55. Kurtenbach E, Curtis CA, Pedder EK, Aitken A, Harris AC, Hulme EC. Muscarinic acetylcholine receptors: Peptide sequencing identifies residues involved in antagonist binding and disulphide bond formation. *J Biol Chem* 1990; 265: 13702–13708.
56. Savarese TM, Wang CD, Fraser CM. Site-directed mutagenesis of the rat m_1 muscarinic acetylcholine receptor: Role of conserved cysteines in receptor function. *J Biol Chem* 1992; 267: 11439–11448.
57. Zhu SZ, Wang SZ, Hu J, El-Fakahany EE. An arginine residue conserved in most G-protein-coupled receptors is essential for the function of the m_1 muscarinic receptor. *Mol Pharmacol* 1994; 45: 517–525.

58. Jones PG, Curtis CAM, Hulme EC. The function of a highly-conserved arginine residue in activation of the muscarinic M₁ receptor. *Eur J Pharmacol* 1995; 288: 251 – 257.
59. Lu ZL, Curtis CA, Jones PG, Pavia J, Hulme EC. The role of aspartate-arginine-tyrosine triad in the m₁ muscarinic receptor: Mutations of aspartate 122 and tyrosine 124 decreases receptor expression but do not abolish signaling. *Mol Pharmacol* 1997; 51: 234–241.
60. Haga T, Haga K, Kameyama K, Nakata H. Phosphorylation of muscarinic receptors: Regulation of G-proteins. *Life Sci* 1993; 52: 421–428.
61. Wess J. Molecular biology of muscarinic acetylcholine receptors. *Crit Rev Neurobiol* 1996; 10: 69–99.
62. Wess J, Liu J, Blin N, Yun J, Lerche C, Kostenis E. Structural basis of receptor/G-protein coupling selectivity studied with muscarinic receptors as model systems. *Life Sci* 1997; 60: 1007–1014.
63. Levey AI. Immunological localization of m₁-m₅ muscarinic receptor subtypes in the peripheral tissues and brain. *Life Sci* 1993; 52: 441–448.
64. Grimm U, Moser U, Mutschler E, Lambrecht G. Muscarinic receptors: Focus on presynaptic mechanisms and recently developed novel agonist and antagonist. *Pharmazie* 1994b; 49: 711–726.
65. Michel AD, Stefanich E, Whiting RL. Direct labeling of rat M₃ muscarinic receptors by (³H)4DAMP. *Eur J Pharmacol* 1989; 166: 459–466.
66. Lazareno S, Buckley NJ, Roberts FF. Characterization of muscarinic M₄ binding sites in rabbit lung, chicken heart and NG108-15 cells. *Mol Pharmacol* 1990; 53: 573–589. 38: 805–815.
67. Caulfield MP. Muscarinic receptors: Characterization, coupling and function. *Pharmacol Ther* 1993; 58: 319–379.
68. Kondou H, Inagaki N, Fukui H. Formation of inositol phosphates mediated by M₃ muscarinic receptors in type-1 and type-2 astrocytes from neonatal rat cerebral cortex. *Neurosci Lett* 1994; 180: 131–134.

69. Lambrecht G, Feifel R, Forth B, Strohmann C, Tacke R, Mutschler E. p-Fluoro-hexahydro-sila-difenidol: The first M₂β- selective muscarinic antagonist. *Eur J Pharmacol* 1988a; 152: 193 – 194.
70. Lambrecht G, Feifel R, Wagner-Röder M, Strohmann C, Zilch H, Tacke R, Waelbroeck M, Christophe J, Boddeke H, Mutschler E. Affinity profiles of hexahydro-sila-difenidol analogues at muscarinic receptor subtypes. *Eur J Pharmacol* 1989b; 168: 71–80.
71. Dörje F, Wess J, Lambrecht G, Tacke R, Mutschler E, Brann MR. Antagonist binding profiles of five cloned human muscarinic receptor subtypes. *The Journal of Pharmacology and Experimental Therapeutics* 1991; 256: 727–733.
72. Simon MI, Strathmann MP, Gautam N. Diversity of G proteins in signal transduction. *Science* 1991; 252: 802 – 8.
73. Gudermann T, Kalkbrenner F, Schultz G. Diversity and selectivity of receptor-G protein interaction. *Annu Rev Pharmacol Toxicol* 1996; 36: 429 – 59.
74. Clapham DE, Neer EJ. G protein βγ subunits. *Annu Rev Pharmacol Toxicol* 1997; 37: 167 – 203.
75. Wu G, Benovic JL, Hildebrandt JD, Lanier SM. Receptor docking sites for G protein βγ subunits. Implications for signal regulation. *J Biol Chem* 1998; 273: 7197 – 200.
76. Wu G, Bogatkevich GS, Mukhin YV, Benovic JL, Hildebrandt JD, Lanier SM. Identification of G βγ binding sites in the third intracellular loop of the M₃-muscarinic receptor and their role in receptor regulation. *J Biol Chem* 2000; 275: 9026 – 25.
77. Buckley NJ. Molecular pharmacology of cloned muscarinic receptors. In: SR Nahorski, ed *Transmembrane Signalling, Intracellular Messengers and Implications for Drug Development*. Wiley and Sons 1990; 11 – 30.
78. Ashkenazi A, Ramachandran J, Capon DJ. Acetylcholine analogue stimulates DNA synthesis in brain-derived cells via specific muscarinic subtypes. *Nature* 1989; 340: 146 – 150.

79. Hulme EC, Birdsall NJM, Buckley NJ. Muscarinic receptor subtypes. *Annu Rev Pharmacol Toxicol* 1990; 30: 633 – 673.
80. Baumgold J. Muscarinic receptor mediated stimulation of adenylyl cyclase. *Trends Pharmacol Sci* 1992; 13: 339 – 340.
81. Parker EM, Kameyama K, Higashijima T, Ross EM. Reconstitutively active G protein-coupled receptors purified from baculovirus-infected insect cells. *J Biol Chem* 1991; 266(1): 519 – 27.
82. Stein R, Pinkas-Kramarski R, Sokolovsky M. Cloned M1 muscarinic receptors mediates both adenylate cyclase inhibition and phosphoinositide turnover. *EMBO J* 1988; 7: 3031 – 3035.
83. Baumgold J, Fishman PH. Muscarinic receptor-mediated increase in cAMP levels in SK-N-SH human neuroblastoma cells. *Biochem Biophys Res Commun* 1988; 154: 1137 – 1143.
84. Olanas MC, Onali P. Properties of muscarinic –stimulated adenylate cyclase in rat olfactory bulb. *J Neurochem* 1992; 58: 1723 – 1729.
85. Watson EL, Singh JC, McPhee C, Beavo J, Jacobson KL. Regulation of cAMP metabolism in mouse parotid gland by cGMP and calcium. *Mol Pharmacol* 1990; 38(4): 547 – 553.
86. Ashkenazi A, Peralta EG, Winslow JW, Ramachandran J, Capon DJ. Functionally distinct G proteins selectively couple different receptors to PI hydrolysis in the same cell. *Cell* 1989; 56: 487 – 493.
87. Pieroni JP, Jacobowitz O, Chen J, Iyengar R. Signal recognition and integration by Gs stimulated adenylyl cyclases. *Curr Opin Neurobiol* 1993; 3: 345 – 351.
88. Jansson CC, Kukkonen J, Akerman KE. Muscarinic receptor-linked elevation of cAMP in SH-SY5Y neuroblastoma cells is mediated by Ca²⁺ and protein kinase C. *Biochem Biophys Acta* 1991; 1095 (3): 255 – 260.
89. Baumgold J. Muscarinic receptor-mediated stimulation of adenylyl cyclase. *Trends Pharmacol Sci* 1992; 13: 339 – 340.
90. Meeker RB, Harden TK. Muscarinic cholinergic receptor-mediated activation of phosphodiesterase. *Mol Pharmacol* 1982; 22: 310 – 319.

91. Rhee SG, Choi KD. Regulation of inositol phospholipid-specific phospholipase C isozymes. *J Biol Chem* 1992; 267: 12393 – 12396.
92. Lambert DG, Burford NT, Nahorski SR. Muscarinic receptor subtypes: inositol phosphates and intracellular calcium. *Biochem Soc Trans* 1992; 20: 130 – 135.
93. Berstein G, Blank JL, Smrcka A, Higashijima T, Sternweis PC, Exton JH, Ross BJ, De Jong P, Reed RR, Simon MI. G protein α subunit multi gene family. *Nat Genet* 1992; 1: 85 – 91.
94. Sawaki K, Hiramatsu Y, Baum BJ, Ambudkar IS. Involvement of $G_{\alpha_q/11}$ in m_3 -muscarinic receptor stimulation of phosphatidylinositol 4,5 bisphosphate-specific phospholipase C in rat parotid gland membranes. *Arch Biochem Biophys* 1993; 305: 546 – 550.
95. Hildebrandt JP, Shuttleworth TJ. A G_q -type G protein couples muscarinic receptors to inositol phosphate and calcium signaling in exocrine cells from avian salt glands. *J Membr Biol* 1993; 133: 183 – 190.
96. Gusovsky F, Lueders JE, Kohn EC, Felder CC. Muscarinic receptor-mediated tyrosine phosphorylation of phospholipase C-gamma. *J Biol Chem* 1993; 268: 7768 – 7772.
97. Dell'Acqua ML, Carroll RC, Peralta EG. Transfected m_2 muscarinic acetylcholine receptors couple to G α_{i2} and G α_{i3} in Chinese hamster ovary cells. Activation and desensitization of the phospholipase C signaling pathway. *J Biol Chem* 1993; 268: 5676 – 5685.
98. Katz A, Wu D, Simon MI. Subunits beta gamma of heterotrimeric G protein activate beta isoform of phospholipase C. *Nature* 1992; 360: 686 – 689.
99. Cohen RI, Almazan G. Rat oligodendrocytes express muscarinic receptors coupled to phosphoinositide hydrolysis and adenylyl cyclase. *Eur J Neurosci* 1994; 6: 1213 – 1224.
100. Moller R, Parker PJ. The extended protein kinase C superfamily. *Biochem J* 1998; 332: 281 – 292.
101. Stephens EV, Kalinec G, Brann MR, Gutkind JS. Transforming G protein coupled receptors transducer potent mitogenic signals in NIH 3T3 cells

102. Hallberg B, Rayter SI, Downward J. Interaction of Ras and Raf in intact mammalian cells upon extracellular stimulation. *J Biol Chem* 1994; 269: 3913 – 3916.
103. Volmat V, Camps M, Arkinstall S, Pouyssegur J, Leonormand P. The nucleus, the site for signal termination by sequestration and inactivation of p42/p44 MAP kinases. *J Cell Sci* 2001; 114: 3433 – 3443.
104. Shaeffer HJ, Weber MJ. Mitogen-activated protein kinases: specific messages for ubiquitous messengers. *Mol Cell Biol* 1999; 19: 2435 – 2444.
105. Nakayama K. Cip/Kip cyclin-dependent kinase inhibitors: brakes of the cell cycle engine during development. *Bioessays* 1998; 20: 1020 – 1029.
106. Lavoie JN, L'Allemain G, Brunet A, Müller R, Pouyssegur J. Cyclin D1 expression is regulated positively by p42/p44 MAPK and negatively by the p38/HOGMAPK pathway. *J Biol Chem* 1996; 271: 20608 – 20616.
107. Lavoie JN, Rivard N, L'Allemain G, Pouyssegur J. A temporal and biochemical link between growth factor-activated MAP-kinases, cyclin D1 induction and cell cycle entry. *Prog Cell Cycle Res* 1996; 2: 49 – 58.
108. Whitmarsh AJ, Davis RJ. A central control for cell growth. *Nature* 2000; 403: 255 – 256.
109. Meloche S, Seuwen K, Pages G, Pouyssegur J. Biphasic and synergistic activation of p44 MAPK (ERK1) by growth factors: correlation between late phase activation. *Mol Endocrinol* 1992; 6: 845 – 854.
110. Kahan C, Seuwen K, Meloche S, Pouyssegur J. Coordinate biphasic activation of p44 mitogen activated protein kinase and S6 kinase by growth factors in hamster fibroblasts. *J Biol Chem* 1992; 267: 13369 – 13375.
111. Gutkind JS, Crespo P, Xu N, Teramoto H, Coso OA. The pathway connecting the m2 receptors to the nucleus involves small GTP-binding proteins acting on divergent MAP kinase cascades. *Life Sci* 1997; 60: 999 – 1006.

112. Crespo P, Xu N, Simonds WF, Gutkind JS. Ras-dependent activation of MAPK pathway mediated by G-protein beta gamma subunits. *Nature* 1994; 369: 418 – 420.
113. Clapham DE, Neer EJ. New roles for G-protein beta gamma-dimers in transmembrane signaling. *Nature* 1993; 365: 403 – 406.
114. Gutkind JS. Cell growth control by G protein-coupled receptors: from signal transduction to signal integration. *Oncogene* 1998; 17(11): 1331 – 1342.
115. Lewis TS, Shapiro PS, Ahn NG. Signal transduction through MAP kinase cascades. *Adv Cancer Res* 1998; 74: 49 – 139.
116. Schmidt A, Hall A. Guanine nucleotide exchange factors for Rho GTPases: turning on the switch. *Genes Dev* 2002; 16: 1587 – 1609.
117. Cox AD, Der CJ. Ras family signaling: therapeutic targeting. *Cancer Biol Ther* 2002; 1: 599 – 606.
118. Van Corven EJ, Hordijk PL, Medema RH, Bos JL, Moolenaar WH. Pertussis toxin-sensitive activation of p21ras by G protein-coupled receptor agonist in fibroblasts. *Proc Natl Acad Sci USA* 1993; 90: 1257 – 1261.
119. Repasky GA, Chenette EJ, Der CJ. Renewing the conspiracy theory debate: does Raf function alone to mediate Ras oncogenesis? *Trends Cell Biol* 2004; 14: 639 – 647.
120. Alblas J, Van Corven EJ, Hordijk PL, Milligan G, Moolenaar WH. Gi-mediated activation of the p21^{ras} mitogen-activated protein kinase pathway by α_2 adrenergic receptors expressed in fibroblasts. *J Biol Chem* 1993; 268: 22235 – 22238.
121. Winitz S, Russell M, Qian XN, Gardner A, Dwyer L, Johnson GL. Involvement of Ras and Raf in the G_i-coupled acetylcholine muscarinic M₂ receptor activation of mitogen-activated protein (MAP) kinase kinase and MAP kinase. *J Biol Chem* 1993; 268: 19196 – 19199.
122. Burgering BM, Pronk GJ, Van Weeren PC, Chardin P, Bose JL. cAMP antagonizes p21ras-directed activation of extracellular signal-regulated kinase 2 and phosphorylation of mSOS nucleotide exchange factor. *EMBO J* 1993; 12: 4211 – 4220.

123. Wu J, Dent P, Jelinek K, Wolfman A, Weber MJ, Sturgill TW. Inhibition of the EGF-activated MAP kinase signaling pathway by adenosine 3',5'-monophosphate. *Science* 1993; 262: 1065 – 1069.
124. Buchsbaum R, Telliez JB, Goonesekera S, Feig LA. The N-terminal pleckstrin, coiled-coil, and IQ domains of the exchange factor Ras-GRF act cooperatively to facilitate activation by calcium. *Mol Cell Biol* 1996; 16: 4888 – 4896.
125. Farnsworth CL, Freshney NW, Rosen LB, Ghosh A, Greenberg ME, Feig LA. Calcium activation of Ras mediated by neuronal exchange factor Ras-GRF. *Nature* 1995; 376: 524 – 527.
126. Ebinu JO, Bottorff DA, Chan EY, Stang SL, Dunn RJ, Stone JC. RasGRP, a Ras guanyl nucleotide-releasing protein with calcium-and diacylglycerol-binding motifs. *Science* 1998; 280: 1082 – 1086.
127. Mattingly RR, Saini V, Macara IG. Activation of the Ras-GRF/CDC25Mm exchange factor by lysophosphatidic acid. *Cell Signal* 1999; 11: 603 – 610.
128. Schonwasser DC, Marais RM, Marshall CJ, Parker PJ. Activation of the mitogen activated protein kinase/extracellular signal –regulated kinase pathway by conventional, novel, and atypical protein kinase C isotypes. *Mol Cell Biol* 1998; 18: 790 – 798.
129. Ueda Y, Hirai S, Osada S, Suzuki A, Mizuno K, Ohno S. Protein kinase C activates the MEK-ERK pathway in a manner independent of Ras and dependent on Raf. *J Biol Chem* 1996; 271: 23512 – 23519.
130. Marais RM, Light Y, Mason C, Paterson H, Olson MF, Marshall CJ. Requirement of Ras-GTP-Raf complexes for activation of Raf-1 by protein kinase C. *Science* 1998; 280: 109 – 112.
131. Chiloeches A, Paterson HF, Marais R, Clerk A, Marshall CJ, Sugden PH. Regulation of RasGTP loading and Ras-Raf association in neonatal rat ventricular myocytes by G protein-coupled receptor agonist and phorbol ester. Activation of the extracellular signal-regulated kinase cascade by phorbol ester is mediated by Ras. *J Biol Chem* 1999; 274: 19762 – 19770.

132. Grobben B, Claes P, Kolen KV, Roymans D, Frnassen P, Sys SU, Slegers H. Agonists of the P2Y_{AC}-receptor activate MAP kinase by a Ras independent pathway in rat C6 glioma. *Journal of Neurochemistry* 2001; 78: 1325 – 1338.
133. Wellbrock C, Karasarides M, Marais R. The Raf protein takes centre stage. *Nature Reviews Molecular Cell Biology* 2004; 5: 875 – 885.
134. Etienne-Manneville S, Hall A. Rho GTPases in cell biology. *Nature* 2002; 420: 629 – 635.
135. Sah VP, Seasholtz TM, Sagi SA, Heller Brown J. The role of Rho in G protein coupled receptor signal transduction. *Annu Rev Pharmacol Toxicol* 2000; 40: 459 – 489.
136. Kumagi N, Morii N, Fujisawa K, Nemoto Y, Narumiya S. ADP-ribosylation of Rho p21 inhibits lysophosphatidic acid-induced protein tyrosine phosphorylation and phosphatidylinositol 3-kinase activation in cultured swis 3T3 cells. *J Biol Chem* 1993; 268: 24535 – 38.
137. Zhang J, King W, Dillon S, Hall A, Feig L, Rittenhouse SE. Activation of platelet phosphotidylinositide 3-kinase requires the small GTP-binding protein Rho. *J Biol Chem* 1993; 268: 22251 – 54.
138. Murga C, Laguinge L, Wetzker R, Cuadrado A, Gutkind JS. Activation of Akt/protein kinase B by G protein-coupled receptors. A role for α and $\beta\gamma$ subunits of heterotrimeric G proteins acting through phosphatidylinositol-3-OH kinasey. *J Biol Chem* 1998; 273: 19080 – 85.
139. Toker A, Cantley LC. Signaling through the lipid products of phosphoinositide-3-OH kinase. *Nature* 1997; 387: 673 – 76.
140. Khosravi-Far R, Solski PA, Clark GJ, Kinch MS, Der CJ. Activation of Rac1, RhoA and mitogen-activated protein kinases is required for Ras transformation. *Mol Cell Biol* 1995; 15: 6443 – 6453.
141. Qiu RG, Chen J, McCormick F, Symons M. A role for Rho in Ras transformation. *Proc Natl Acad Sci USA* 1995; 92: 11781 – 11785.

142. Zhong C, Kinch MS, Burridge K. Rho-stimulated contractility contributes to the fibroblastic phenotype of Ras-transformed epithelial cells. *Mol Cell Biol* 1997; 8: 2329 – 2344.
143. Izawa I, Amano M, Chihara K, Yamamoto T, Kaibuchi K. Possible involvement of the inactivation of the Rho-Rho-Kinase pathway in oncogenic Ras-induced transformation. *Oncogene* 1998; 17: 2863 – 2871.
144. Sahai E, Ishizaki T, Narumiya S, Treisman R. Transformation mediated by RhoA requires activity of ROCK kinases. *Curr Biol* 1999; 9: 136 – 145.
145. Itoh K, Yoshioka K, Akedo H, Uehata M, Ishizaki T, Narumiya S. An essential part for Rho associated kinase in the transcellular invasion of the tumor cells. *Nature Med* 1999; 5: 221 – 225.
146. Seasholtz TM, Brown JH. Rho signaling in vascular diseases. *Molecular interventions* 2004; 4: 348 – 357.
147. Yamamoto M, Marui N, Sakai T, Morii N, Kozaki S. ADP ribosylation of the RhoA gene product by botulinum C3 exoenzyme causes Swiss 3T3 cells to accumulate in the G1 phase of the cell cycle. *Oncogene* 1993; 8: 1449 – 1455.
148. Kureishi Y, Kobayashi S, Amano M, Kimura K, Kanaide H, Naekano T, Kaibuchi K, Ito M. Rho-associated kinase directly induces smooth muscle contraction through myosin light chain phosphorylation. *J Biol Chem* 1997; 272: 12257 – 12260.
149. Liu Y, Suzuki YJ, Day RM, Fanburg BL. Rho-kinase induced nuclear translocation of ERK1/ERK2 in smooth muscle cell mitogenesis caused by serotonin. *Circ Res* 2004; 95: 579 – 586.
150. Stoyanov B, Volonia S, Hanck T, Rubio I, Loubtchenkov M, Malek D, Stoyanova S, Vanhaesebroeck B, Dhand R, Nurnberg B, Gierschik P, Seedorf K, Hsun JJ, Waterfield MD, Wetzker R. Cloning and characterization of a G protein-activated human phosphoinositide 3-kinase. *Science* 1995; 269: 690 – 693.
151. Domin J, Pages F, Volina S, Rittenhouse SE, Zvelebil MJ, Stein RC, Waterfield MD. Cloning of human phosphoinositide 3-kinase with C2 domain

- that displays reduced sensitivity to the inhibitor wortmannin. *J Biochem* 1997; 326: 139 – 147.
152. Seasholtz TM, Zhang T, Morissette MR, Howes AL, Yang AH, Brown JH. Increased expression and activity of RhoA are associated with increased DNA synthesis and reduced p^{27Kip1} expression in the vasculature of hypertensive rats. *Circulation Res* 2001; 89: 488 – 495.
 153. Phillips-Mason PJ, Raben DM, Baldassare JJ. Phosphatidylinositol 3-kinase activity regulates α -thrombin-stimulated G1 progression by its effects on cyclin D1 expression and cyclin dependent kinase 4 activity. *J Biol Chem* 2000; 275: 18046 – 18053.
 154. Goel R, Phillips-Mason PJ, Raben DM, Baldassare JJ. α -Thrombin induces rapid and sustained Akt phosphorylation by β -arrestin 1-dependent and independent mechanisms, and only the sustained Akt phosphorylation is essential for G1 phase progression. *J Biol Chem* 2002; 277: 18640 – 18648.
 155. Keenan SM, Bellone C, Baldassare JJ. Cyclin dependent kinase 2 nucleocytoplasmic translocation is regulated by extracellular regulated kinase. *J Biol Chem* 2001; 276: 22404 – 22409.
 156. Iwasaka LM, Crespo P, Giuseppe P, Gutkind JS, Wetzker R. Linkage of G protein-coupled receptors to the MAPK signaling pathway through PI 3-kinase. *Science* 1997; 275: 394 – 396.
 157. Rhee SG. Regulation of phosphoinositide-specific phospholipase C. *Annu Rev Biochem* 2001; 70: 281 – 312.
 158. Kolch W, Heldecker G, Kochs G, Hummel R, Vahidi H, Mischak H, Finkenzeller G, Marme D, Rapp U. Protein kinase C α activates Raf-1 by direct phosphorylation. *Nature* 1993; 364: 249 – 255.
 159. Lev S, Moreno H, Martinez R, Canoll P, Peles E, Musacchio JM, Plowman GD, Rudy B, Schlessinger J. Protein tyrosine kinase PYK2 involved in Ca(2+)-induced regulation of ion channel and MAP kinase functions. *Nature* 1995; 376: 737 – 745.

160. Dikic I, Tokiwa G, Lev S, Courtneidge SA, Schlessinger J. A role for PYK2 and Src in linking G-protein-coupled receptors with MAP kinase activation. *Nature* 1996; 383: 547 – 550.
161. Della Rocca GJ, Maudsley S, Daaka Y, Lefkowitz RJ, Luttrell LM. Pleiotropic coupling of G-protein-coupled receptors to the MAP kinase cascade: role of focal adhesions and receptor tyrosine kinases. *J Biol Chem* 1999; 274: 13978 – 13984.
162. Kim JY, Yang MS, Oh CD, Kim KT, Ha MJ, Kang SS, Chun JS. Signaling pathway leading to an activation of mitogen-activated protein kinase by stimulating M3 muscarinic receptors. *J Biochem* 1999; 337: 275 – 280.
163. Arthur DB, Akassoglou K, Insel PA. P2Y(2) and TrkA receptors interact with the Src family kinase for neuronal differentiation. *Biochem Biophys Res Commun*, epub ahead of print, 2006.
164. Filardo EJ. Epidermal growth factor transactivation by estrogen via the G-protein-coupled receptor, GPR30: a novel signaling pathway with potential significance for breast cancer. *J Steroid Biochem Mol Biol* 2002; 80: 231 – 238.
165. Jeanneteau F, Chao MV. Promoting neurotrophic effects by GPCR ligands. *Novartis Found Symp* 2006; 276: 181 – 189.
166. Kanno H, Norikawa Y, Hodges RR, Zoukhri D, Shatos MA, Rios JD, Dartt DA. Cholinergic agonists transactivate EGFR and stimulate MAPK to induce goblet cell secretion. *Am J Physiol Cell Physiol* 2003; 284: C988 – 998.
167. Mori K, Kitayama J, Shida D, Yamashita H, Watanabe T, Nagawa H. Lysophosphatidic acid induced effects in human colon carcinoma DLD1 cells are partially dependent on transactivation of epidermal growth factor receptor. *J Surg Res* 2006; 132: 56 – 61.
168. Amos S, Martin PM, Polar GA, Parsons SJ, Hussaini IM. Phorbol 12-myristate 13-acetate induces epidermal growth factor receptor (EGFR) and c-erbB-2 protein overexpression in adenocarcinoma of uterine cervix. *Eur J Gynaecol Oncol* 2005; 17: 267 – 270.

169. Roelle S, Grosse R, Aigner A, Krell HW, Czubyko F, Gudermann T. Matrix metalloproteinases 2 and 9 mediate epidermal growth factor receptor transactivation by gonadotropin-releasing hormone. *J Biol Chem* 2003; 278: 47307 – 47318.
170. Kue PF, Taub JS, Harrington LB, Polakiewicz RD, Ullrich A, Daaka Y. Lysophosphatidic acid regulated mitogenic ERK signaling in androgen-insensitive prostate cancer PC-3 cells. *Int J Cancer* 2002; 102: 572 – 579.
171. Pandiella A, Bosenberg MW, Huang EJ, Besmer P, Massague J. Cleavage of membrane-anchored growth factors involves distinct protease activities regulated through common mechanisms. *J Biol Chem* 1992; 267: 24028 – 24033.
172. Schlondorff J, Blobel CP. Metalloprotease-disintegrins: modular proteins capable of promoting cell-cell interactions and triggering signals by protein-ectodomain shedding. *J Cell Sci* 1999; 112: 3603 – 3617.
173. Lesser M, Gschwind A, Ullrich A. Epidermal growth factor receptor signal transactivation. *IUBMB Life* 2000; 49: 405 – 409.
174. Lucchesi PA, Sabri A, Belmadani S, Matrougui K. Involvement of metalloproteinases 2/9 in epidermal growth factor receptor transactivation in pressure-induced myogenic tone in mouse mesenteric resistance arteries. *Circulation* 2004; 110: 3587 – 3593.
175. Koch WJ, Hawes BE, Allen LF, Lefkowitz RJ. Direct evidence that G $\beta\gamma$ coupled receptor stimulation of mitogen-activated protein kinase is mediated by the G $\beta\gamma$ activation of the p21ras. *Proc Natl Acad Sci USA* 1994; 91: 12706 – 12710.
176. Faure M, Voyno-Yasenetskaya TA, Bourne HR. cAMP and $\beta\gamma$ subunits of heterotrimeric G proteins stimulate the mitogen-activated protein kinase pathway in COS-7 cells. *J Biol Chem* 1994; 269: 7851 – 7854.
177. Luttrell LM, Della Rocca GJ, Van Biesen T, Luttrell DK, Lefkowitz RJ. G $\beta\gamma$ subunits mediate Src-dependent phosphorylation of the epidermal growth factor receptor. *J Biol Chem* 1997; 272: 4637 – 4644.

178. Prenzel N, Zwick E, Daub H, Leserer M, Abraham R, Wallasch C, Ullrich A. EGF receptor transactivation by G protein-coupled receptors requires metalloproteinase cleavage of proHB-EGF. *Nature* 1999; 402: 884 – 888.
179. Hawes BE, Van Biesen T, Koch WJ, Luttrell LM, Lefkowitz RJ. Distinct pathways of Gi and Gq mediated mitogen activated protein kinase activation. *J Biol Chem* 1995; 270: 17148 – 17153.
180. Seo B, Choy EW, Maudsley S, Miller WE, Wilson BE, Luttrell LM. Pasturella multocida toxin stimulates MAP kinase via Gq/11-dependent transactivation of epidermal growth factor receptors. *J Biol Chem* 2000; 275: 2239 – 2245.
181. Eguchi S, Numaguchi K, Iwasaki H, Matsumoto T, Yamakawa T, Utsunomiya H, Motley ED, Owada KM, Hirata Y, Marumo F, Inagami T. Calcium dependent epidermal growth factor receptor transactivation mediates the angiotensin II-induced mitogen-activated protein kinase activation in vascular smooth muscle cells. *J Biol Chem* 1998; 273: 8890 – 8896.
182. Herr I, Debatin KM. Cellular stress response and apoptosis in cancer therapy. *Blood* 2001; 98: 2603 – 2614.
183. Fadeel B, Orrenius S, Zhivotovsky B. The most unkindest cut of all: on the multiple roles of mammalian caspases. *Leukemia* 2000; 14: 1514 – 1525.
184. Martinou JC, Green DR. Breaking the mitochondrial barrier. *Nat Rev Mol Cell Biol* 2001; 2: 63 – 67.
185. Zhu WZ, Zheng M, Koch WJ, Lefkowitz RJ, Kobilka BK, Xia RP. Dual modulation of cell survival and cell death by β 2 adrenergic signaling in adult mouse cardiac myocytes. *Proc Natl Acad Sci USA* 2001; 98: 1607 – 1612.
186. Budd DC, McDonald J, Emsley N, Cain K, Tobin AB. The C-terminal tail of the M₃ muscarinic receptor possesses anti-apoptotic properties. *J Biol Chem* 2003; 278: 19565 – 19573.
187. Tobin AB, Budd DC. The anti-apoptotic response of the G_{q/11}-coupled muscarinic receptor. *Biochem Soc Trans* 2003; 31: 1182 – 1185.
188. Budd DC, Willars GB, McDonald JE, Tobin AB. Phosphorylation of the Gq/11-coupled M3-muscarinic receptor is involved in receptor activation of

- the ERK-1/2 mitogen-activated protein kinase pathway. *J Biol Chem* 2001; 276: 4581 – 4587.
189. Jacobs. Characteristics of a human diploid cell designated MRC-5. *Nature* 1970; 277: 168.
 190. Cook AK, Carty M, Singer CA, Yamboliev IA, Gerthoffer WT. Coupling of M(2) muscarinic receptors to ERK MAP kinases and caldesmon phosphorylation in colonic smooth muscle. *Am J Physiol Gastrointest Liver Physiol* 2000; 278: G429 – G437.
 191. Wylie PG, Challiss RA, Blank JL. Regulation of extracellular-signal regulated kinase and c-Jun N-terminal kinase by G protein-linked muscarinic acetylcholine receptors. *Biochem J* 1999; 338: 619 – 628.
 192. Zhou L, Hershenson MB. Mitogen signaling pathways in airways smooth muscle. *Respir Physiol Neurobiol* 2003; 137: 295 – 308.
 193. Zhang W, Liu HT. MAPK signal pathways in regulation of cell proliferation in mammalian cells. *Cell Res* 2002; 12: 9 – 18.
 194. Fang JY, Richardson BC. The MAPK signaling pathways and colorectal cancer. *Lancet Oncol* 2005; 6: 322 – 327.
 195. Hey C, Wessler I, Racke K. Muscarinic inhibition of endogenous noradrenaline release from rabbit isolated trachea: receptor subtype and receptor reserve. *Naunyn Schmiedebergs Arch Pharmacol* 1994; 350: 464 – 472.
 196. Disse B, Speck GA, Rominger KL Jr, Hammer R. Tiotropium (Spiriva): mechanistical considerations and clinical profile in obstructive lung disease. *Life Sci* 1999; 64: 457 – 464.
 197. Gosen R, Zaagsma J, Meurs H, Halayko AJ. Muscarinic receptor signalling in the pathophysiology of asthma and COPD. *Respir Res* 2006; 7: 73.
 198. Marinissen MJ, Gutkind JS. G-protein-coupled receptors and signaling networks: emerging paradigms. *Trends in Pharmacological Sciences* 2001; 22: 368 – 376.
 199. Ashkenazi A, Winslow JW, Peralta EG, Peterson GL, Schimerlik MI, Capon DJ, Ramachandran J. An M₂ muscarinic receptor subtype coupled to both

adenylyl cyclase and phosphoinositide turnover. *Science* 1987; 238: 672 – 675.

200. Pulcinelli FM, Gresele P, Bonuglia M, Gazzaniga PP. Evidence for separate effects of U73122 on phospholipase C and calcium channels in human platelets. *Biochem Pharmacol* 1998; 56: 1481 – 1484.
201. Racké K, Haag S, Bahulayan A, Warnken M. Pulmonary fibroblasts, an emerging target for anti-obstructive drugs. *Naunyn-Schmiedeberg's Arch Pharmacol* 2008; 378: 193 – 201.

7. Seminars and Publications

Matthiesen S, Kempkens S, Bahulayan A, Juergens UR, Racké K. Muscarinic stimulation of human lung fibroblast proliferation. Proceeding of British Pharmacological Society 2006; 3: A37P

'Muscarinic receptor stimulation of human lung fibroblast' [Conference Presentation] Second International Symposium on Non-neuronal Acetylcholine August 31-September 2, 2006 Academy of Science and Literature, Mainz, Germany

Matthiesen S, Bahulayan A, Kempkens S, Haag S, Fuhrmann R, Stichnote C, Jurgens UR, Racké K. Muscarinic Receptors Mediate Stimulation of Human Lung Fibroblast Proliferation. American Journal of Respiratory Cell and Molecular Biology 2006; 35: 621 – 627.

Matthiesen S, Bahulayan A, Holz O, Racké K. MAPK pathway mediates muscarinic receptor-induced human lung fibroblast proliferation. Life Science 2007; 80: 24 – 25.

Racké K, Haag S, Bahulayan A, Warnken M. Pulmonary fibroblasts, an emerging target for anti-obstructive drugs. Naunyn-Schmiedeberg's Arch Pharmacol 2008; 378: 193 – 201.

8. Acknowledgements

I would first and foremost like to thank my Professor, Dr. Kurt Racké for developing a scientist out of me; I will always be indebted for his guidance and support contributing to my work and for his compassion and understanding as an individual.

My special thanks go to my supervisor Dr: Sonja Matthiesen and my colleagues Marielle Warnken and Susanne Haag for their valuable contribution and assistance in my project, and for providing a very amicable working environment.

I would also like to thank Rita Fuhrmann for excellent technical assistance.

Last but not the least I would like to express my gratitude and thank the Department of Pharmacology and Toxicology for offering me the opportunity to complete my project in a stimulating scientific environment.

This project was funded by Boehringer Ingelheim Germany.

9. Curriculum Vitae

Name: Amit Bahulayan

Date of Birth: 27.1.1978

Nationality: Indian

Marital Status: Single

Educational Background:

Name of institute	Degree obtained	Duration of course	Score/Grade
Griffith university Brisbane, Australia	Masters of Health Services Management	Feb2002- Sept2003	5GPA
Bharati Vidyapeeth's college of Pharmacy Mumbai, India	Bachelor of Pharmaceutical Sciences	May1995- May1999	Passed with First Class
Mithibai college of Science Mumbai, India	Higher Secondary State Board Examination	March1993- March1995	First Class
St.Xaviers High School Mumbai, India	Secondary School Certificate Examination	March1983- March1993	Distinction

Current Status:

July 2005 to date: Pursuing a doctorate degree at the Institute for Pharmacology and Toxicology, University of Bonn.